HVdc Commutation Failures

by: Lorne E. Midford

A Thesis

Submitted to the Faculty of Graduate Studies

in Partial Fulfillment of the Requirements for the

Degree of Master of Science.

Electrical Engineering Department

Winnipeg, Manitoba

August, 1991

ISBN 0-315-76880-0

HVdc COMMUTATION FAILURES

BY

LORNE E. MIDFORD

A thesis submitted to the Faculty of Graduate Studies of
the University of Manitoba in partial fulfillment of the requirements
of the degree of

MASTER OF SCIENCE

Abstract

A commutation failure will occur if commutation of current from one valve to another has not completed before the commutating voltage reverses across the outgoing valve. A commutation failure is not usually caused by the misoperation of a valve, but either by disturbances outside of the valve group, or by misoperation of the valve firing controls. It will be shown that commutation failures, as well, are inherent in converter operation and can never be completely avoided with conventional thyristors.

This report analyzes the problem of commutation failures as it relates to inverter commutating voltage, dc loading, ac system strength, thyristor deionization time and steady state extinction angle. Through computer simulations and field results from the Manitoba Hydro HVdc transmission system, analysis of commutation failures caused by remote single line to ground faults was carried out. The major focus was on the chance of a commutation failure occurring. Previously published material on this subject was scarce, emphasizing the significance of the results.

In addition, the effectiveness of several dc controls was analyzed in reducing the probability of a commutation failure. A zero sequence control strategy was also designed and tested for the Manitoba Hydro HVdc system.

Results indicate that the incidence of a commutation failure by a remote single line to ground fault is dependent on a number of system conditions which are analyzed in detail in the report. The most effective way of reducing the probability of a commutation failure is to operate the inverter at a larger extinction angle. However, a decision to increase the extinction angle must not only consider commutation failure performance, but also extra capital and operating costs for a converter which can operate continuously at the higher extinction angle.

Acknowledgement

The author wishes to acknowledge C.V. Thio (Manitoba Hydro) for suggesting the topic for this thesis. The author also wishes to extend his gratitude to M.Z. Tarnawecky (University of Manitoba) for his contributions to this project, as well as to Dr. D.G. Chapman, K.L. Kent, and P. Kuffel (Manitoba Hydro) for their input and comments.

The use of Manitoba Hydro computing resources is also very greatly appreciated.

Table Of Contents

Table Of Figures

Table Of Figures

Table Of Symbols

Tabulated below are some of the more frequently occurring symbols and acronyms:

α	firing angle
β	inverter ignition angle
γ	inverter extinction angle
γ_o or γ_{min}	deionization time
μ	angle of overlap
Ω	ohms
ΔA	commutation area
ΔI_d	current margin
AORD	α_{order}
AMEAS	$\alpha_{measured}$
BP1	Bipole 1
BP2	Bipole 2
CEA	constant extinction angle
CEC	current error control
CF	commutation failure
EMTDC	Electromagnetic Transient Program for DC systems
HVdc	High Voltage Direct Current
Hz	hertz
I_{ac}	alternating current
I_{dc}	direct current
I_s	ac short circuit current on the secondary side of the converter transformer
kV	kilovolts
L_c	commutating inductance
L-L	line to line
L_r	smoothing reactor
MAV	mercury arc valve
MW	megawatt
PACF	pole kick
pu	per unit
SCR	short ciruit ratio

S-L-G	single line to ground
Q_{rr}	excess stored charge
R_{line}	dc line resistance
VAOUT	α valve group control loop
V_{dc}	dc voltage
VDCOL	voltage dependent current order limit
V_{do}	ideal no-load direct voltage
VG	valve group
VGCF	valve group commutation failure indicator
VGOUT	γ valve group control loop
$V_{L\text{-}L}$ or $E_{L\text{-}L}$	line to line voltage
$V_{L\text{-}n}$ or $E_{L\text{-}n}$	line to neutral voltage
VZERO	zero sequence commutation failure indicator
X_c	commutating reactance

Problem

Commutation failures have always been inherent in inverter operation, and is the focus of research in this thesis. When there is a commutation failure, a short circuit occurs across the bridge, decreasing the power by the percentage of bridges that failed commutation. The incidence of commutation failures has been known to be related to the commutating voltage at the inverter, but there has been no research into the probability of commutation failures as a direct result of remote single line to ground faults.

Purpose

The study objectives are summarized below:

- To determine the probability of the incidence of a commutation failure as well as the percentage of valve groups that fail commutation at Dorsey Converter Station for remote single line to ground faults of varying severity, and compare this with field data.
- To determine the effect of voltage depression on the incidence of commutation failures.
- To determine the effect of the thyristor deionization time on the incidence of commutation failures.
- To determine the effect of the direct current on the incidence of commutation failures.
- To determine the effect of the phase shift and voltage distortion associated with a single line to ground fault on the incidence of commutation failures.
- To determine the effect of an improved pole-kick based on a zero sequence detection rather than a commutation failure detection.

Scope

There has not been a lot of published material on the causes of commutation failures, which makes the results of Chapters 4 and 5 very significant. However, before the results are presented, a detailed explanation of commutation failures is presented including, thyristor characteristics, fault analysis and control strategies.

The first chapter is a general introduction to thyristor physics, which is necessary to develop the concept of a commutation failure. A basic understanding of HVdc converter six pulse and twelve pulse operation is assumed. The thyristor turn-on and turn-off characteristics are described in detail, with the thyristor turn-off noted as being fundamentally important in the occurrence of commutation failures.

The second chapter begins by first defining the inverter and rectifier angle definitions that are used in this study. A detailed discussion of commutation failures is then presented with specific detail to the commutation area for a valve. The effect of both phase shift and voltage depression of several different ac disturbances is also described as they relate to commutation failures. Finally, a waveform analysis of the valve voltages and currents during a commutation failure demonstrates the short circuit in the bridge, and the resulting rise in valve current.

The subject of the third chapter is control strategies. Typical control strategies of HVdc systems are first introduced, with specific detail to inverter control strategies. Based on the Manitoba Hydro Bipole 1 controls, response of the inverter controls to a commutation failure is presented. As well, a zero sequence commutation failure detection scheme is designed for the Manitoba Hydro system.

The fourth chapter contains all of the results to the EMTDC computer simulations. By modelling the complete Manitoba Hydro Bipole 1 HVdc system, the problem of commutation failures as they relate to inverter commutating

voltage, direct current, deionization time of the thyristors, steady-state extinction angle and ac system strength is presented. A detailed description of the ac and dc models used in the studies is also included.

The fifth chapter presents commutation failure results from the Manitoba Hydro HVdc system. The Manitoba Hydro system is described, and the field results are presented. A direct comparison of computer simulation to field results is also included.

The sixth and seventh chapters contain the summary and the conclusions, respectively. These chapters provide a concise analysis of the entire thesis.

Method

A validated computer model of the Manitoba Hydro Bipole 1 HVdc transmission system was used to research commutation failures through digital simulations. As well, field results from the Manitoba Hydro system were also analysed and compared to the computer results.

Contributions

Several significant contributions were made in researching the problem of commutation failures as they relate to inverter commutating voltage, direct current, deionization time of the thyristors, steady-state extinction angle and ac system strength. Knowing the relation of commutation failures to all of these aforementioned variables, it is hoped that commutation failure performance may be included in future specifications for HVdc inverter performance.

Thyristors

Introduction

This chapter provides a very brief description of an HVdc bridge, with more emphasis on thyristor voltage and current characteristics. The thyristor turn-on and turn-off characteristics are also described.

HVdc Bridge

Although details vary between designs, the general composition of an HVdc valve is illustrated in *Figure 1.1*.

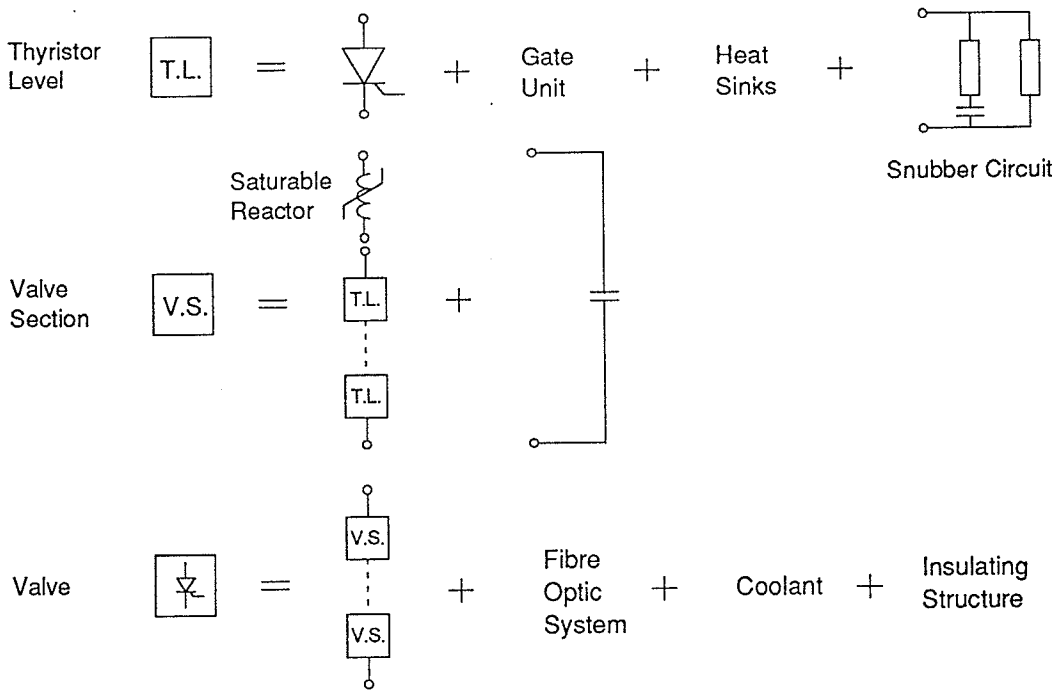

Figure 1.1 - Composition of an HVdc valve.

The valve can be considered at three levels: the thyristor level, the valve section level, and the complete valve level[1]. The valve sections contain several

thyristor levels in series, while the thyristor level contains the thyristor, the gate firing units, as well as the snubber circuits.

An HVdc three phase bridge is made up of 6 valves, which is also known as a 6-pulse system. The connection of two bridges in series is known as a twelve pulse system. The connection of two bridges in series not only doubles the dc voltage, but if the transformer bank of one bridge is connected Y-Y, and the transformer of the other bridge is connected Y-Δ, the 5^{th} and 7^{th} ac harmonics as well as the 6^{th} dc harmonic are eliminated[2]. *Figure 1.2* shows a six-pulse bridge and a twelve-pulse bridge cascade.

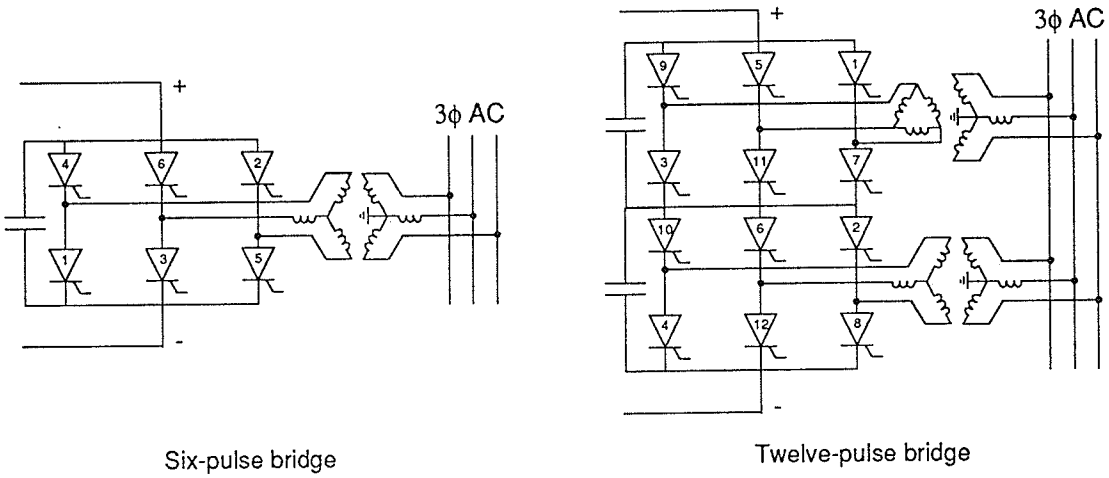

Figure 1.2 - Six-pulse bridge and twelve-pulse bridge cascade.

Thyristor Characteristics

A thyristor is a three terminal, four layer, semiconductor device that can be thought of as a simple diode with turn-on gate control *(Figure 1.3)*. The voltage versus current (V-I) characteristic curve consists of the reverse blocking mode, the forward blocking mode, and the on-state mode. In the reverse blocking mode, the anode is made negative with respect to the cathode; thereby allowing a high voltage to be maintained between the anode and cathode with only a small leakage current flowing *(Figure 1.4, curve ABC)*. This characteristic is the same

as a reverse biased diode, where an increase in reverse voltage beyond the breakdown voltage will cause very large reverse currents, and ultimately destroy the thyristor.

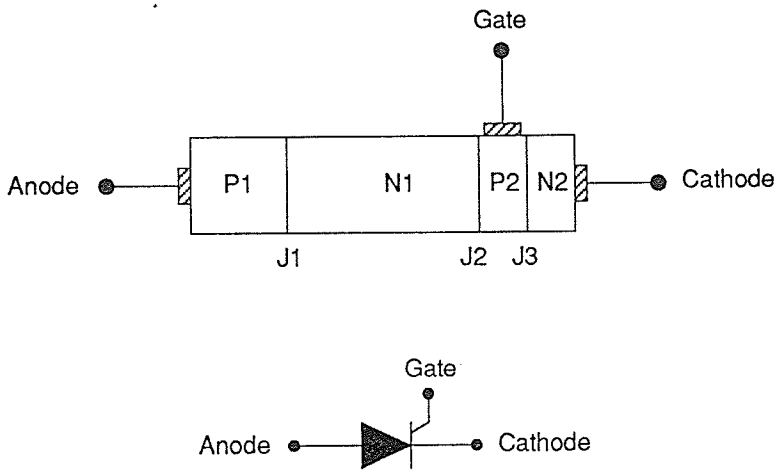

Figure 1.3 - Thyristor structure.

As long as no gate current flows from the gate terminal to the cathode terminal, a thyristor will remain blocked even if the anode is made positive with respect to the cathode *(Figure 1.4, curve AD)*. This characteristic is referred to as the forward blocking mode. However, if the anode voltage is increased beyond the zero breakover voltage, a thyristor with no gate current can turn on *(Figure 1.4, curve DEFG)*. Random triggering in this manner can be tolerated in the event of faults.

In the normal turn on mode, with the anode voltage positive with respect to the cathode, a gate current flowing from the gate terminal to the cathode terminal will turn on the device *(Figure 1.4, curve AFG)*. This characteristic is similar to a forward biased diode, although the voltage drop will be slightly greater for a thyristor. Once on, the gate cannot control the thyristor, which will only turn off when the anode to cathode current drops to zero.

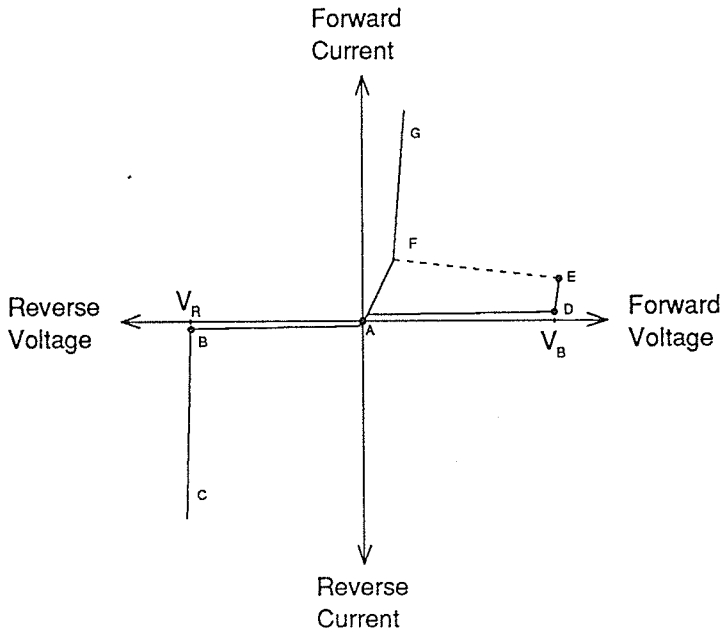

Figure 1.4 - Thyristor characteristics.

Turn-On/Off

With the thyristor forward biased (the anode voltage greater than the cathode voltage), a gate current pulse will turn the thyristor on. The turn on process occurs in three stages: first there is a small gate-controlled time delay where the anode voltage does not change significantly; second, the voltage across the thyristor suddenly collapses while the thyristor current rises at a finite rate known as the rise time; finally, the spreading phase of the turn on process is characterized by a steady state voltage as the conduction spreads to the entire silicon area. These turn on characteristics are illustrated in *Figure 1.5*. The turn-on time is defined as the sum of the delay time and rise time only, and is typically only several microseconds long (less than one tenth of a degree). For an HVdc valve consisting of several thyristors in series, each thyristor will have a slightly different turn-on characteristic due to the non-uniform manufacturing process. Although identical gate pulses can be sent to each thyristor simultaneously, there is no guarantee that the thyristors will all turn on at

exactly the same time. This non-uniform on-state is important when considering valve stresses and applicable protective schemes, but is relatively small compared to the turn-off time of a thyristor.

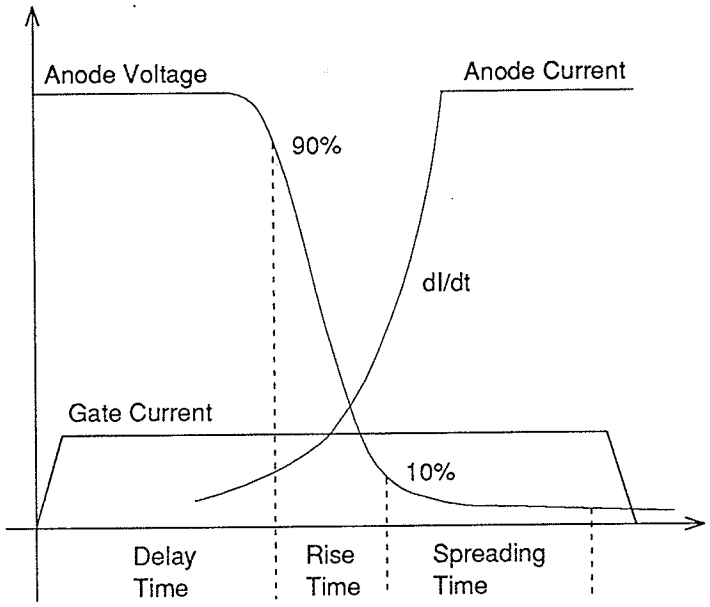

Figure 1.5 - Turn-on characteristics.

The turn-off characteristic of a thyristor is illustrated in *Figure 1.6*. Turn-off is achieved in the reverse blocking mode, where the anode current is forced to flow in the opposite direction by applying a reverse breakdown voltage to the thyristor. The anode current will fall at a high rate of change and then continue to swing negative until all of the excess stored charge Q_{rr} is removed from the thyristor. Once the thyristor current has been turned off, a reverse voltage must continue to be applied to the thyristor to remove any surplus charge carriers. If a forward bias is applied too soon, the thyristor can turn-on again even with no gate control. The time of the reverse voltage after the current has gone to zero is defined as the hold-off interval, and is a characteristic of the thyristor. In addition, thyristor characteristics such as the excess stored charge Q_{rr} and turn-off time are also temperature and circuit dependent.

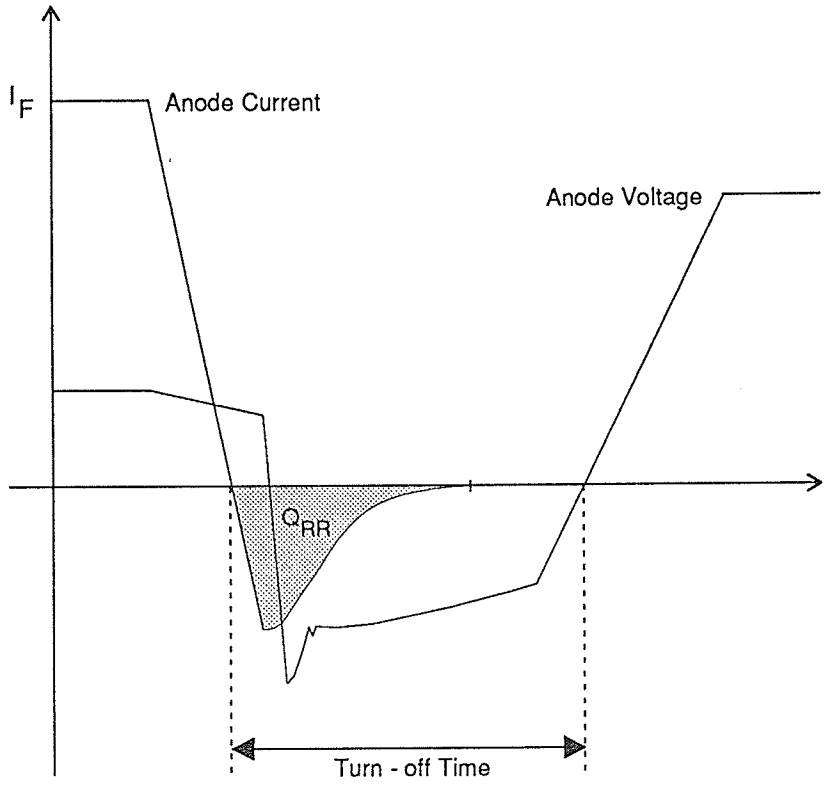

Figure 1.6 - Turn-off characteristics.

In an HVdc valve, thyristors are connected in series to provide the necessary voltage rating for the bridge. The differences in the individual thyristor characteristics for turn-off can become significant. For example, if the stored charge Q_{rr} differs between several thyristors, the thyristor with the smaller Q_{rr} will recover first and experience a higher recovery voltage than the rest of the stack. This effect is minimized by trying to match thyristor characteristics of thyristors placed in series, and also by providing adequately sized damping capacitors in the snubber circuits.

Mercury Arc Valves

Mercury arc valves were developed for HVdc transmission before thyristors became practical in the early 1970's. Although the physics may differ from thyristors, the turn-off process still requires deionization before a reverse voltage can successfully be applied across the valve. The actual turn-off times of mercury arc valves are slightly higher than an equivalent thyristor valve. Since mercury arc valves have a higher turn-off time, the occurrence of commutation failures for mercury arc valves can be slightly higher than thyristor valves.

Conclusions

This chapter introduced thyristor voltage and current characteristics as they relate to the turn-on and turn-off process of thyristors. The difference between thyristor and mercury arc valves was also described. As well, it was noted that a forward bias applied too soon across a thyristor could turn the thyristor on without any gate control. It is this involuntary turn-on that is fundamental to the occurrence of commutation failures.

Commutation Failures

Introduction

This chapter introduces both the inverter and the rectifier angle relationships adopted for this study As well, a detailed analysis of commutation failures, and how they relate to ac system faults is included, with special attention to commutation area. Finally, a detailed waveform analysis is performed for a commutation failure to illustrate the total effect of the failure on the valve voltage and current.

Notation

The following diagram *(Figure 2.1)* illustrates the angle relationships and angle definitions for both a rectifier and an inverter. In both cases, current is being commutated from valve 1 to valve 3.

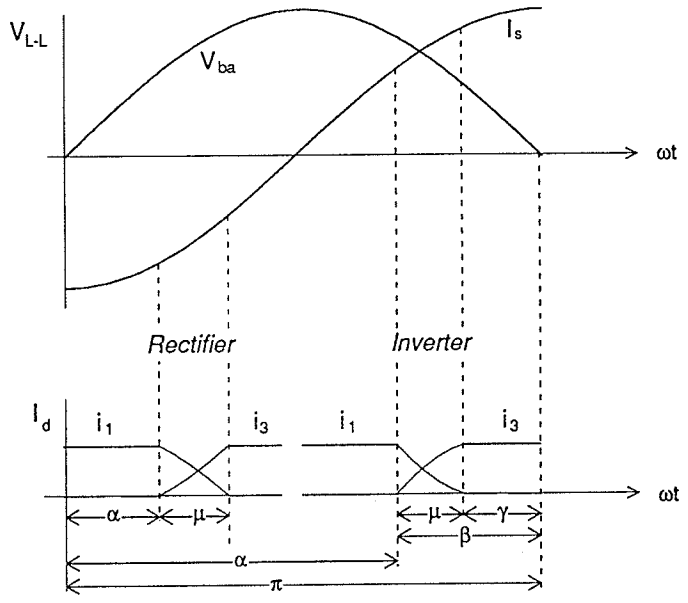

Figure 2.1 - Inverter and rectifier angle relations.

Since a converter transformer has inductance, the transformer current cannot change instantly. The finite rate of change of current means that the transfer of

current from one valve to another requires a finite commutation time (referenced as the angle of overlap (μ)). Typical full load values of μ are in the range of 20° to 25° for a 60 Hz system under normal steady-state operation.

As described in Chapter 1, once a thyristor has completed commutation of current, a finite duration of reverse voltage is necessary to sweep away any excess stored charge. This time is known as the deionization time of the valve, and the time from the instant when the valve current goes to zero to the time that the line-to-line voltage is zero is defined as the extinction angle (γ). If the thyristor becomes positively biased before complete deionization occurs, this thyristor will regain current. Typical values for the deionization time of an individual mercury arc valve ranges from 5° to 8° [3]. Thyristor valves will have a slightly lower deionization time, since the actual turn-off time of mercury arc valves are slightly higher than equivalent thyristor valves. The ordered extinction angle at Dorsey Converter Station and many other inverters on 60 Hz systems is 18°. Inverters on 50 Hz systems typically operate at 15°, which is the same time duration.

Commutation Failures

A commutation failure can occur if the commutation of current from one valve to another has not completed before the commutating voltage reverses across the outgoing valve. A commutation failure is not usually caused by misoperation of a valve, but either by disturbances outside the valve group, or by misoperation of the valve timing. It is therefore important to realize, as will be shown, that commutation failures are inherent in converter operation and can never be completely avoided with conventional thyristors. In addition, the overall ability of a valve to commutate is very dependant on the ac commutating voltage waveform. Therefore, for successful commutation, it is imperative that the controlled firing angle have enough margin to allow transfer of current to the next valve before the minimum extinction angle is reached.

Commutation failures are more frequent at an inverter than at a rectifier because the extinction angle at an inverter can more often decrease below the minimum required for successful commutation during an ac system disturbance. While at

a rectifier, there is substantially more time after firing for commutation to be completed.

As long as the dc current does not increase, the voltage drop due to commutation will remain independent of the firing angle, and the commutation area (ΔA), as shown in *Figure 2.2*, will remain the same for the same current. Thus as the firing angle increases, the extinction angle decreases for the same dc current.

The following line-to-neutral source voltages were adopted for the following analysis of the commutation area (ΔA).

$$V_a = E_{ln} \cos(\omega t + 60) \tag{1}$$

$$V_b = E_{ln} \cos(\omega t - 60) \tag{2}$$

$$V_c = E_{ln} \cos(\omega t - 180) \tag{3}$$

The corresponding line-to-line voltages are:

$$\begin{aligned} V_{ba} = V_b - V_a &= \sqrt{3}\, E_{ln} \cos(\omega t - 90) \\ &= \sqrt{3}\, E_{ln} \sin(\omega t) \end{aligned} \tag{4}$$

$$V_{ac} = V_a - V_c = \sqrt{3}\, E_{ln} \cos(\omega t + 30) \tag{5}$$

$$V_{cb} = V_c - V_b = \sqrt{3}\, E_{ln} \cos(\omega t + 150) \tag{6}$$

An equation can now be derived to calculate the commutation area (ΔA) based on the commutating phase voltages on the dc side of the converter transformer.

$$\Delta A = \int_{\alpha}^{\pi-\gamma} \frac{V_b + V_a}{2} - V_a \, d\theta$$

$$= \int_{\alpha}^{\pi-\gamma} \frac{V_b - V_a}{2} \, d\theta$$

$$= \frac{1}{2} \int_{\alpha}^{\pi-\gamma} E_{ll}\, d\theta \tag{7}$$

$$= \frac{\sqrt{3}E_{ln}}{2} \int_{\alpha}^{\pi-\gamma} \sin(\theta)\, d\theta$$

$$= \frac{\sqrt{3}E_{ln}}{2} \left[-\cos\theta\right]_{\alpha}^{\pi-\gamma}$$

Therefore, $$\Delta A = \frac{\sqrt{3}E_{ln}}{2} (\cos\alpha - \cos(\pi-\gamma)) \tag{8}$$

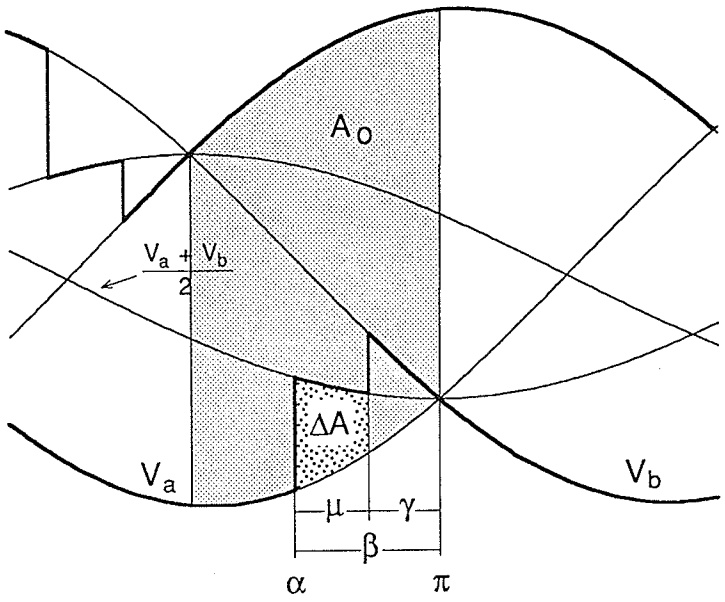

Figure 2.2 - Commutation area definition.

Reevaluating the commutation area based on the commutating line to line voltage on the dc side of the converter transformer and using *Figure 2.3a* as a reference for normal commutation, the principals of converter commutation can be illustrated for several different conditions. For a line to line representation, the commutation area is twice the commutation area previously defined as (ΔA) on a phase voltage representation (Eq. 7). In all cases, the area (ΔA) will not

change for constant direct current. Therefore, advancing the firing angle *(Figure 2.3b)* will cause an increase in the extinction angle ($\gamma_b > \gamma_{min}$) and a decrease in the angle of overlap ($\mu_b < \mu_a$), with the commutation area unchanged ($2\Delta A_a = 2\Delta A_b$).

If, on the other hand, the commutating ac line to line voltage decreases because of an ac disturbance *(Figure 2.3c)*, the commutation area will again remain the same ($2\Delta A_c = 2\Delta A_a$), causing the angle of overlap to increase ($\mu_c > \mu_a$) and the extinction angle to decrease. Therefore, to maintain the minimum extinction angle required for successful commutation, the valve must be fired earlier ($\alpha_c < \alpha_a$) in the event of an ac voltage depression to maintain the required commutation area.

The examples so far assumed a constant direct current with changes in commutating voltage and delay angle. If the direct current is now considered to increase with the commutating voltage unchanged, the overlap angle would increase ($\mu_d > \mu_a$) thereby increasing the commutation area ($2\Delta A_d > 2\Delta A_a$). This would again require an advance in the firing angle to maintain the minimum extinction angle required for successful commutation *(Figure 2.3d)*.

A commutation failure will occur if the commutation area increases enough to cause the angle of overlap to infringe on the deionization time required for the valve. This may occur for several reasons: the ac line-to-line voltage may be suppressed due to an ac system fault; a dc disturbance may cause the direct current to increase; or the dc controls may cause a misfire by not supplying the firing pulse to the valve at the right instant. If any of these disturbances occurred once a valve started commutating current to another valve, there is no control action available to prevent a commutation failure from occurring, since the delay angle cannot be changed for this commutation. Controls can be used to advance the firing angle of other valves upon the detection of a commutation failure, but once a valve has fired nothing can be done for that valve. The chance of a specific valve failing commutation is therefore very dependent on when the disturbance occurs and which phases are affected.

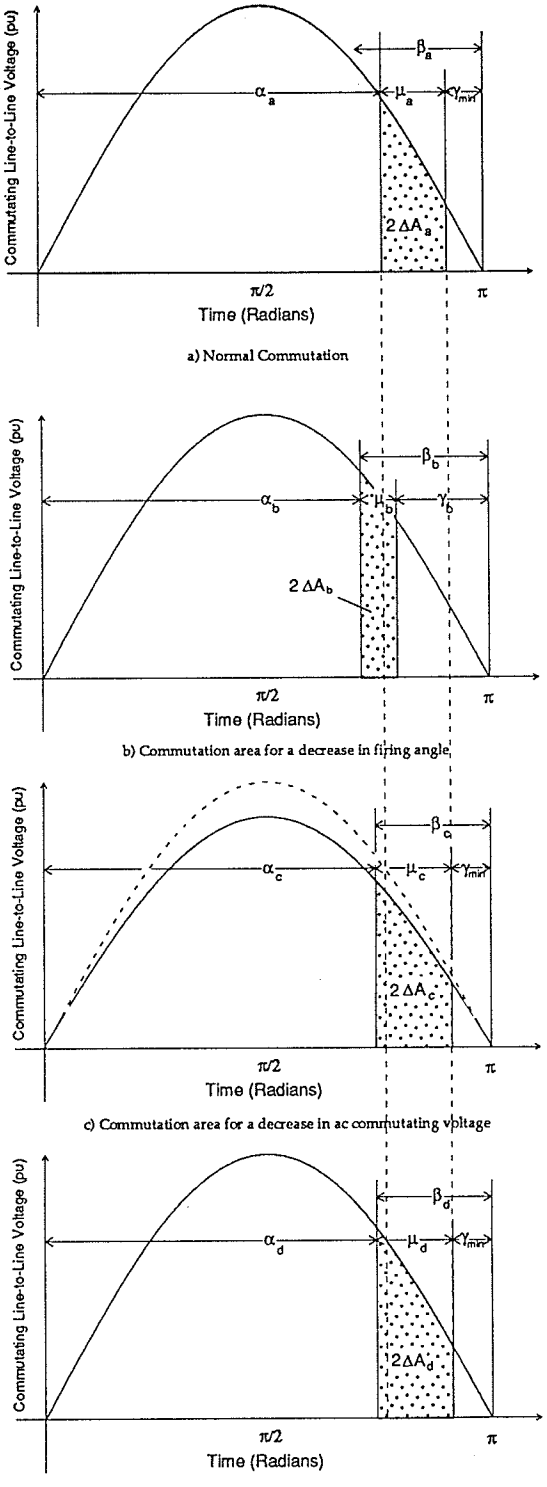

Figure 2.3 - Commutation area Relations.

Usually an inverter is operated in constant extinction angle control (CEA), where the extinction angle is controlled to some value higher than the minimum required by the valves. This margin is to allow changes in the ac system (small decreases in commutating voltage, or small increases in direct current above full load) without resulting in commutation failures.

It would seem that an easy solution to prevent commutation failures is to simply increase the controlled extinction angle to a large value, thereby allowing enough deionization time for almost all faults. Unfortunately, because the current leads the voltage at an inverter, reactive power is absorbed. The approximate expression for the power factor at the inverter is given by (eq. 9)[4].

$$\cos(\phi) \cong \frac{1}{2}[\cos\gamma + \cos(\gamma+\mu)] \tag{9}$$

To maintain a reasonably high power factor, γ should be kept as low as possible. There are a number of reasons to keep the power factor high at an inverter:

- To keep the rated real power of the converters as high as possible for given current and voltage ratings of valves and transformers.
- To reduce the stress on the valves and damping circuits, which applies more to mercury arc valves.
- To minimize the required current rating and copper losses in the ac lines to the converter.
- To minimize voltage regulation drops at the ac terminals of the converter as the loading increases.
- To decrease the level of reactive compensation required at the inverter.

Considering the above reasons, there is a trade-off between keeping the power factor as high as possible, but still keeping γ high enough to minimize the number of commutation failures. The controlled value of extinction angle must provide sufficient commutation margin above the minimum angle

required for deionization of the valve due to possible changes in direct current and alternating voltage even after commutation has begun.

Fault Analysis

Single Line To Ground Faults

Figure 2.4 shows a phasor diagram, as well as the actual waveform, of the commutating bus voltage at the inverter. A decrease in voltage in one phase will cause a drop in two line-to-line voltages. As well, a phase shift will occur in the line-to-line voltages: one will advance, while the other will retard in reference to the natural commutation point.

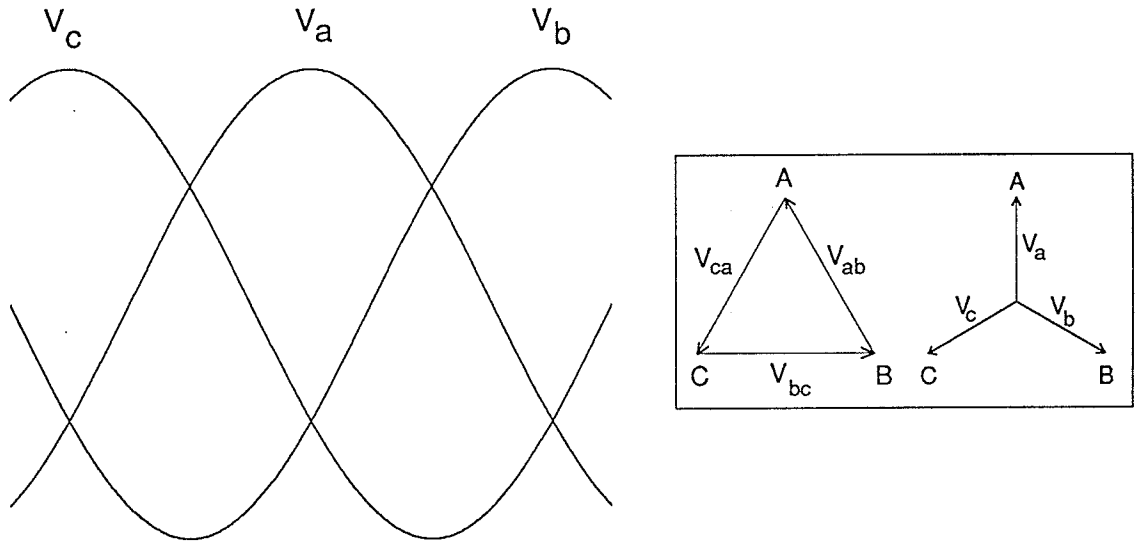

Figure 2.4 - AC commutating voltage.

While the phase advance will increase the probability of commutation failure, a phase retard will decrease this probability. This relation is illustrated in *Figure 2.5*. Again, the probability of a commutation failure is inversely related to the margin for deionization of the valve.

The valve timing is taken from the line-to-line voltages on the ac side of the converter transformers. Therefore, the actual phase shift from the fault is seen

by the change in the measured firing angle and extinction angle, causing the valve firing controls to respond to phase shifts.

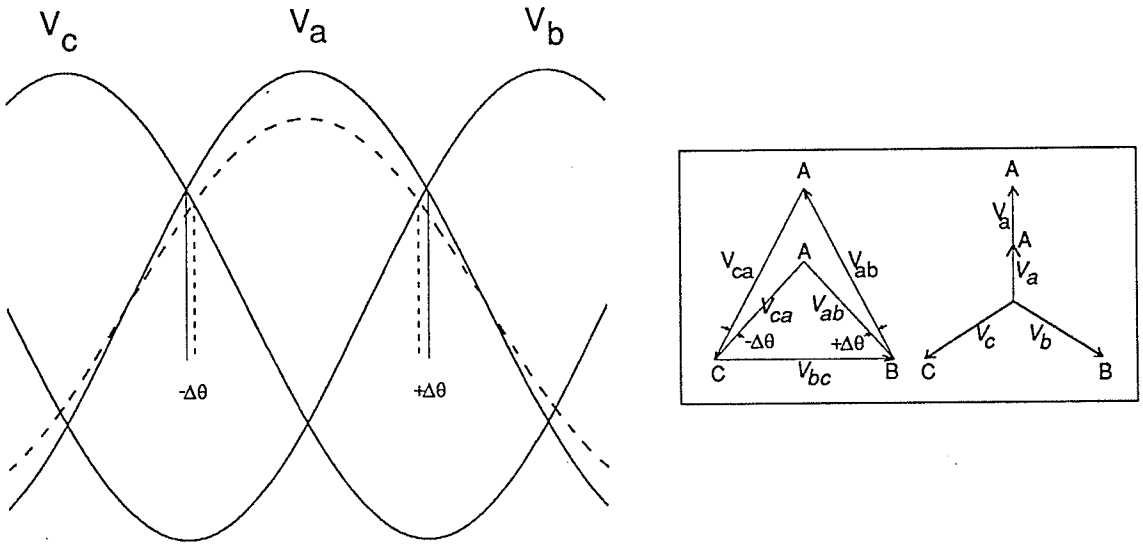

Figure 2.5 - Single-line-to-ground fault.

Line To Line Faults

For a line-to-line fault, two phase voltages decrease while the third remains unchanged *(Figure 2.6)*. All three line-to-line voltages are affected with this disturbance. Two L-L voltages are shifted in phase (one leading, the other lagging), while the third L-L voltage decreases in value but does not experience any phase shift.

Three Phase Fault

A three phase fault is the least likely to occur, yet has the lowest probability of causing a commutation failure. This is because there is no phase shift in any of the line-to-line voltages, only voltage depressions. This fault is illustrated in *Figure 2.7*

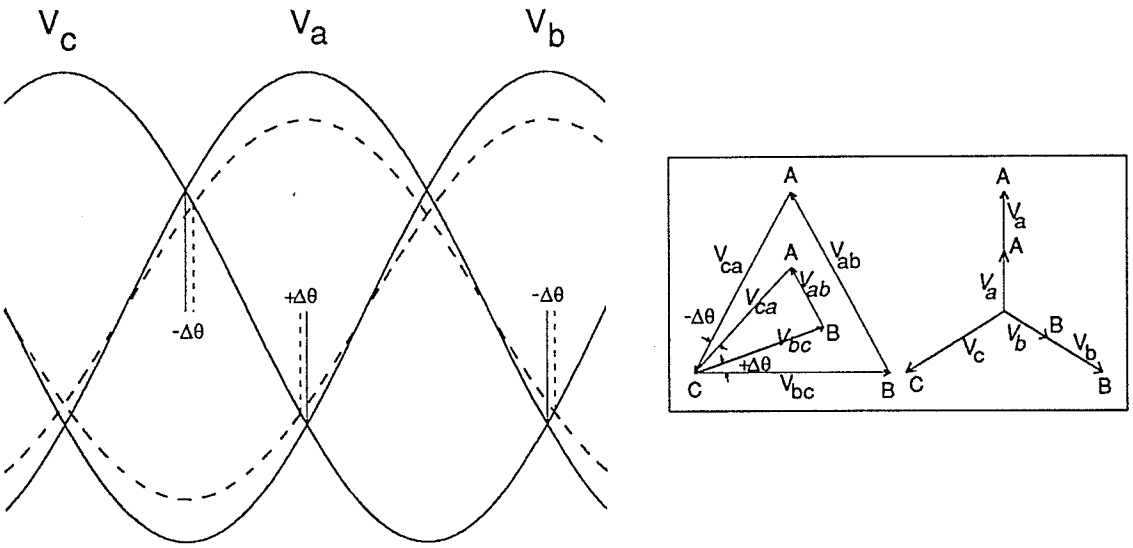

Figure 2.6 - Line-to-line fault.

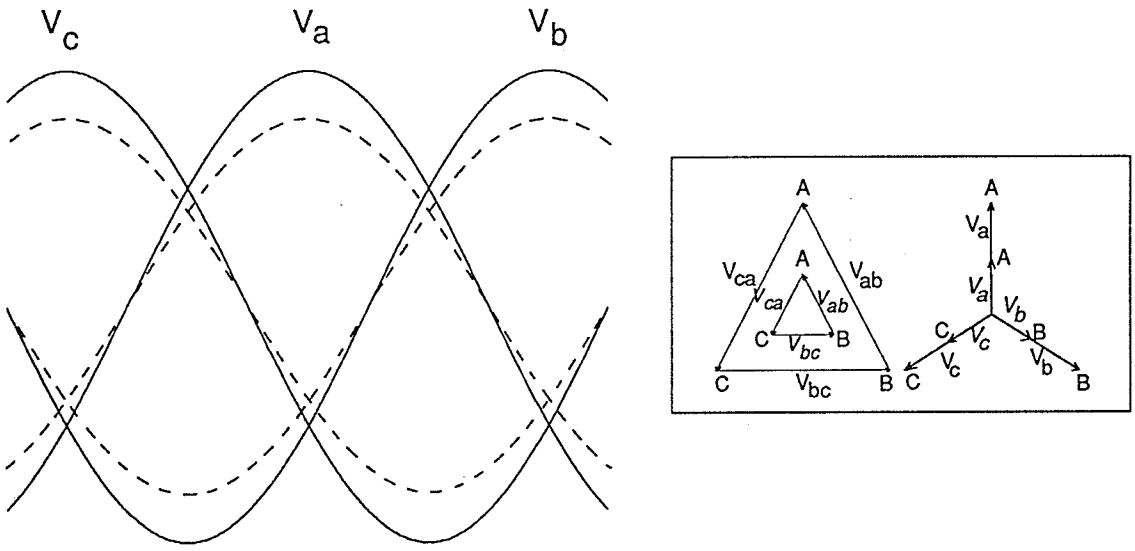

Figure 2.7 - Three phase fault.

For a three phase fault, the theoretical voltage depression, above which there would be no chance of a commutation failure occurring can be estimated by a calculation based on the deionization time required by the valve. This calculation is based solely on the magnitude of the voltage depression, and does

not take into account voltage distortions, or increases in direct current due to the drop in voltage.

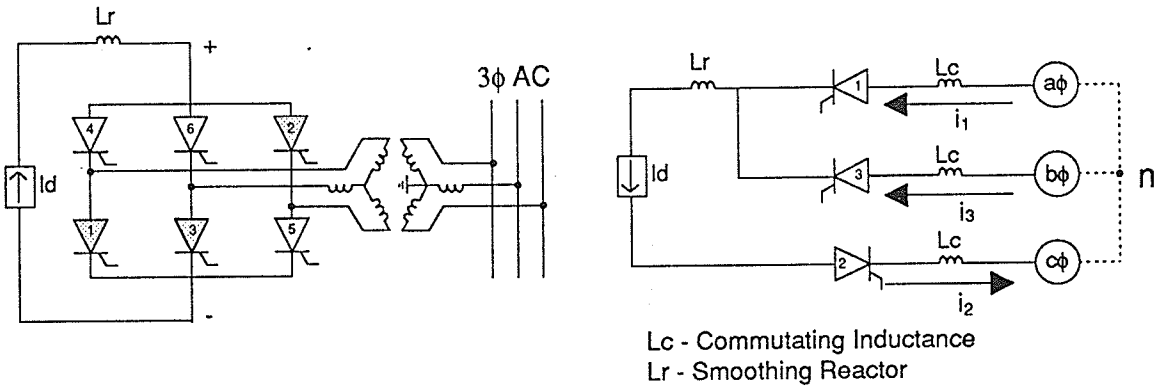

Figure 2.8 - Valves 1,2,3 conducting.

The interval in which valves 1,2, and 3 are conducting *(Figure 2.8)* will be analyzed.

$$V_b - V_a = L_c \frac{di_3}{dt} - L_c \frac{di_1}{dt} \tag{10}$$

but from Eq. (5) $$V_b - V_a = \sqrt{3}\, E_{ln} \sin \omega t \tag{11}$$

Also, $$i_1 = I_d - i_3$$

Therefore, $$\frac{di_1}{dt} = 0 - \frac{di_3}{dt} \tag{12}$$

Substituting (12) into (10),

$$V_b - V_a = 2\, L_c \frac{di_3}{dt} \tag{13}$$

Substituting (13) into (11),

$$\sqrt{3}\,E_{ln} \sin \omega t = 2\,L_c \frac{di_3}{dt} \tag{14}$$

At the beginning of commutation (at $\omega t = \alpha$) $i_1 = I_d$ and $i_3 = 0$

Therefore, integrating Eq. (14) with respect to (t) gives:

$$\frac{\sqrt{3}E_{ln}}{2L_c} \int_{\frac{\alpha}{\omega}}^{t} \sin \omega t \, dt = \int_{0}^{i_3} di_3$$

$$I_s (\cos \alpha - \cos \omega t) = i_3 = I_d - i_1 \tag{15}$$

Where, $$I_s = \frac{\sqrt{3}E_{ln}}{2\omega L_c} \tag{16}$$

At the end of commutation (at $\omega t = \pi - \gamma$) $i_1 = 0$ and $i_3 = I_d$

Substituting in Eq. (15):

$$I_d = I_s (\cos \alpha - \cos (\pi - \gamma)) \tag{17}$$

Since the voltage across a valve is made up of 60 degree intervals of the line-to-line voltage[5], the average dc voltage can be expressed as $V_{do} = \frac{3}{\pi} A_o$, where A_o was previously defined in *Figure* 2.2. Similarly, the voltage drop due to commutation can be expressed as $\Delta V_d = \frac{3}{\pi} \Delta A$, where ΔA was also defined in *Figure* 2.2

Therefore, $$\Delta V_d = \frac{3}{\pi} \frac{\sqrt{3}E_{ln}}{2} (\cos \alpha - \cos (\pi - \gamma))$$

But since, $$V_{do} = \frac{3\sqrt{3}E_{ln}}{\pi} \tag{18}$$

$$\Delta V_d = \frac{V_{do}}{2}(\cos\alpha + \cos\gamma) \tag{19}$$

From Eq. (17) and Eq. (19),

$$\frac{\Delta V_d}{V_{do}} = \frac{I_d}{2I_s} \tag{20}$$

Since $$V_d = V_{do}\cos\alpha - \Delta V_d \tag{21}$$

From Eqs. (20) and (21),

$$V_d = V_{do}\left(\cos\alpha - \frac{I_d}{2I_s}\right)$$

From Eqs. (16) and (18)

$$V_d = V_{do}\cos\alpha - \frac{3}{\pi}X_c I_d \tag{22}$$

From Eqs. (21) and (22),

$$\frac{3\sqrt{3}E_{ln}}{2\pi}(\cos\alpha + \cos\gamma) = \frac{3}{\pi}X_c I_d \tag{23}$$

A calculation of E_{ln} from (23) gives the minimum 3 phase ac voltage before commutation failure. The following example of a calculation of the minimum 3 phase ac voltage before commutation failure is based on the Manitoba Bipole 1 HVdc transmission system

Given:
- V_{dcr} = 463.5 kV (rectifier dc voltage)
- R_{line} = 13.88 ohms (dc line resistance)
- I_{dc} = 1800 amps (dc current)
- X_c = 10.20 ohms (commutating reactance)
- γ = 18.0° (inverter steady-state extinction angle)
- γ_o = 8.0° (deionization time of the valves)

The dc voltage at the inverter is given by:

$$V_{dci} = V_{dcr} - R_{line} * I_{dc}$$

Therefore, $V_{dci} = 463.5 \times 10^3 - (13.88)(1800)$

$= 438{,}516$ Volts

Also, $$\frac{V_{dci}}{3} = V_{do} \cos \gamma - \frac{3X_c I_d}{\pi}$$

Therefore, $$146{,}172 = V_{do} \cos (18) - \frac{(3)(10.20)(1800)}{\pi}$$

Solving for V_{do} $V_{do} = 172{,}129.11$ Volts

Substituting into the following dc equation, and solving for β,

$$\frac{V_{dci}}{3} = V_{do} \cos \beta + \frac{3X_c I_d}{\pi}$$

$\beta = 41.64°$

Therefore, $\alpha = 180.00° - \beta$

$= 180.00° - 41.64°$

$= 138.36°$

From Eq.(18), $E_{ln} = 104{,}069.22$ Volts

Substituting into Eq. (23),

$$\frac{3\sqrt{3}E_{ln}}{2\pi} [\cos (138.36) + \cos (8)] = \frac{3}{\pi} (10.20)(1800)$$

$E_{ln} = 87{,}267.86$ Volts

$$= \frac{87267.86}{104069.22} (100) = 83.86 \text{ \% of the original voltage.}$$

This value represents the lowest three phase voltage allowable before a commutation failure will occur, assuming that the direct current remains constant. This result is therefore optimistic since a drop in commutating voltage will result in an increase in the direct current through the valve, thereby

increasing the angle of overlap. A commutation failure could therefore occur at and above the calculated value, dependent on the rate of rise of direct current.

Waveform Analysis

To demonstrate the waveforms and short circuit across a bridge resulting from a commutation failure, a commutation failure was simulated using the Electomagnetic Transient DC simulation program (EMTDC). Three valve groups per pole were modelled with a full bipole model. The direct current was set at 0.4pu. The waveforms shown in *Figure 2.9* for this discussion are for one of the valve groups that failed commutation (valve group 21). The sinusoidal phase voltages on the converter side of the transformer were calculated and plotted with the positive and negative dc voltage of the valve group with respect to a fictitious neutral point of the transformer. As well, the current through each valve was plotted on a separate graph.

The commutation failure was initiated with a decrease in the commutating voltage of phase 'a' by 20%. An infinite bus ac representation was used to negate any consequential effects on the other two ac phases. The disturbance persisted for 1 cycle.

This simulation demonstrates the voltage and current waveforms associated with a commutation failure.

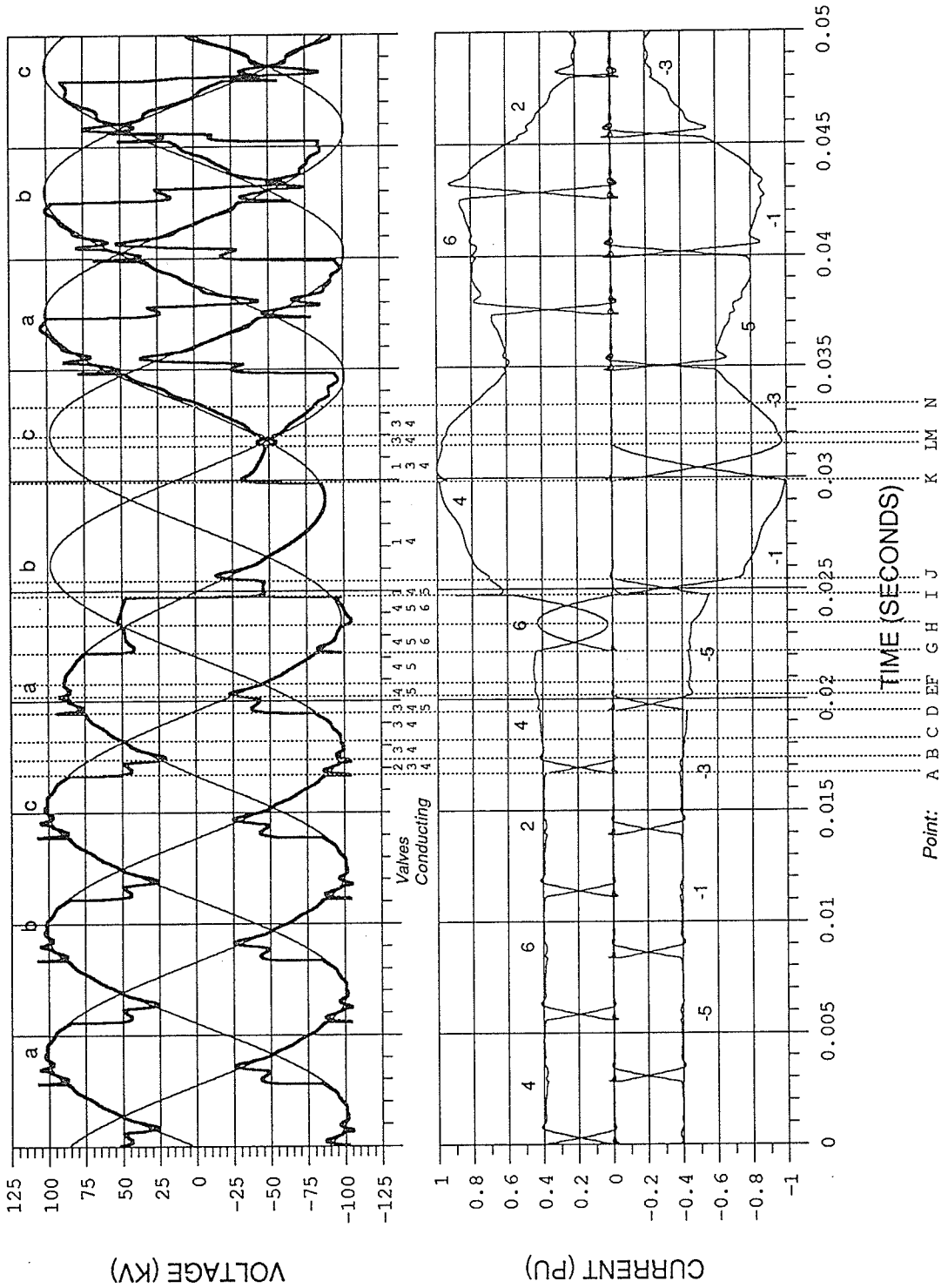

Figure 2.9 - Waveform analysis.

Point	Time (seconds)	Description
A	0.01667	The phase 'a' commutating bus voltage is decreased to 80% for 1 cycle, which corresponds to the following voltages on the converter side of the transformer. $V_a = 0.8667, 0°$. $V_b = 0.9684, -116.58°$. $V_c = 0.9684, 116.58°$. Coincidentally, normal commutation begins from Valve 2 to Valve 4. Valves 2,3,&4 are conducting: 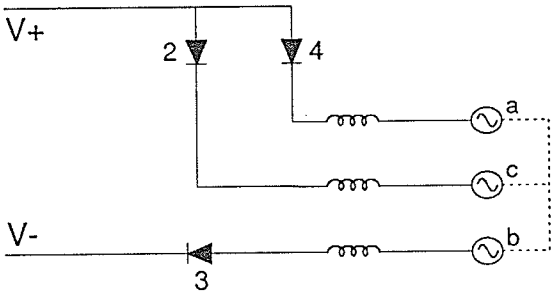 $V- = Vb$ $V+ = \frac{Va + Vc}{2}$ The angle of overlap is 12.52°.
B	0.01725	Commutation from Valve 2 to Valve 4 is complete. It is interesting to see the effect the disturbance has on the extinction angle γ, now at 20.3°. The voltage depression of phase 'a' has caused an increase in the extinction angle, while the phase shift in phase 'c' from 120° has decreased the extinction angle - with the net effect of a 2.3° increase in γ.
C	0.01819	Since the extinction angle is greater than the deionization time of the valve (in this case the deionization time is modelled at 0°), successful commutation from Valve 2 to Valve 4 is complete.

D	0.01944	Normal commutation begins from valve 3 to valve 5. Valves 3,4,&5 are conducting: 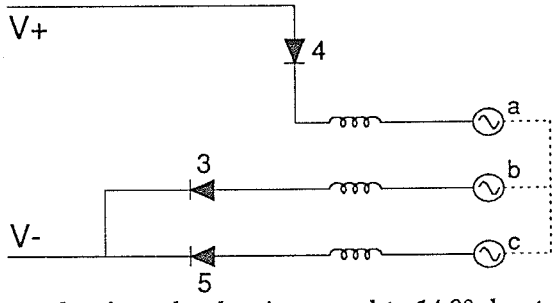 $V+ = Va$ $V- = \frac{Vb + Vc}{2}$ The angle of overlap has increased to 14.9° due to an increase in the direct current from the drop in commutating voltage.
E	0.02015	Commutation from valve 3 to valve 5 is complete. The extinction angle has decreased to 13.49° due to the phase shift in the phase 'c' voltage.
F	0.02075	Since the extinction angle is greater than the deionization time of the valve (0°), successful commutation from Valve 3 to Valve 5 is complete.
G	0.02220	Valves 4,5,&6 are conducting: 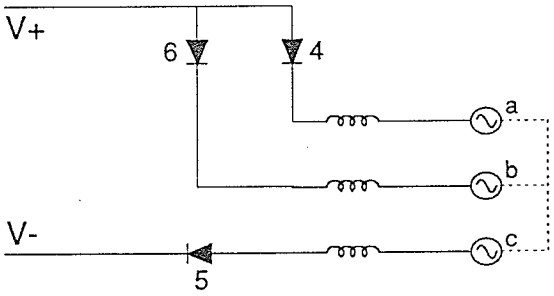 $V- = Vc$ $V+ = \frac{Va + Vb}{2}$ The angle of overlap is 25.7°.
H	0.02339	The commutating voltage (V_a - V_b) reverses before commutation is complete. This denotes a failure of commutation, and reverse transfer of current begins.

I	0.02474	At the same time that valve 4 fails commutation to valve 6, valve 1 is fired and commutation from 5 to 1 begins. Valves 1,4,5 are conducting: 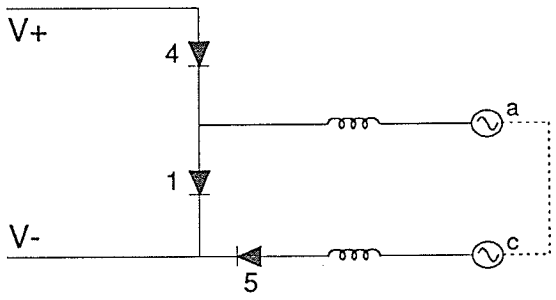 $V- = V+ = \frac{Va + Vc}{2}$ The dc voltage is short circuited causing the voltage across the valve group to be zero.
J	0.02549	Commutation from valve 5 to valve 1 is complete. Now only valves 1 and 4 are conducting. 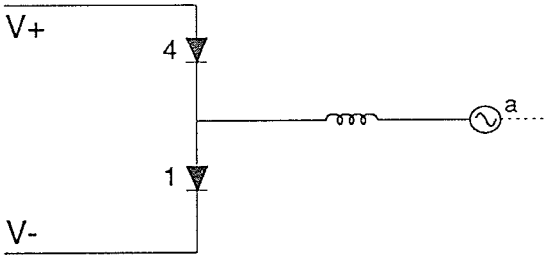 $V- = V+ = Va$ The angle of overlap is 14.9°, and the voltage across the valve group remains zero.

K	0.02990	Commutation begins from valve 1 to valve 3. Notice the increased current through the valve. This is due to the firing angle advance as well as the pole voltage decreasing to zero (because all of the valve groups in the pole coincidentally fail commutation as well). Valves 1,3,&4 are conducting: 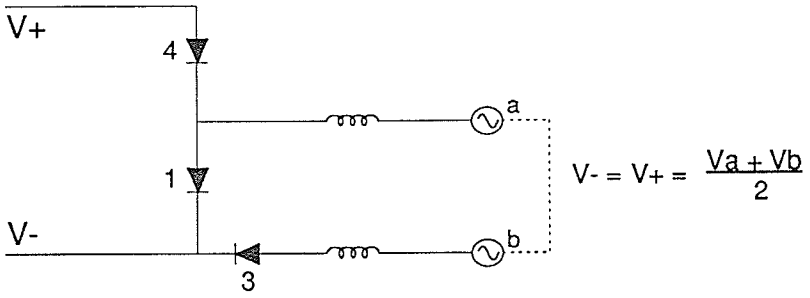 Due to the higher current through the valve, the angle of overlap has increased significantly (35°). Successful commutation is only possible in this case because the deionization time after the current has completed commutation is modelled at 0°.
L	0.03149	Commutation is completed between valves 1 and 3, therefore, only valves 3 and 4 are now conducting: 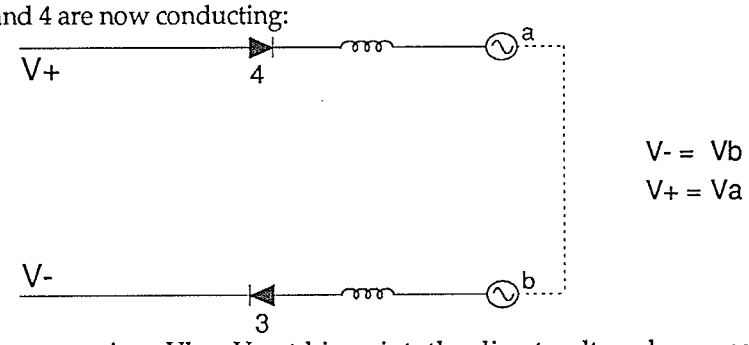 However, since Vb > Va at his point, the direct voltage becomes negative until point M is reached.
M	0.03198	The direct voltage becomes positive again since Vb<Va.
N	0.03333	The voltage depression on phase 'a' is cleared. The resulting phase voltages on the primary side of the transformer are now: $V_a = 1.0, 0°$ $V_b = 1.0, -120°$. $V_c = 1.0, 120°$.

>N	>0.03333	Once the fault has been removed, there are no more commutation failures. The effect of the phase advance control can be seen from the positive and negative valve group dc voltage. As well, the current starts to decrease once the pole voltage starts recovering from the short circuit due to the commutation failures.

Conclusions

In this chapter, commutation failures were analyzed in detail for several ac system disturbances. The concept of commutation area was also introduced, with a theoretical calculation of the lowest three phase voltage depression before commutation failure for the Manitoba Hydro Bipole 1 HVdc transmission system. Finally, a detailed waveform analysis of the valve voltage and current during a commutation failure illustrated the short circuit across the bridge, and the corresponding increase in current.

Control Strategies

Introduction

This chapter reviews general control strategies for an HVdc transmission scheme, with specific references to the Manitoba Hydro Bipole 1 HVdc transmission system. Commutation failure alpha advance circuits are then analyzed for predictive and non-predictive control strategies. The detection of commutation failures, and a zero sequence detection scheme are also introduced.

Control Characteristics

The steady-state rectifier and inverter control characteristics of DC voltage and current are shown in *Figure 3.1*. The intersection of the two characteristics *(Figure 3.1, point A)* represents the voltage and current operating point, defined here as the receiving end of the dc line.

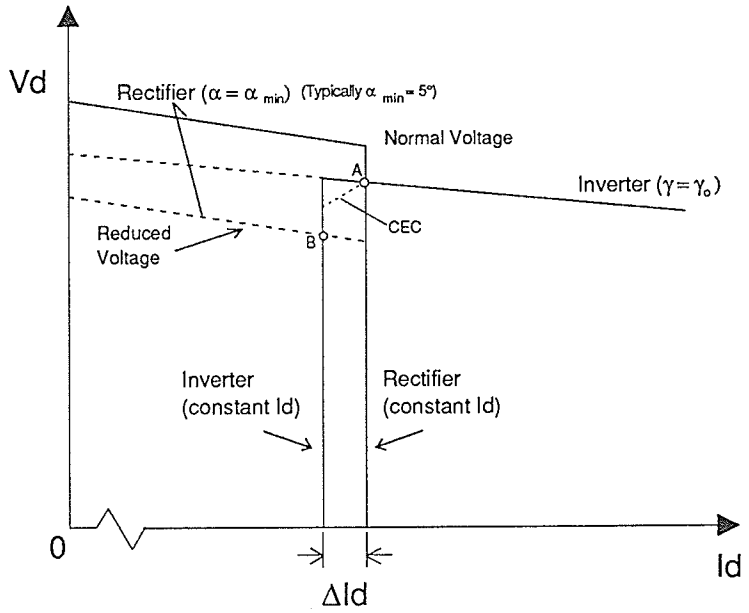

Figure 3.1 - Steady state rectifier and inverter characteristics.

The rectifier is normally operated as a constant current regulator, whereas the inverter is normally operated as a constant extinction angle (CEA) regulator. The

inverter is actually equipped with a current regulator as well, but the setpoint is lower than that of the rectifier's current regulator. The difference between the current setpoints at the rectifier and the inverter is known as the current margin (ΔI_d). The current margin is set at 10% of rated current at Dorsey Converter Station. On the occurrence of a large rectifier voltage reduction, the constant firing angle characteristic of the rectifier will shift downward, crossing the inverter constant current characteristic *(Figure 3.1, point B)*. In this case, the inverter will be controlling the direct current with the rectifier at α_{min} transiently. If the current margin did not exist, the rectifier characteristic would be unable to intersect the inverter characteristic, resulting in a current and power reduction to zero.

The rectifier current control characteristic can be shifted horizontally along the x-axis with a current order change. If the measured current is less than the current order, the rectifier will decrease the firing angle in an attempt to increase the rectifier dc voltage, thereby increasing direct current.

The CEA inverter characteristic can be shifted along the y-axis by means of the tap changer on the converter transformer at the inverter station. A change in the tap will cause an increase or decrease in the alternating voltage on the valve side of the transformer. Since the extinction angle is constant, any change in the alternating voltage will directly affect the dc voltage at the inverter, which will change the direct current. However, any change in current will be corrected by the rectifier current regulator.

If the inverter voltage is raised through a tap change the rectifier voltage will also have to be raised to keep the direct current constant. The current regulator at the rectifier can only control α until α_{min} is reached (typically 5°). Therefore, the rectifier will also have to undergo a tap change to raise the voltage. In practice, the rectifier will control the firing angle in the range of 12° to 20° to allow a fast increase in rectifier voltage, while keeping the power factor relatively high. If the ac system at the inverter has a low short circuit ratio (ratio of the short circuit level at the commutating bus to the dc power), then the CEA characteristic at the inverter will have a more negative slope. In this case, a condition can exist where there are two possible operating points, leading to

hunting between these points. To remove this possibility, the extinction angle reference can be increased in proportion to the current error. This is called Current Error Control (CEC). As well, a voltage dependent current order limit has been represented to reduce the stress on the inverter valves in the case of a severe commutation failure involving a complete short circuit of the pole. Current limits are also included at low voltage. These modifications are illustrated in *Figure 3.2*.

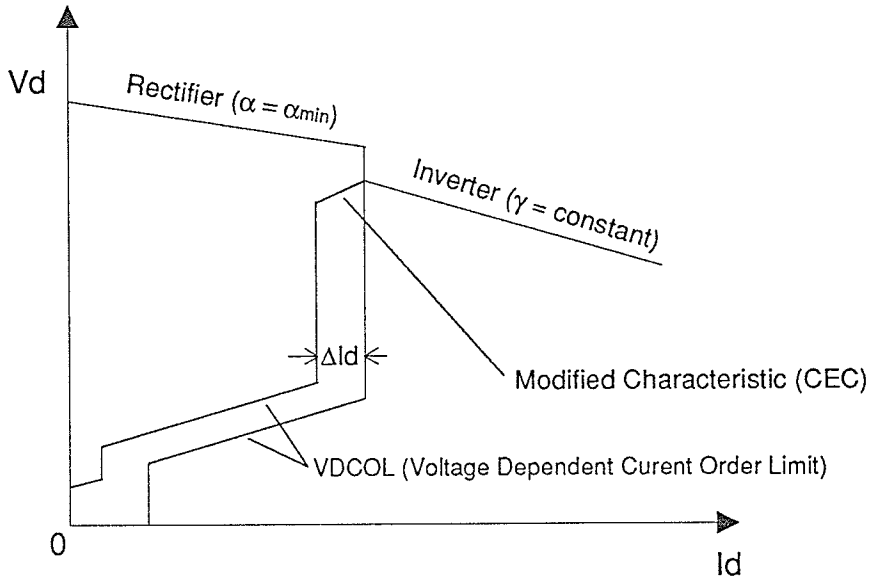

Figure 3.2 - Modified steady state characteristic.

If a commutation failure occurs, the controls should act to increase the extinction angle of the valve failing commutation. This, of course, will not affect the commutation of the failed valve, but it can reduce the likelihood of subsequent failures. If the initial commutation failure is a result of low ac voltage, then the reappearance of normal operating voltage should help to eliminate further commutation failures as well. However, due to the first commutation failure, the inverter dc voltage will be reduced in proportion to the number of valve groups that failed commutation, since the failure will result in a short circuit across the failing valve. This voltage reduction will in turn cause the direct current to increase. The current order will also increase with a decrease in inverter dc voltage, since the current order is defined as the power order divided

by the measured dc voltage for a typical constant power control. To solve this problem, the current order is limited to 10% above the rated current.

Once a commutation failure occurs, the extinction angle is increased by one of two methods: use of a a predictive circuit , or use of a a closed loop control method using the measured extinction angle. In either case, by increasing γ, the inverter dc voltage will be reduced further, where the amount of voltage decrease will depend on the magnitude of the angle advance and any control limits.

There seems to be a contradiction with an extinction angle advance strategy upon the detection of a commutation failure. Since there has been a commutation failure, the extinction angle was obviously too low to allow enough commutation area to complete commutation. It therefore seems logical to increase the extinction angle to prevent further commutation failures, however by increasing γ, the inverter dc voltage is further reduced - increasing the dc current further. An increase in the direct current will in turn increase the commutation area required for successful commutation. The keys to this control strategy are the dc smoothing reactor and the rectifier current controller. Since the rate of increase in direct current will be limited to a rate dependent on the value of the smoothing reactor, the direct current increase can, in effect, transiently be held down while the control circuits advance the extinction angle.

The rectifier current control will also limit the increase in direct current by increasing its firing angle. At the time of a commutation failure, the rectifier still has the old current order because of a 20 msec telecom delay (Manitoba Hydro). As well, since the current order signal is relatively slow, the rectifier will increase α to control the increase in direct current. The combination of the dc smoothing reactor and the rectifier current controller decreases the reaction of the extinction angle advance to any rise in direct current.

In addition, CEA controllers utilize the lowest measured extinction angle historically occurring over the last cycle (6 commutations for a 6 pulse valve group, and 12 commutations for a 12 pulse valve group). This control method

helps to avoid successive commutation failures from phase shifts or voltage distortions in the commutating bus voltage.

Once the disturbance causing the commutation failure has been removed, the extinction angle will be controlled back to its original steady-state value.

Non-Predictive γ – Control

Non-predictive control of the extinction angle must increase γ based on the worst steady-state operating condition that could occur when a commutation failure occurs. This worst condition would be at full power, since the actual commutation area would be the largest in this case. However, the firing angle phase advance must not be too large since increases in gamma will cause a decrease in the power factor, which in turn can cause higher reactive power consumption at the converter bus. This in turn would decrease the line-to-line ac voltage increasing the angle of overlap further, which would cause more commutation failures by decreasing the extinction angle below the deionization time required by the valve. Therefore, it is important to increase γ to a predetermined level based mostly on the strength of the ac system being supplied by the inverter. At Dorsey Converter Station, there are gamma advance circuits (gamma-kick) at the pole and the valve group level. Upon the detection of a commutation failure, a large advance in γ is delivered to the valve that failed, while a smaller and slower advance is delivered to the rest of the valve groups in the pole.

As well, combined with a higher var consumption at the converter bus due to an alpha advance control, there can also be a rejection of reactive power from any failing groups. This must also be considered in the design of the gamma-kick circuits.

Dorsey Bipole 1 Pole-Kick

The Dorsey pole-kick block diagram is shown in *Figure 3.3*. Each valve group in the pole contributes to the pole kick depending when each valve group fails. A single commutation failure of one valve group will result in a kick directly to the current controller of the pole *(Figure 3.4)*.

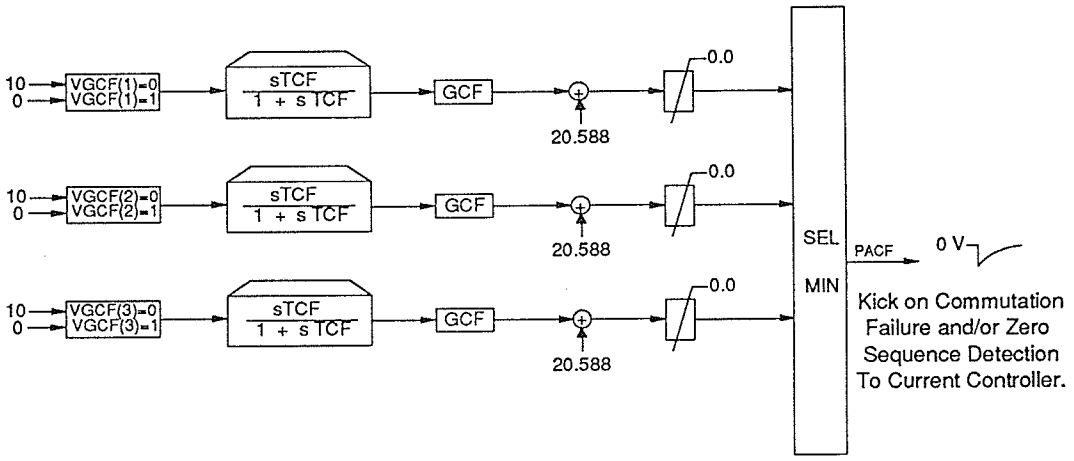

Figure 3.3 - Dorsey pole-kick block diagram (© Manitoba Hydro).

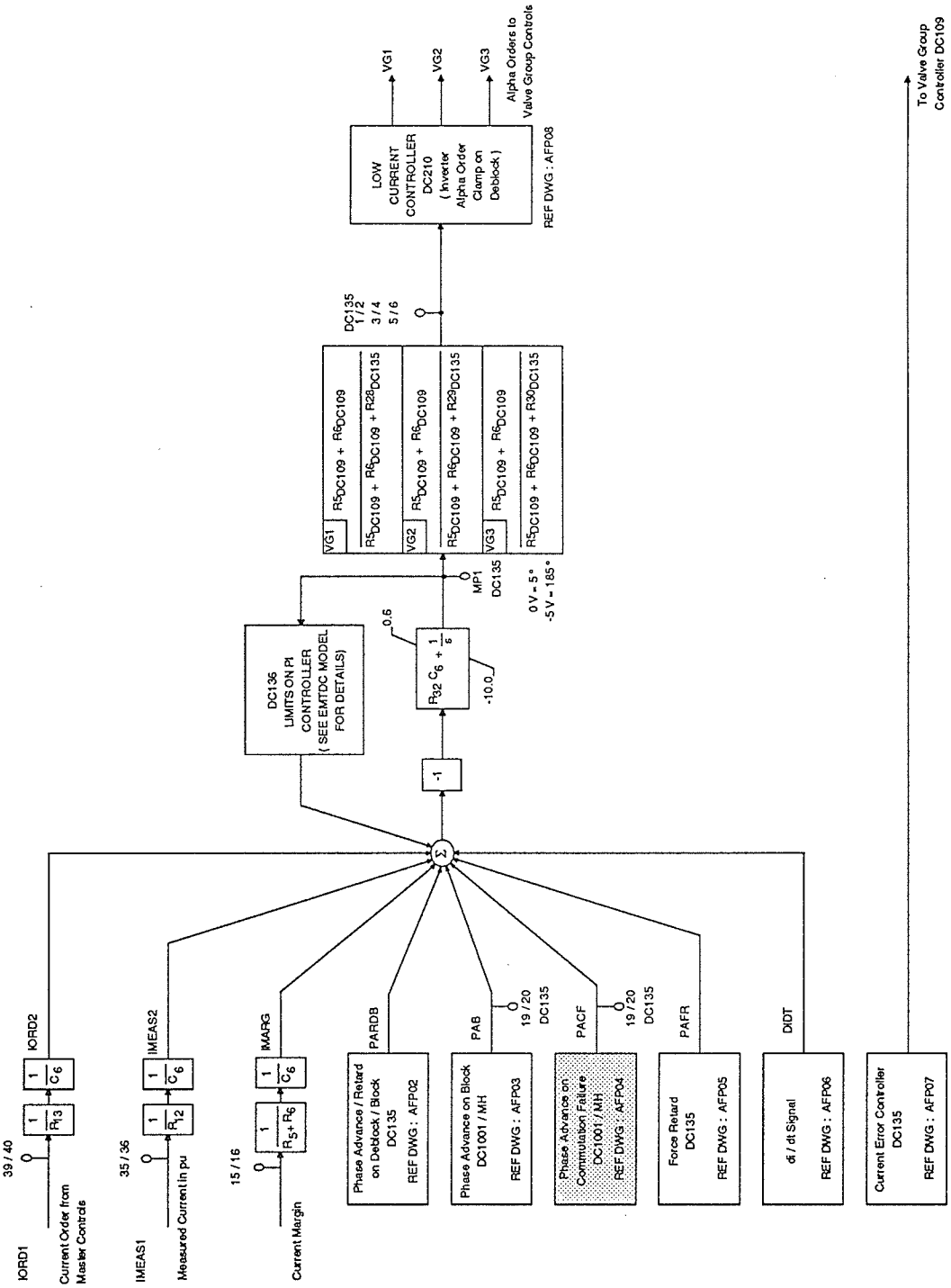

Figure 3.4 - Dorsey pole controller (© Manitoba Hydro).

If the commutation failure ends before the pole kick has reached zero, the kick automatically resets to zero. In the same way, if one valve group has failed commutation and a second valve group starts failing commutation during the pole kick, the kick will be reissued to the current controller. The kicks do not add together, rather, the largest kick is chosen to advance to the current controller. The kick that is issued to the current controller upon detection of a single valve group failing commutation is shown in *Figure 3.5*

The pole kick is issued directly to the current controller, which issues α orders to the valve group controllers. *Figure 3.6* shows the block diagram of the valve group controls. In this diagram, the pole-kick directly affects the AORD (α_{order}) signal to the valve group.

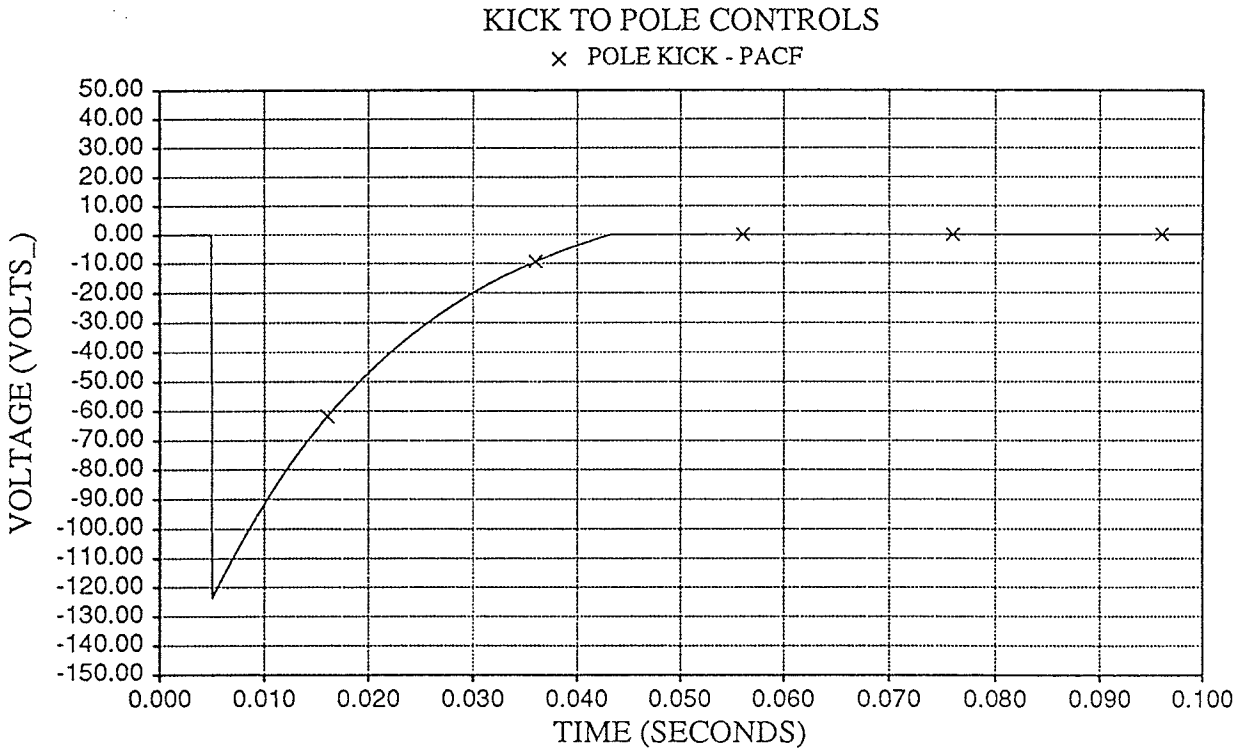

Figure 3.5 - The pole kick that is issued to the current controller upon detection of a single valve group failing commutation.

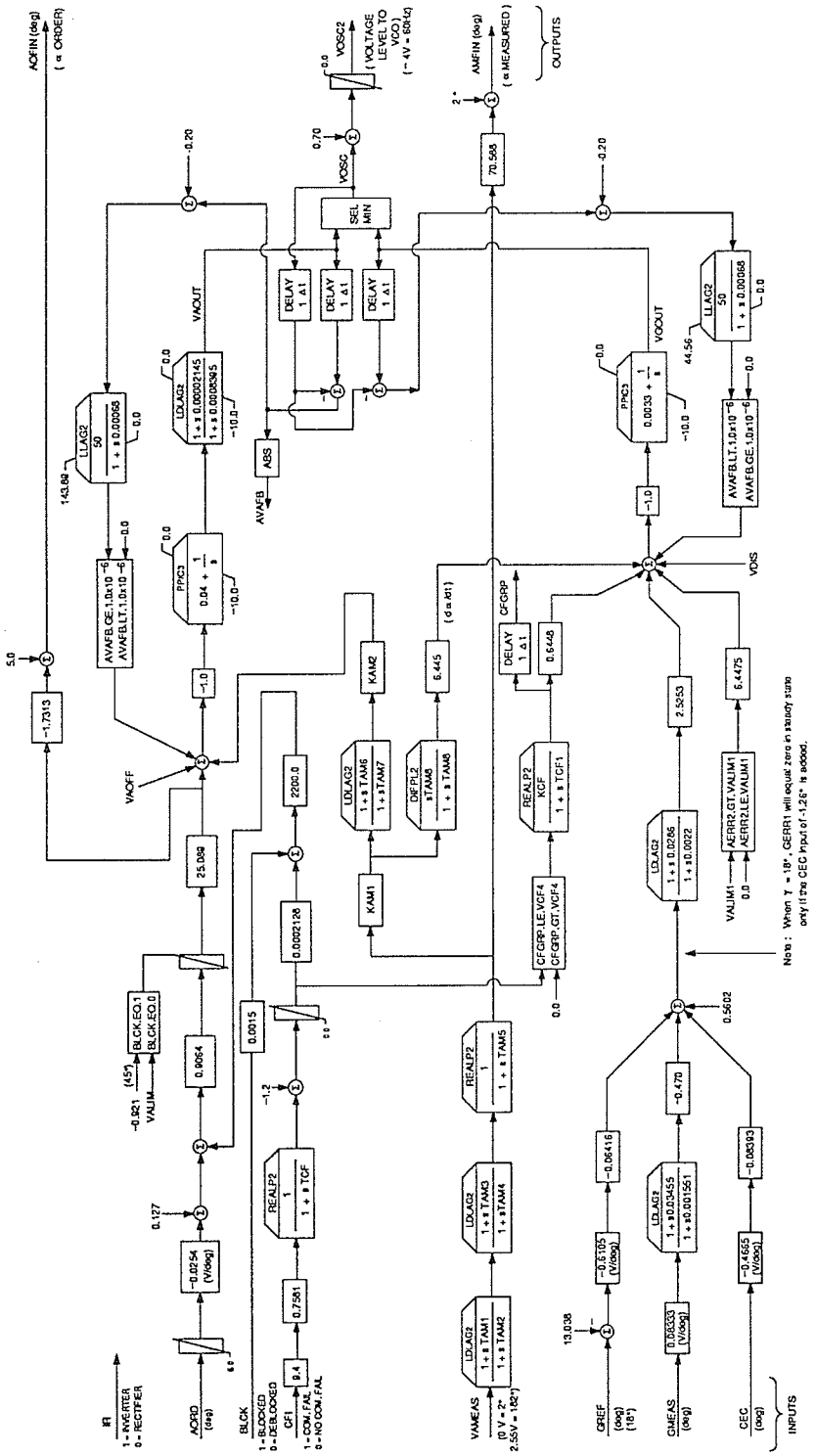

Figure 3.6 - Dorsey valve group controller (© Manitoba Hydro).

The valve group control issues a voltage to a voltage controlled oscillator, which in turn determines the firing angle of the valve. To determine the oscillator voltage, there are two control loops in the valve group controls. There is the α response loop, and the γ response loop, where the minimum value is chosen as the oscillator voltage.

At the inverter, under steady-state operation, the γ loop is usually in control. This is known as constant extinction angle control, where a $\gamma_{reference}$ is compared to a $\gamma_{measured}$, producing an error signal through a PI controller to the voltage controlled oscillator. Both loops, however, contain a feedback signal from the respective oscillator voltage levels biasing the two loops (α and γ) very close to one another. In the event of a commutation failure, the pole kick affects the α loop by the change in the α order. The α loop takes control at the inverter, decreasing the voltage to the oscillator, thereby decreasing α. This response is shown in *Figure 3.7*.

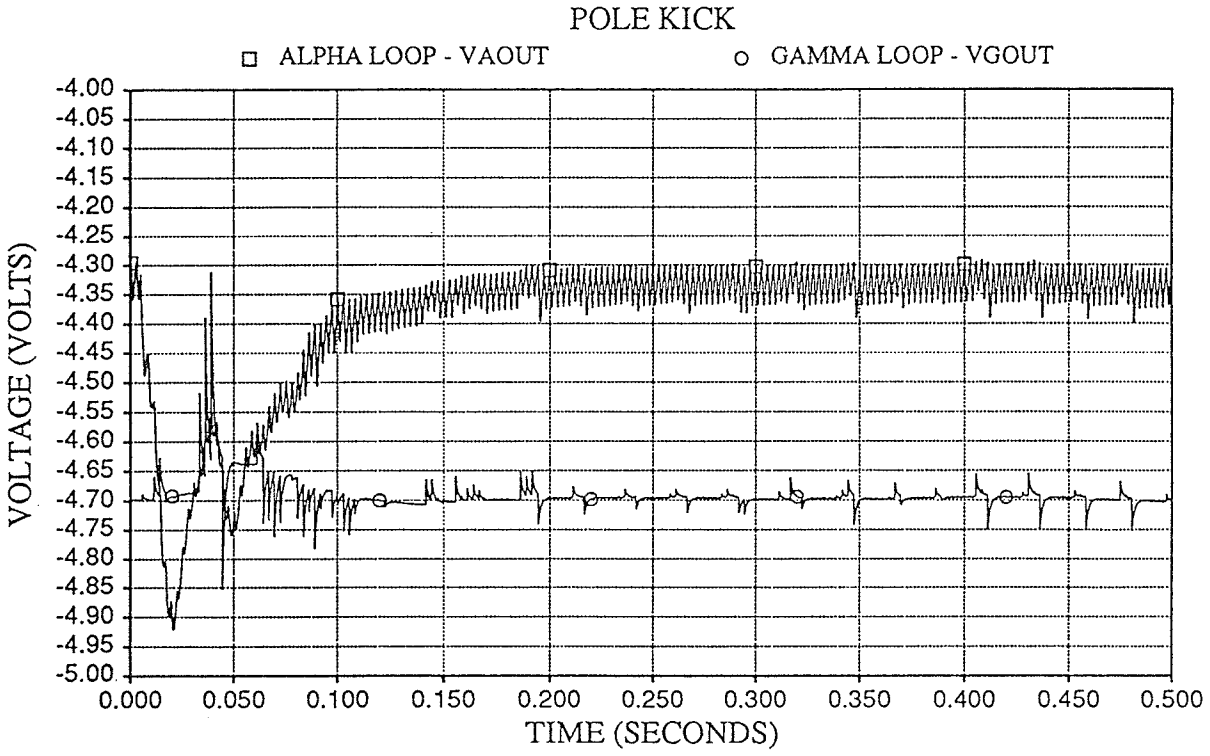

Figure 3.7 - α and γ loop response to a pole kick at Dorsey.

The actual effect this pole-kick has on the extinction angle at the inverter is shown in *Figure 3.8*. This was the response to an individual kick from a single simulated commutation failure.

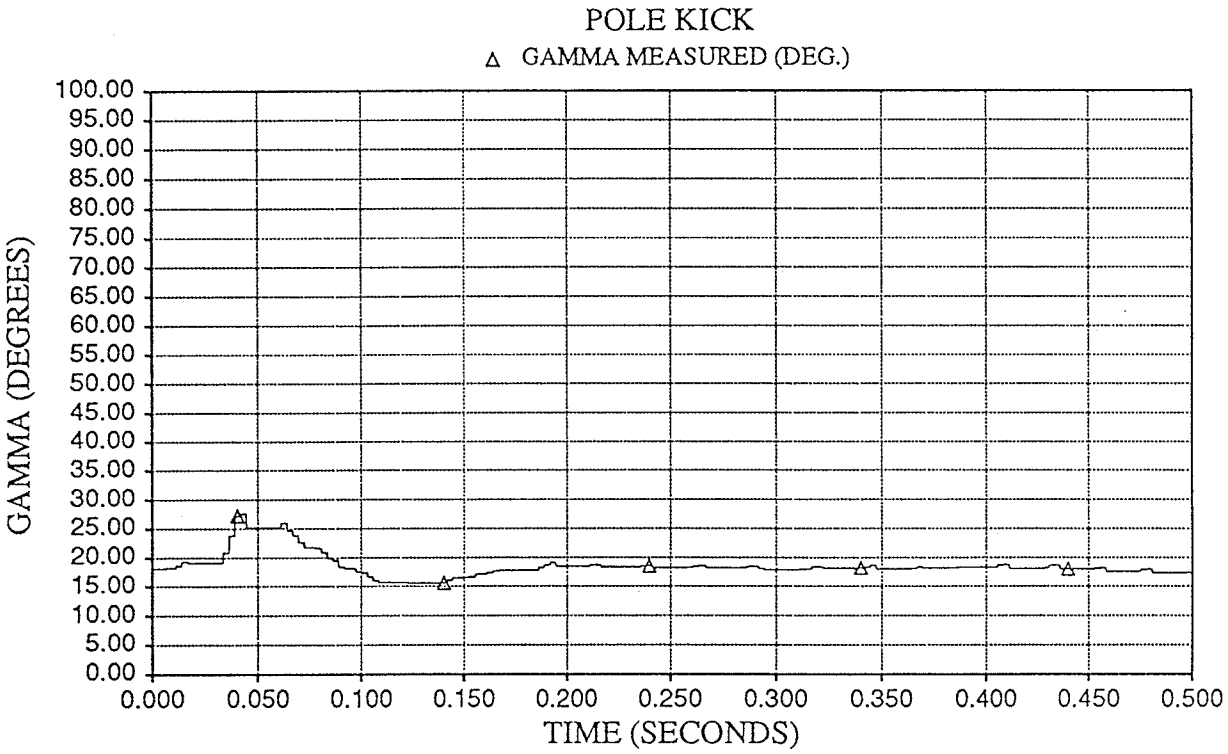

Figure 3.8 - Extinction angle response to a pole-kick.

Although it is true that further kicks will not add to the original kick, additional kicks at varying time intervals may produce a larger α advance because of the integral action from the P-I circuit in the pole controller. The α_{order} will remain lower for a longer time, which will allow the α response loop to affect the oscillator voltage for a longer time, in effect giving the extinction angle more time to change.

Dorsey Bipole 1 Valve Group Kick

The Bipole 1 valve group controller, upon the detection of a commutation failure, affects both the α response loop as well as the γ response loop in the valve group controls. A 100 msec commutation failure was simulated by setting the commutation failure indicator high. This allowed the controller to react as if a commutation failure occurred without initially reacting to any change in direct current or voltage. A 100 msec duration was chosen to emphasize the action of the controller. The simulated commutation failure resulted in the α and γ loop responses shown in *Figure 3.9*.

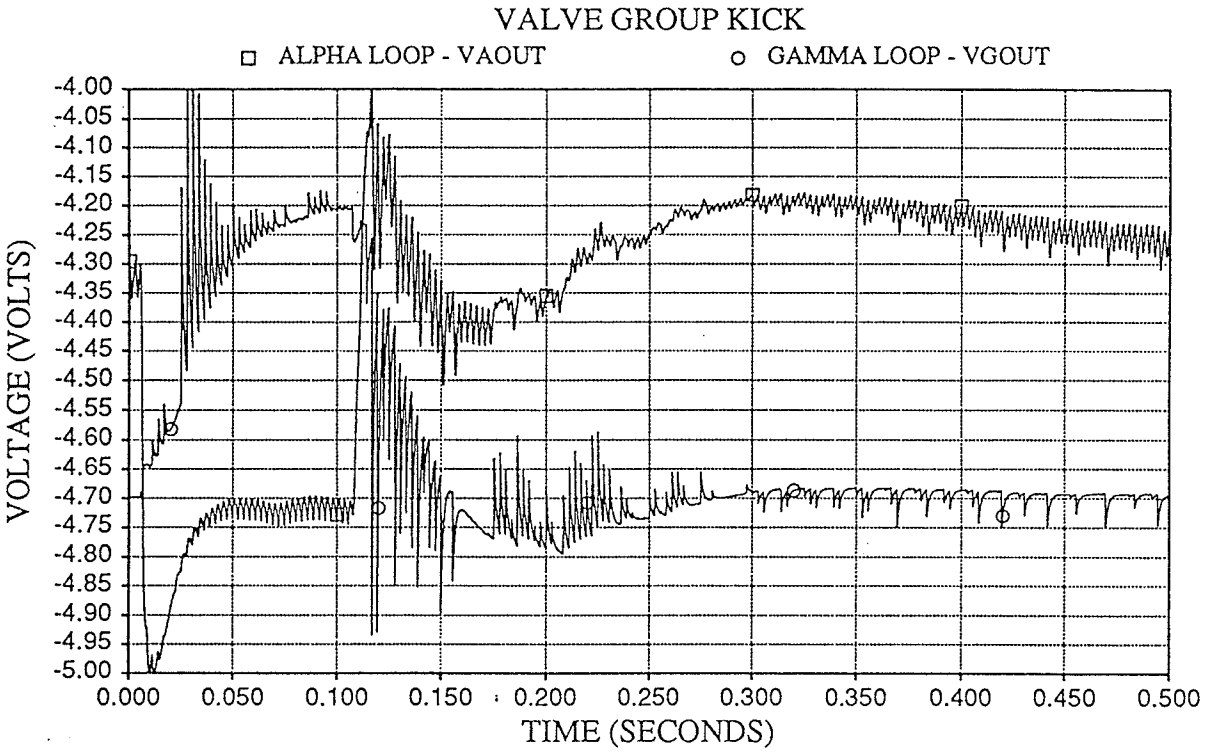

Figure 3.9 - α and γ loop responses to a valve group-kick.

In this case, compared to the pole kick, the response is much faster with the α loop taking control very quickly. The α_{order} and $\alpha_{measured}$ traces in *Figure 3.10* show that the α_{order} is immediately pinned to the minimum limit of 110°.

With the valve group kick, however, the α response loop as well as the γ response loop are affected. The signal to the voltage controlled oscillator will be the minimum of the α and γ response signals. The faster α response loop is almost immediately brought into control when the γ response loop is quickly increased, while the α response loop is decreased. Once the simulated commutation failure ends, the γ loop effectively provides the controls with a $\gamma_{reference}$ change to 38°, whose value decays with a large time constant *(Figure 3.11)*. This change in the extinction angle reference will aid system recovery from commutation failures, especially at a weak inverter.

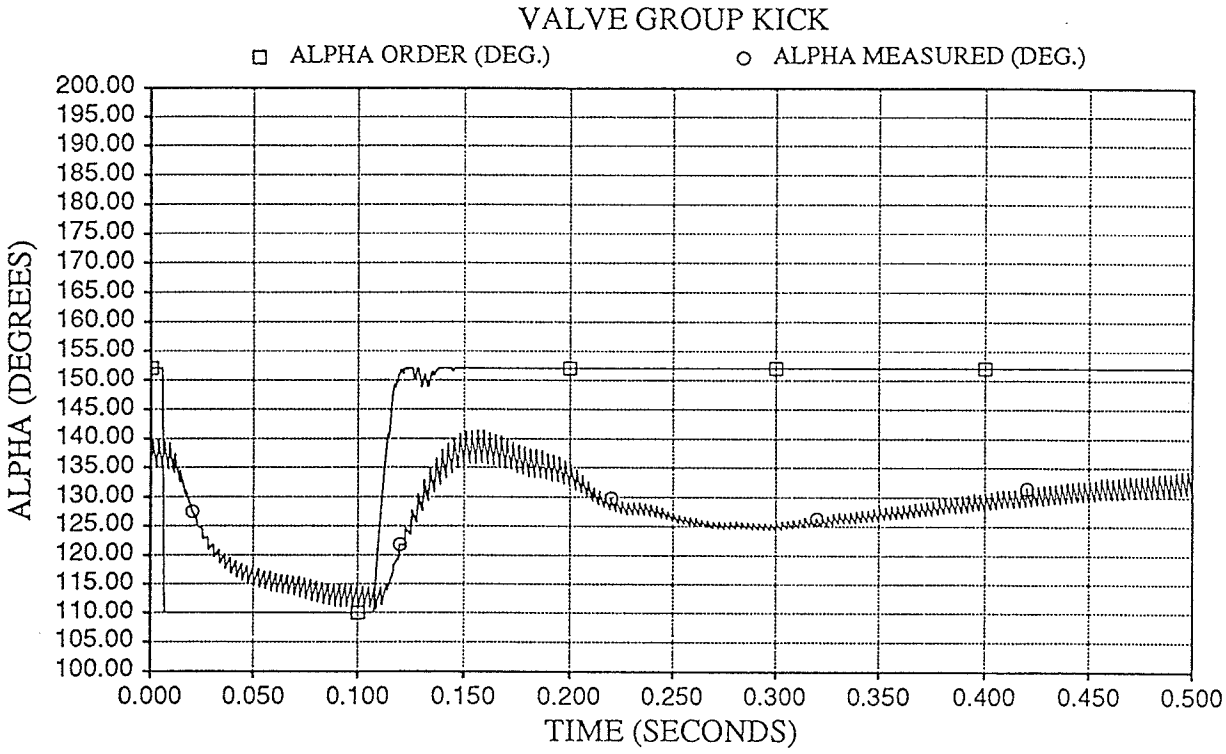

Figure 3.10 - α_{order} and $\alpha_{measured}$ response to a valve group-kick.

It is worthwhile noting the response of the extinction angle in *Figure 3.11*, which increases to approximately 55° while there is a simulated commutation failure. Just after 100 msec the commutation failure indicator is reset and the controller decreases the extinction angle rapidly to approximately 9° - barely avoiding

another commutation failure. The controller then increases the extinction angle to 38° where it is slowly brought back to the reference of 18°.

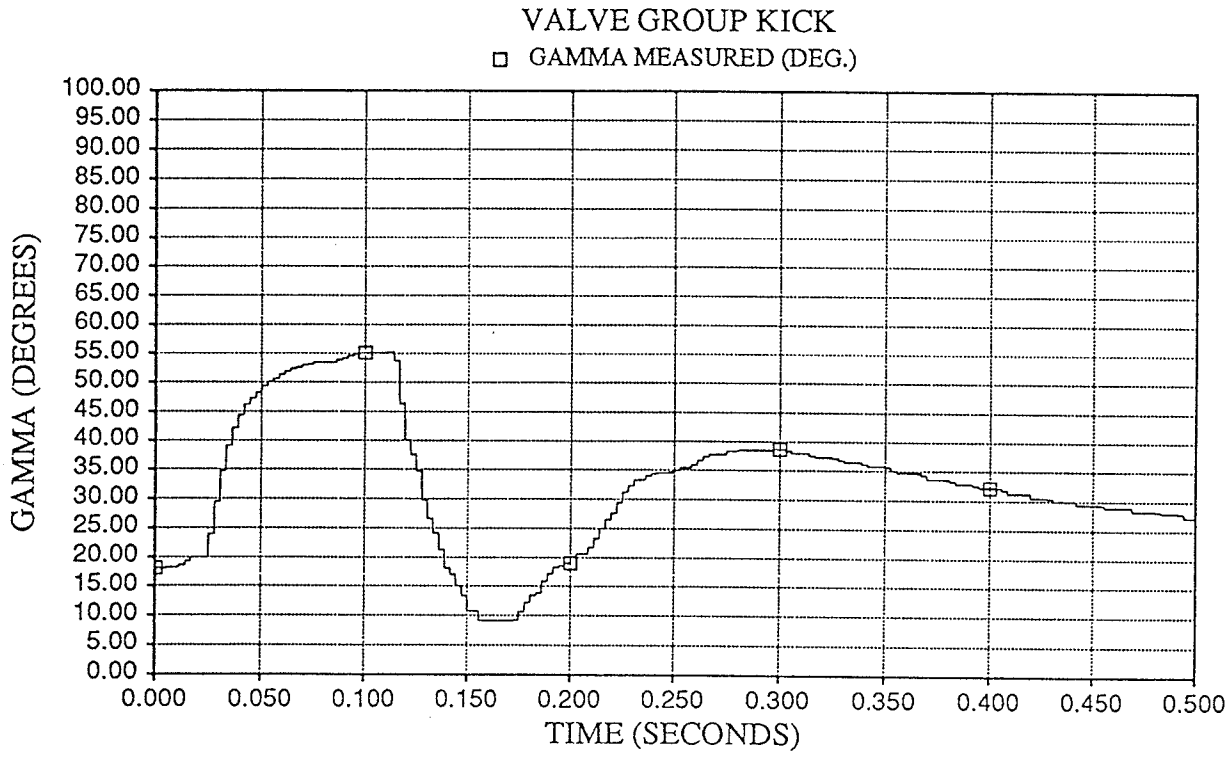

Figure 3.11 - Extinction angle response to the Dorsey valve group-kick.

Predictive γ – Control

A predictive control calculates the commutation area based on direct current, and the desired area based on a reference line to line commutating voltage on the converter side of the transformer, and compares the sum of these two quantities to a predicted area based on the firing angle and the line to line voltage on the converter side of the transformer. This is demonstrated in the following analysis:

(1) Desired area (Figure 3.12):

Based on the steady-state line-to-line voltage on the converter side of the transformer, and the nominal extinction angle, a reference area can be calculated. This area should not change, since neither nominal γ nor the steady-state line-to-line ac voltage change.

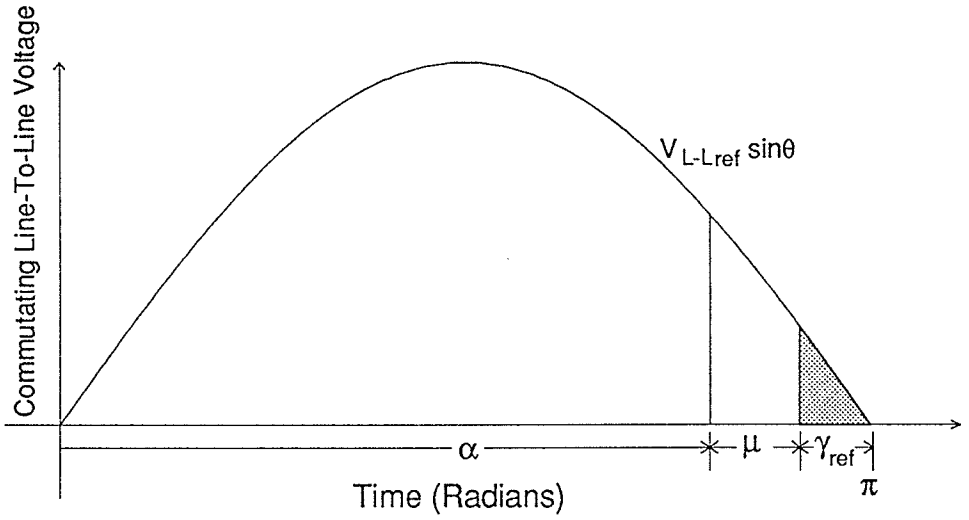

Figure 3.12 - Desired area.

$$\text{Area}_{\text{desired}} = \int_{\pi-\gamma_{ref}}^{\pi} V_{LL\text{-}ref} \sin\theta \, d\theta$$

$$= V_{LL\text{-}ref} \left[-\cos\theta\right]_{\pi-\gamma_{ref}}^{\pi}$$

$$= V_{LL\text{-}ref} \left[-\cos(\pi) + \cos(\pi - \gamma_{ref}) \right]$$

$$= V_{LL\text{-}ref} \left[1 + \cos(\pi - \gamma_{ref}) \right] \qquad (24)$$

(2) Commutation area (Figure 3.13):

Depending on the desired current and the commutating reactance, a commutation area can also be calculated. This area will change as the direct current changes, reflecting an increased angle of overlap. This area was calculated earlier in Eq. (8). It is reproduced now as twice the value calculated earlier simply because a line-to-line voltage representation is used in this analysis, rather than a phase voltage representation that was shown in Chapter 2.

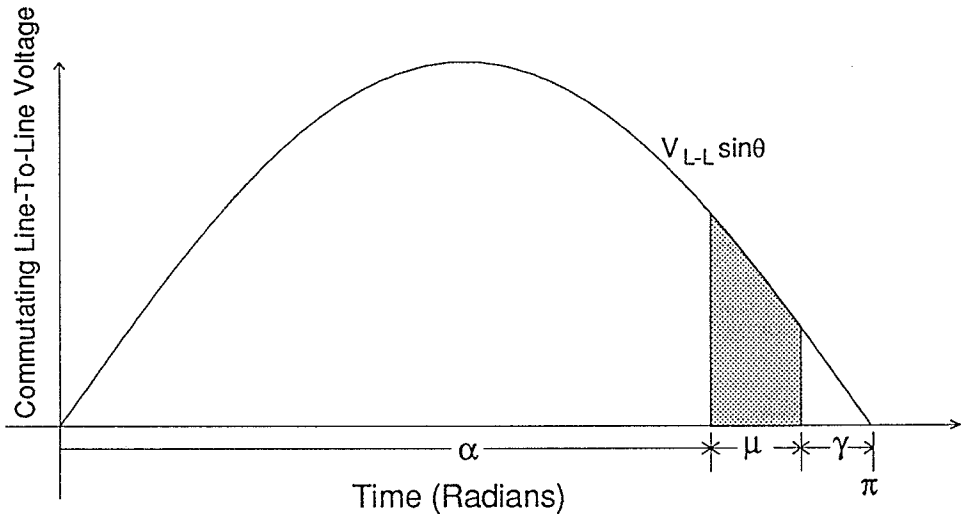

Figure 3.13 - Commutation area.

$$\text{Area}_{\mu} = (2)(R_c)(I_{dc})$$

$$= (2)\left(\frac{3}{\pi}\right)(X_c)(I_{dc})$$

$$= \frac{6}{\pi} X_c I_{dc} \qquad (25)$$

(3) Predicted area (Figure 3.14):

Here, predicted area includes both the desired area as well as the commutation area. Based strictly on the firing angle and line-to-line voltage on the converter side of the transformer, an area is calculated that would result from the present operating conditions.

$$\text{Area}_{\text{pred}} = \int_{\alpha}^{\pi} V_{LL} \sin\theta \, d\theta$$

$$= V_{LL} [-\cos\theta]_{\alpha}^{\pi}$$

$$= V_{LL} [\, -\cos(\pi) + \cos(\alpha)]$$

$$= V_{LL} [\, 1+\cos(\alpha)] \qquad (26)$$

The predictive control strategy uses all three calculated areas to determine the largest firing angle at the inverter that will allow successful commutation.

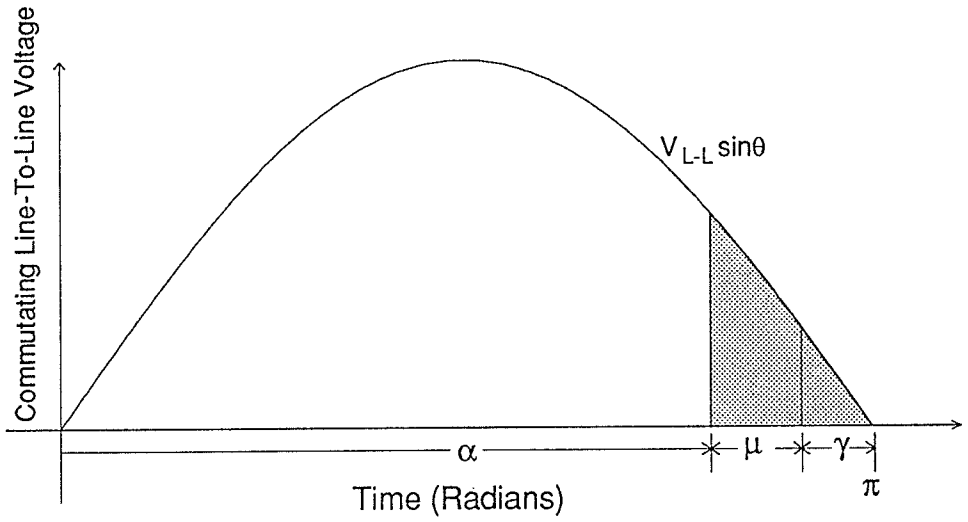

Figure 3.14 - Predicted area.

Predicted area = Desired area + Commutation area

$$\text{Area}_{pred} = \text{Area}_{desired} + \text{Area}_{\mu}$$

$$V_{LL}\,[\,1+\cos(\alpha)] = \text{Area}_{\gamma} + \frac{6}{\pi} X_c I_{dc}$$

Solving for α,

$$\alpha = \cos^{-1}\left(\frac{\text{Area}_{\gamma} + \frac{6}{\pi} X_c I_{dc}}{V_{LL}} - 1\right) \tag{27}$$

Where, $\text{Area}_{\gamma} = V_{LL\text{-}ref}\,[\,1 + \cos(\pi - \gamma_{ref})]$

The block diagram of this predictive control is shown in *Figure 3.15*.

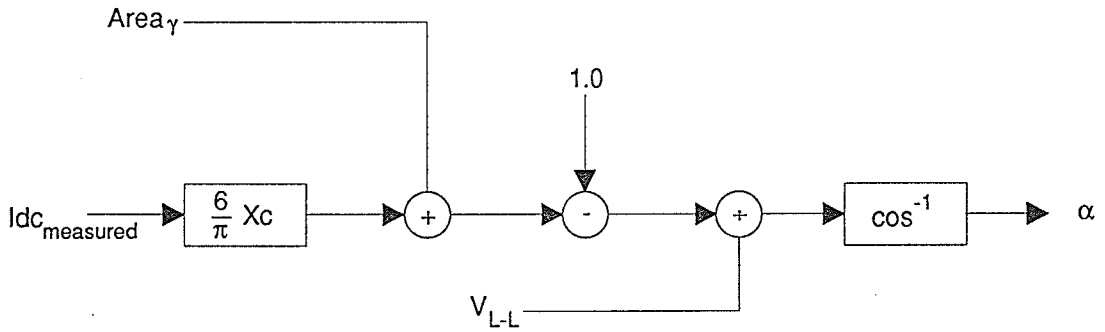

where: $\text{Area}_{\gamma} = V_{L\text{-}L\,ref}\,[1+\cos(\pi - \gamma_{ref})]$

$V_{L\text{-}L}$ = line to line voltage on the converter side of the transformer

Figure 3.15 - Block diagram of a predictive controller.

Commutation Failure Detection

There are a number of ways to detect a commutation failure. The method described in this section is based on the Dorsey Bipole 1 technique. For Bipole 1, the currents through the valve side windings of the converter transformers are rectified with a three phase bridge, and the result is compared to the measured

direct current. In the event of a commutation failure, a by-pass valve pair occurs, causing the current through the converter transformer to drop to zero. Otherwise, the measured direct current and the converter current should be equal. When $I_{ac} < I_{dc}$ by a specified tolerance, a commutation failure is registered.

Zero Sequence Detection

There are probabilities associated with commutation failure based on the point-on-wave when the disturbance occurs. A disturbance just after the natural commutation point would have a higher probability of commutation failure, while a disturbance just before the natural commutation point would have a lower probability. The overall probability will depend greatly on the severity of the disturbance. It is therefore important to act quickly to prevent the presently conducting valve from failing commutation or, if this is not possible, to prevent subsequent failures. Rather than try to react after a commutation failure occurs, the zero sequence voltage can be monitored at the commutating bus and controls can start advancing the firing angle before the actual commutation failure occurs. Since the control will be acting before a commutation failure occurs, the problems associated with rise in current due to a short circuit across a valve group will not be evident initially.

For any fault except a 3 phase fault there will be a zero sequence voltage due to the imbalance between phases. This voltage can be measured at the neutral point of the grounded Y winding of the converter transformer on the ac side. Zero sequence voltage is defined as the instantaneous sum of the three phase voltages in a three phase system. A three phase fault will have no zero sequence voltage because all three phases retain their balanced relationship during this disturbance. A three phase fault, however, has the lowest probability of occurring as well as the lowest probability of causing a commutation failure. Also, zero sequence detection will only apply to commutation failures occurring from ac system disturbances which do not appear on the secondary of a Δ or an ungrounded Y winding transformer. As well, dc side disturbances will not be detected with a zero sequence detection scheme. It is difficult to predict how

much advance warning a zero sequence detector will provide. The performance will depend on the severity of the disturbance, when the disturbance occurred, detection time, and which phase(s) were affected.

A flow chart of the zero sequence detection scheme studied in later sections is shown in *Figure 3.16*

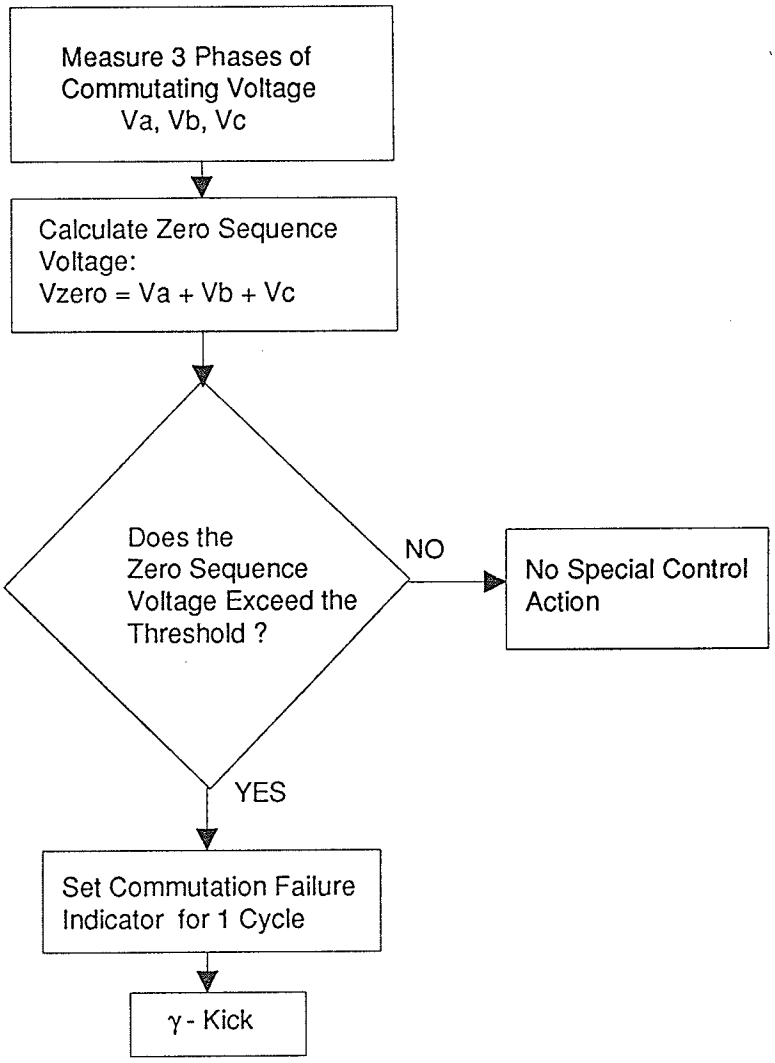

Figure 3.16 - Flow chart of a zero sequence detection scheme.

Conclusions

This chapter initially reviewed HVdc control strategies, and developed these ideas as they relate to alpha advance controls in the event of a commutation failure. A detailed analysis of the Manitoba Hydro advance circuits was also included, highlighting the difference between predictive and non-predictive controls. As well, a zero sequence detection scheme was introduced as an alternative to the more common commutation failure detection strategies. This zero sequence detection scheme will be analyzed in more detail in Chapter 4.

Computer Study

Introduction

This chapter provides original computer analysis of commutation failures using EMTDC. The dc and ac system models are described in detail, with the emphasis of the chapter on the computer results. The effect of commutating voltage depression, direct current, deionization time, steady-state extinction angle, ac system strength, and a zero sequence detection scheme are all investigated as they affect commutation failures.

DC Representation

EMTDC was used to simulate the response of a dc system to several ac system disturbances. The dc system consisted of a detailed model of the Manitoba Hydro Bipole 1 transmission system, including: three 6-pulse valve groups per pole, a smoothing reactor, sixth and twelfth dc side harmonic filters, and a distributed parameter dc line model. *Figure 4.1* shows the Bipole 1 dc system represented in this study. The model also included detailed representation of the master power controller, pole and valve group controls, but did not include frequency and angle damping controls, or synchronous compensator models.

The Manitoba Hydro Bipole 2 transmission system was simply modelled by a dc source at either end of a transmission line. Therefore, interactions between Bipole 1 and Bipole 2 were not studied, nor were subsequent commutation failures. The Bipole 1 model was chosen to study commutation failures because it allowed a comparison to field results. As well, a detailed model of Bipole 2 was unavailable at the time of this study.

Although Bipole 1 uses mercury arc valves, the physics of operation are analogous to thyristor valves - although mercury-arc valves typically have a longer deionization time. A minimum extinction angle model was developed in order to set the deionization time required before a commutation failure occurred. For a mercury-arc valve, this value is in the order of 5° to 8°, while a

thyristor valve would typically be smaller. If the minimum extinction angle was reached before the reverse voltage was applied across the valve, the valve was refired - simulating a commutation failure. A block diagram of this model is shown in *Figure 4.2*

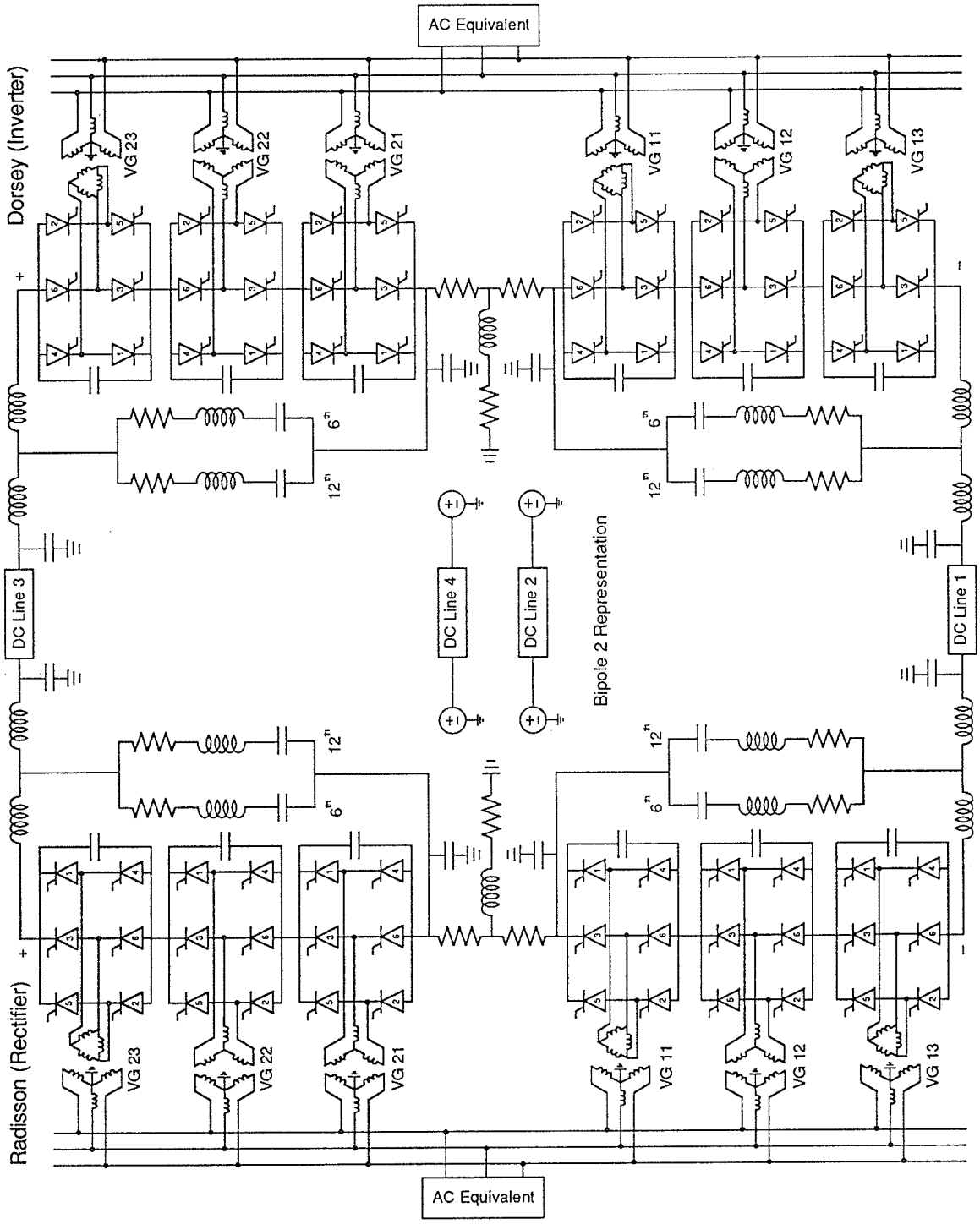

Figure 4.1 - Bipole 1 representation for the computer study.

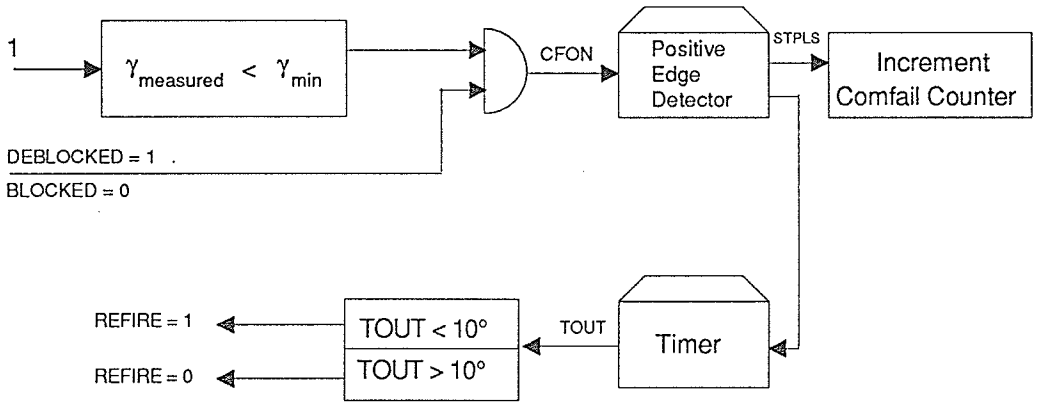

Figure 4.2 - Deionization model.

AC System Representation

HVdc converters produce steady state voltage and current harmonics of the ac supply frequency which appear on both the ac side as well as the dc side of the converters. The ac harmonics are attenuated in the ac system by connecting filters to the commutating bus. At Dorsey, both Bipole 1 and Bipole 2 filters were represented, consisting of the 5^{th}, 7^{th}, 11^{th}, 13^{th}, and high pass harmonic filters. Although the impedance versus frequency characteristic for an ac system is generally complex, at frequencies below the 5^{th} harmonic of the supply frequency the characteristic is typically inductive[6]. Therefore, depending on the system strength, there can be several points of resonance between the ac system and the ac filters. These characteristics will be defined in respective sections for the equivalents defined in this study. The ac system Thevenin equivalent circuit used to represent different ac system strengths is shown in *Figure 4.3*.

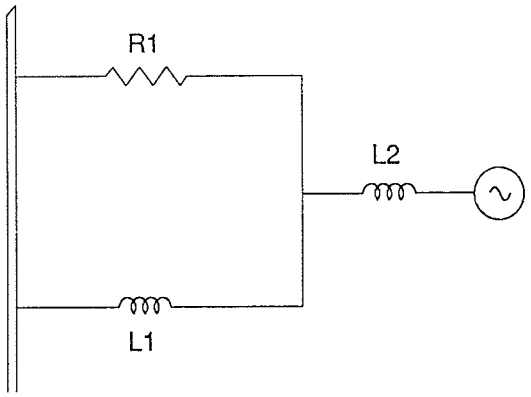

Figure 4.3 - AC equivalent circuit.

The amount of damping represented in the ac equivalent is dependent on the impedance angle chosen to represent the ac system at two specified frequencies. In the ac representation of *Figure 4.3* the impedance angle was defined at fundamental as well as third harmonic frequency to be -80° at the inverter, and

-85° at the rectifier. These values were previously determined to most accurately represent the Dorsey ac system for computer simulations.[7]

Infinite Bus

An infinite bus ac representation was initially used to determine the effect of a drop in ac voltage to the incidence of commutation failures. A voltage drop in only one phase was simulated to determine the effect of a voltage drop during a S-L-G fault on the incidence of commutation failures. This representation will not represent any phase shift or voltage distortions at the commutating bus that can occur with a S-L-G fault.

Thevenin Equivalent circuit

Two separate Thevenin ac equivalents were represented at the inverter (*Figure 4.4)*, providing short circuit ratios (SCR) of 3.0 and 6.0 with a damping angle of –80° at the first and third harmonic. The short circuit ratio is defined as the ratio of the short circuit level at the commutating bus to the dc power. This representation, during a S-L-G fault, would more adequately represent any phase shift, voltage distortion, and voltage depression up to the 5^{th} harmonic of the supply frequency. Beyond the 5^{th} harmonic, the ac supply can no longer be accurately represented as a truly inductive system. Any equivalent representation, however, cannot truly be relied upon to accurately represent an ac system at all times, since a practical ac system may not maintain a linear impedance vs frequency profile[8].

The difference in SCR provides a reference to the strength of the ac system, and its effect on the incidence of commutation failures. The synchronous compensators were not modelled, since the simulations in this study were executed over the first 50 milliseconds after the incidence of a S-L-G fault. The voltage regulation from the synchronous compensators are in the range of 80 - 100 milliseconds so were not required to be modelled in the analysis of the incidence of commutation failures. Studies involving subsequent failures may require the modelling of the synchronous compensators. Since the synchronous compensators connected to the tertiary of the Bipole 1 converter transformers

would normally affect the commutating reactance for this model, the effect of the synchronous compensators were represented in the SCR of the equivalent system. The actual values of commutating reactance is defined at Dorsey in the following table[9], however, this value was kept constant at 10.20 Ω, implying all of the synchronous compensators were in service during any studies performed.

Description	Commutating Reactance (Ω)
Radisson VG	10.831
Henday VG	10.770
Dorsey BP1 VG without SC	11.358
Dorsey BP1 VG with SC	*10.20*
Dorsey BP2 VG	10.280

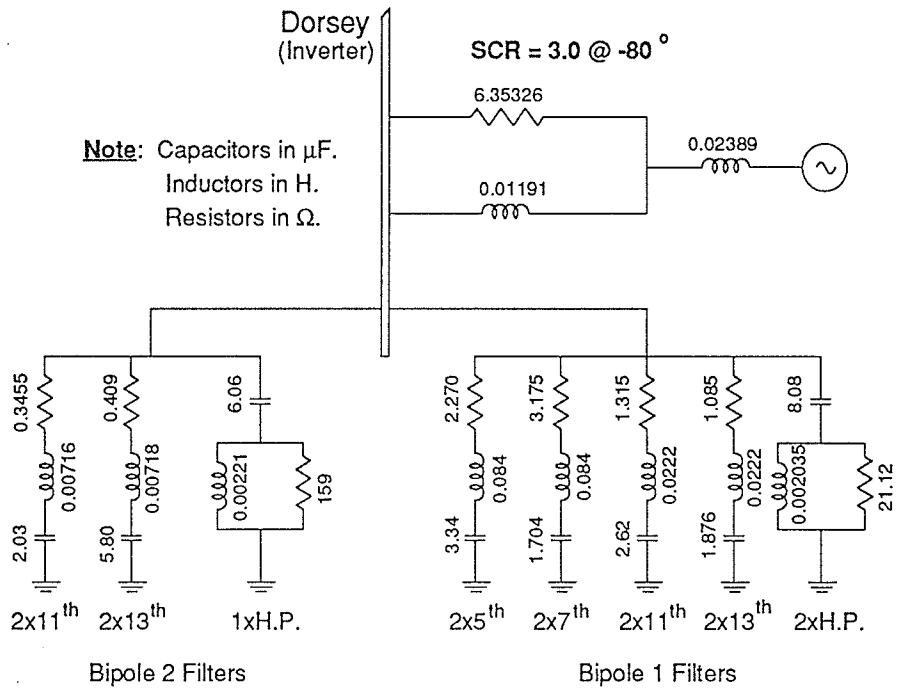

a) SCR = 3.0 : Inverter AC Representation

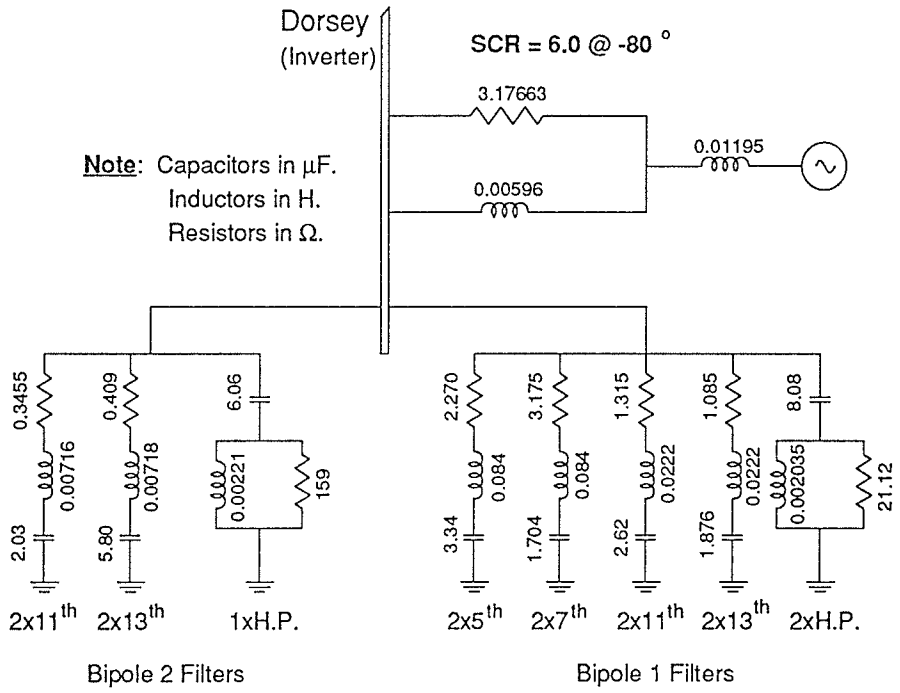

b) SCR = 6.0 : Inverter AC Representation

Figure 4.4 - Inverter AC equivalent circuits.

At the rectifier, the ac equivalent represented an SCR of 3.0 with a damping angle of -85° at the fundamental and third harmonic. This equivalent properly represents the isolated generating units of the northern collector system (*Figure 4.5*). The impedance profile of the ac equivalent is inductive, and where this characteristic crosses the capacitive impedance profile of the filters, a resonance will occur. The overall impedance profile from the converter bus terminal verifies this result and shows the harmonic impedance profile of the bus.

The impedance profiles are included for all of the equivalent circuits used at the inverter as well as the rectifier in *Figures 4.6* and *4.7* respectively.

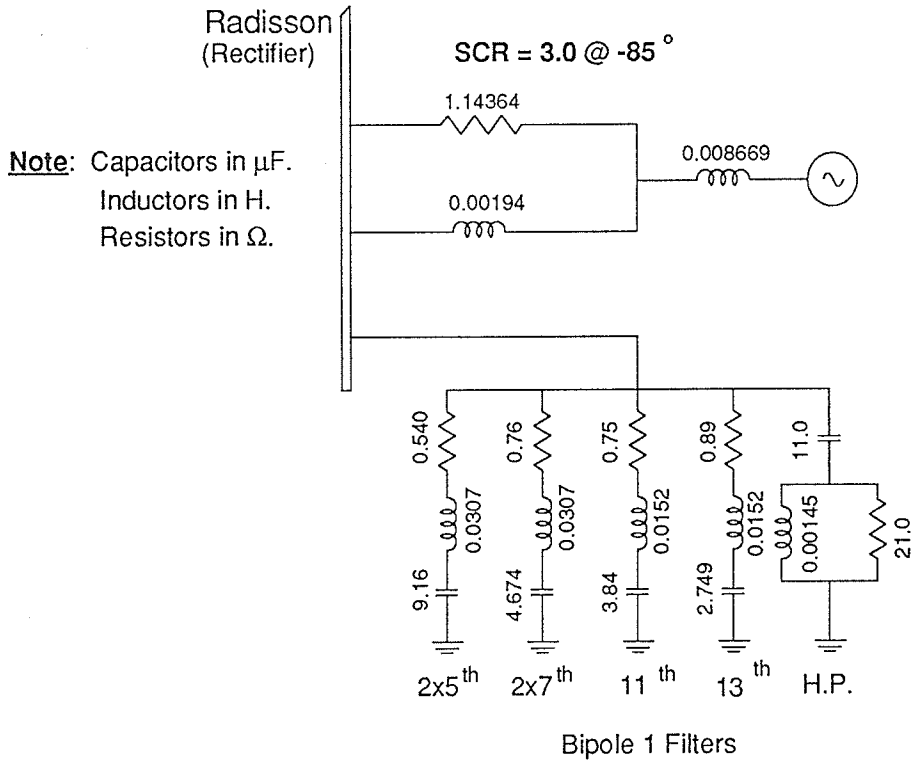

Figure 4.5 - Rectifier AC equivalent circuit.

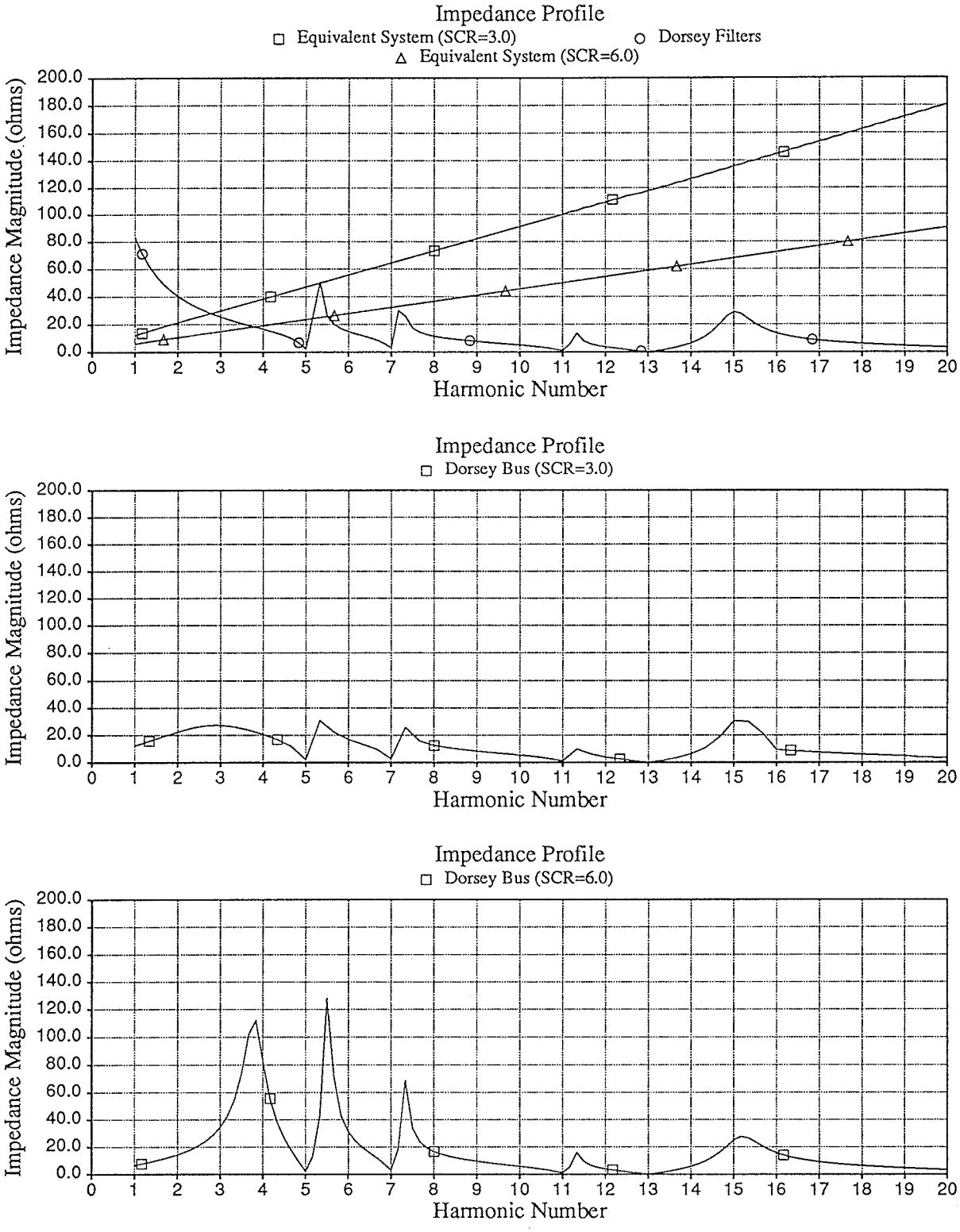

Figure 4.6 - Impedance profiles of the inverter.

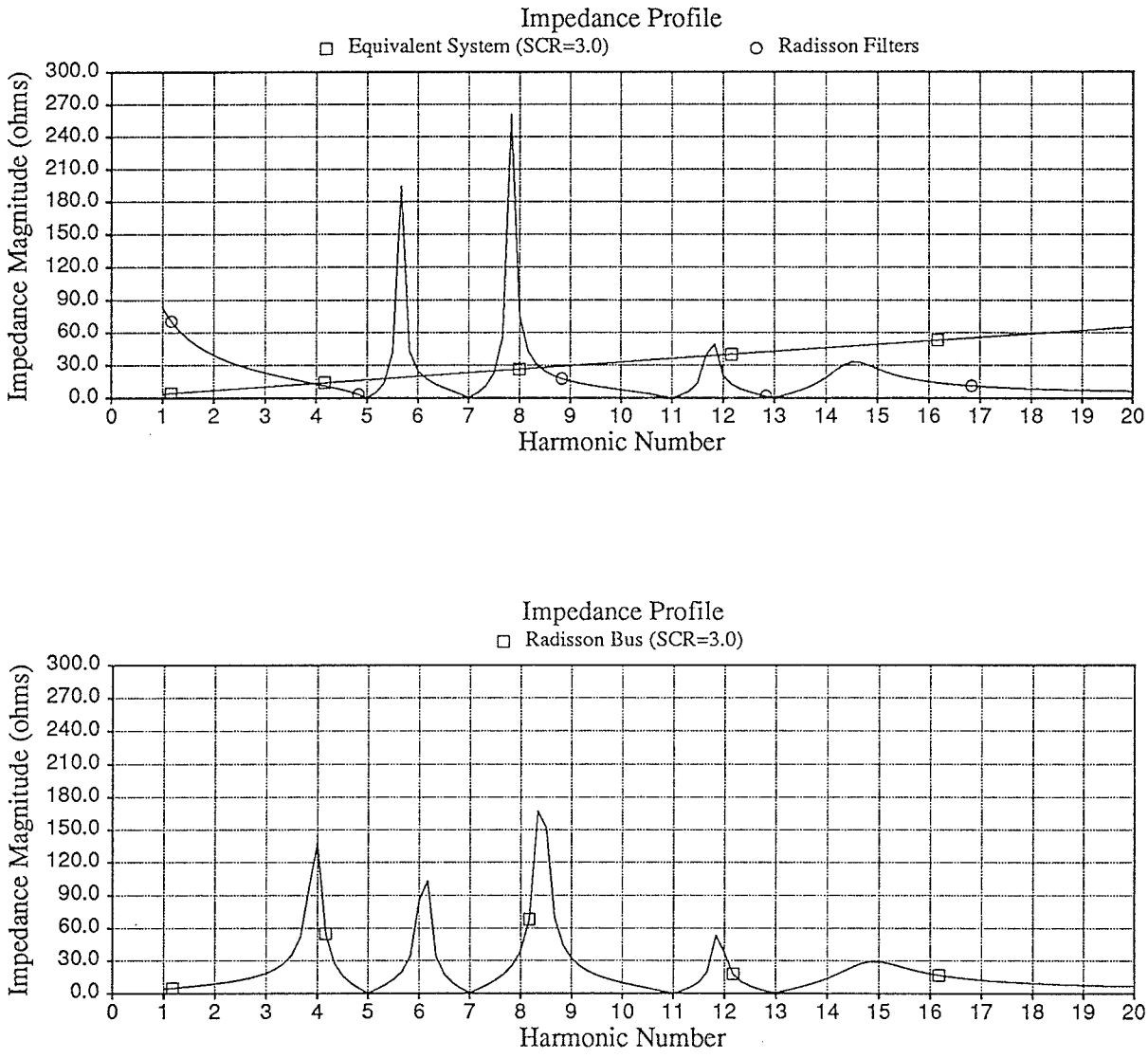

Figure 4.7 - Impedance profiles of the rectifier.

Simulation of a S-L-G Fault

Because the incidence of a commutation failure depends on the point-on-wave that the disturbance occurs, multiple simulations were executed for the same S-L-G fault representation. The time of the incidence of the disturbance was varied randomly over the first cycle of the simulation, however the fault duration was kept constant at one cycle. One hundred simulations were executed with random point-on-wave disturbance times, to provide data for statistical analysis.

The study objectives are summarized below:

- To determine the probability of the incidence of a commutation failure as well as the percentage of valve groups that fail commutation at Dorsey Converter Station for remote S-L-G faults of varying severity, and compare this with field data.
- To determine the effect of voltage depression on the incidence of commutation failures.
- To determine the effect of the minimum extinction angle required to successfully commutate from one valve to another.
- To determine the effect of direct current on the incidence of commutation failures.
- To determine the effect of the phase shift and voltage distortion associated with a S-L-G fault on the incidence of commutation failures.
- To determine the effect of an improved pole-kick based on a zero sequence detection rather than a commutation failure detection.

In all of these cases, the primary interest is in the incidence of commutation failures in each valve, and not in the number of subsequent failures that may occur for each valve. For this reason, as well as to decrease computation time, a one cycle disturbance was used with the start of the disturbance randomly occurring during the first cycle of the run. A good measure of the severity of a S-

L-G fault for comparison to field data is the minimum phase voltage during the fault. This method was used throughout this study to compare statistical results observed for each of the previously outlined objectives. As well, the existing pole and valve group kicks at Dorsey Bipole 1 were modelled throughout this study.

With these kicks and a one cycle fault, a 50 millisecond run time was found to be the minimum time required to observe the incidence of a commutation failure.

The remote S-L-G fault was represented by simply decreasing the voltage of one phase of the ac equivalent source, rather than varying a shunt inductance at the source. This simplification allowed the voltage depression associated with a S-L-G fault to be defined, but may have simplified any harmonic interaction between the ac system impedance and the fault impedance profiles.

Model Validation

Validation of the Bipole 1 EMTDC model was accomplished at Manitoba Hydro through several system tests[10]. The validation results provided in this section are for a single commutation failure introduced by suppressing the firing pulse at the pulse amplifier to valve 5 of valve group 11. The predisturbance dc operation was +450/−150 kV for Bipole 1, with a power order of 450 MW. This indicates that there were three valve groups in service in the positive pole, and only one valve group in service in the negative pole. The system configuration is shown in detail in *Figure 4.8*. The positive pole was modelled with only two valve groups: a Y-Y, and a Y-Δ. The Y-Y valve group was scaled by a factor of two, to properly represent the system configuration. This simplification allowed faster computer execution times, while not jeopardizing the accuracy of the simulation. This simplified model was only used for the model validation tests.

The Bipole 2 dc configuration was modelled by a dc source at each end of the polar transmission line. The actual predisturbance system configuration for Bipole 2 consisted of 1-12 pulse valve group per pole at Henday and Dorsey, with a power order of 350 MW.

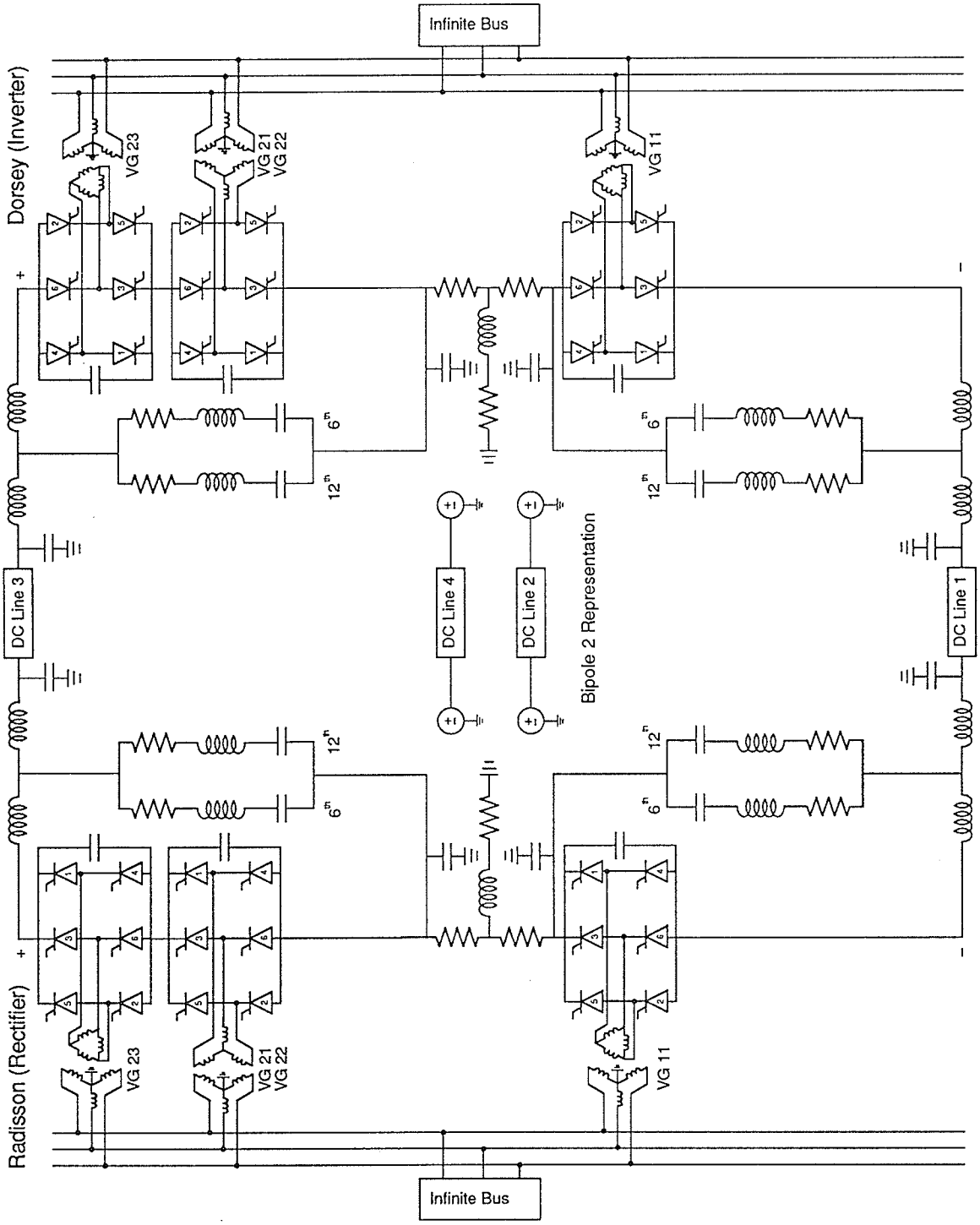

Figure 4.8 - The dc system model used for model validation.

The ac systems at the rectifier and the inverter were modelled with infinite sources, which should be an accurate approximation with the low power order on the Bipole as well as the 5 Bipole 1 synchronous compensators that were in service. As well, there was no need to model the synchronous compensators or the angle damping and frequency damping controls at Dorsey since the commutating bus was modelled with an infinite source.

The dc voltage and line current were plotted for both the computer simulation and the field test results. The field results were digitized and plotted on the same scale as the computer simulation results. These plots can be seen in *Figures 4.9* and *4.10* respectively. As illustrated, the simulation matches the field results very closely.

Effect of Voltage Depression

To determine the sole effect of the voltage depression associated with a single line to ground fault, an infinite bus ac equivalent was placed at the Dorsey commutating bus. This allowed the voltage of one phase to be varied without seeing any phase shift associated with the change in power or from the voltage distortions typically seen from a S-L-G fault. As mentioned, the disturbance was applied for one cycle, with 100 random start times over the first cycle of the simulation. *Figure 4.11* illustrates the effect of the random disturbance start times to the percentage of valve groups that failed commutation. A commutation failure indicator flag was monitored to detect the incidence of a commutation failure for each valve group. Because the EMTDC program models do not take into account the time required before a reverse voltage can be applied across the valve, a valve will only fail commutation if a valve is still commutating when the line to line voltage goes to zero. In reality, approximately 5° to 8° leeway is required between the time that the current completes commutation and the line to line voltage goes to zero. In the tests described in subsequent sections this effect was modelled; however initially it was set to 0°. The results *(Figure 4.12)* show that for a given direct current (in this case I_{dc} = 0.6pu), as one phase voltage decreases, the probability of a commutation failure

increases. As well, an indication of the severity of the disturbance can be seen from a plot of the percentage of valve groups that failed commutation.

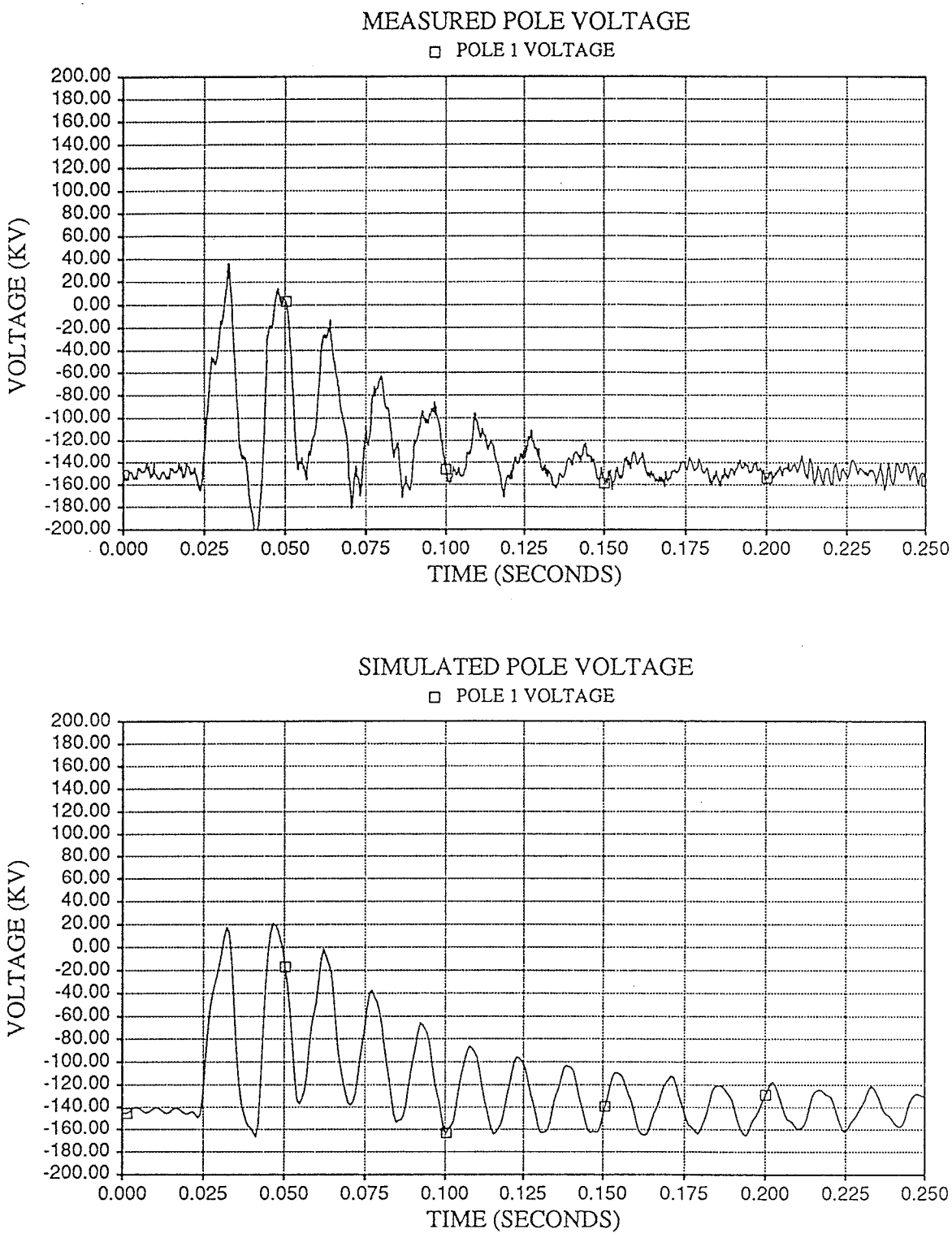

Figure 4.9 - DC voltage comparison between system measurements and model validation simulations.

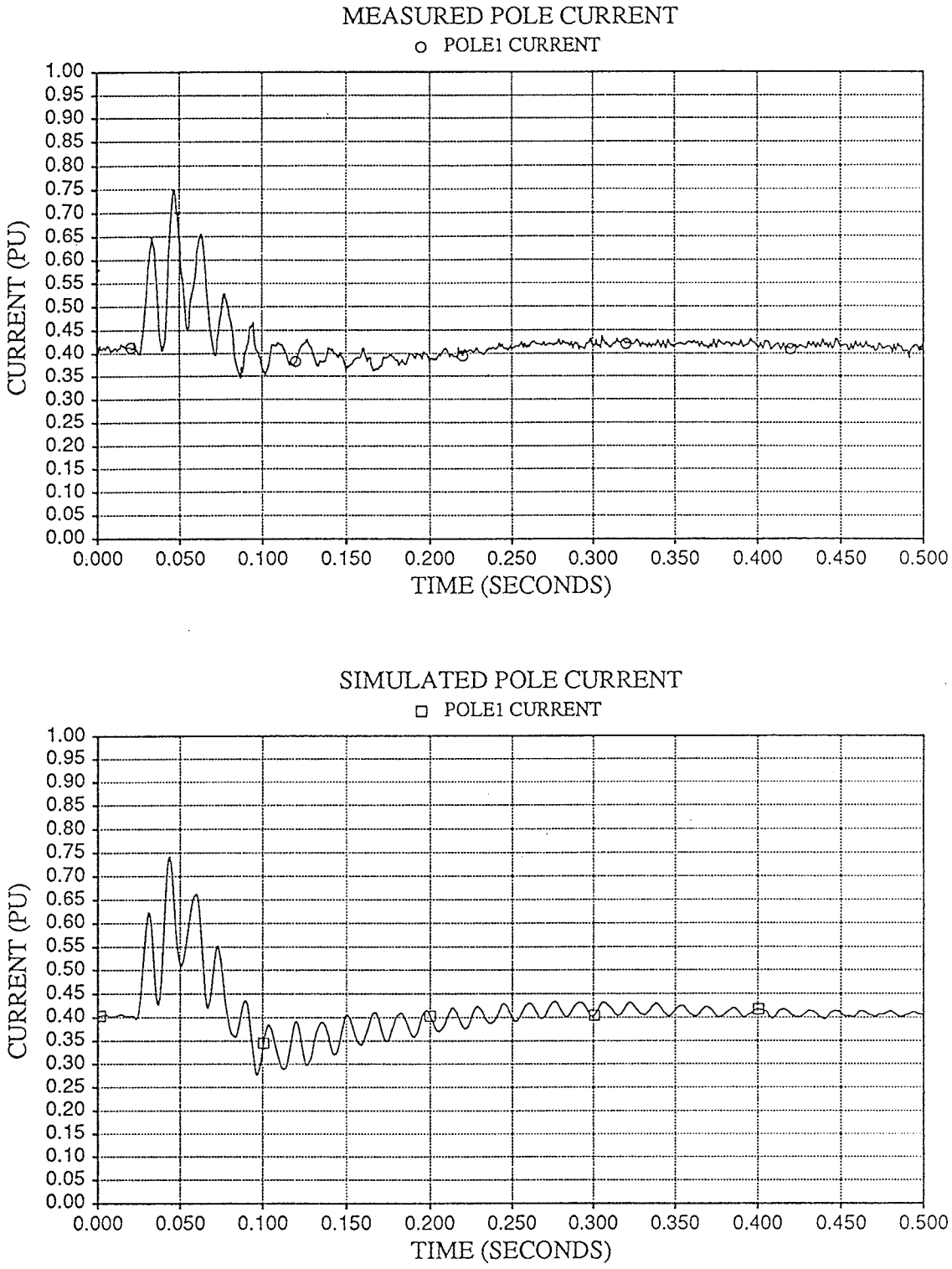

Figure 4.10 - Line current comparison between system measurements and model validation simulations.

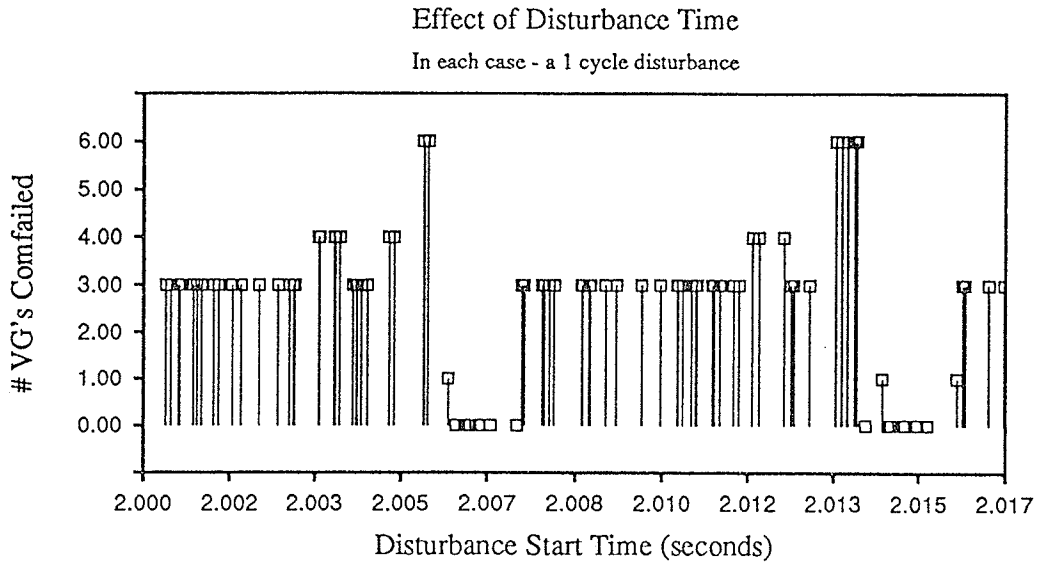

Figure 4.11 - Effect of random disturbance times.

The percent of valve groups that failed commutation is based on the following analysis. For each voltage depression there were 100 simulations with varied disturbance start times. As well, there were 3 valve groups modelled per pole. Therefore, the percentage of valve groups that failed commutation is defined by the total number of valve groups that failed commutation divided by the total of all of the valve groups in service.

ie,

$$\%\ \text{VG's CF'd} = \frac{\text{Total Number of VG's that failed commutation in 100 simulation}}{(100\ \text{simulations}) \times (6\ \text{VG's in service})}$$

Although this value is representative of the severity of the disturbance in relation to commutation failures, it is still possible to have no valve groups fail commutation or have all valve groups fail commutation, depending on when the disturbance was initiated, and the severity of the disturbance.

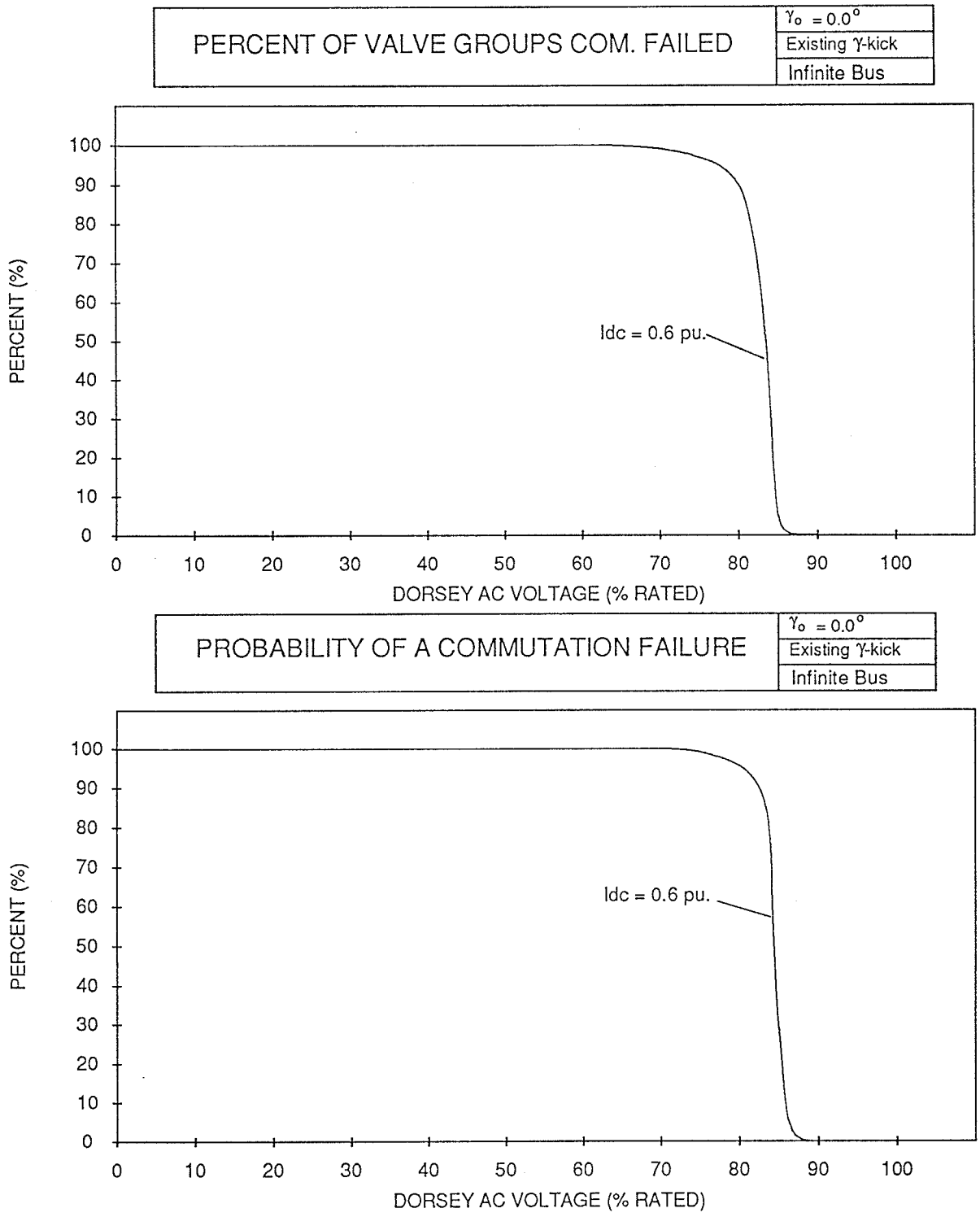

Figure 4.12 - Effect of voltage depression.

The probability of a commutation failure is simply an indication of the chance of one or more valve groups failing commutation for a given voltage level, and system representation. Again, this value will be dependent on the point on wave that the disturbance was initiated.

Effect of Direct Current

To determine the effect of direct current on the incidence of commutation failures, the previous simulation was redone at Idc=0.4 pu, and Idc=1.0 pu. As expected, with a higher direct current, the angle of overlap increased, causing the incidence of commutation failures to increase for the same disturbance. As well, for a decrease in direct current, the incidence of commutation failures decreased. This is shown in *Figure 4.13*.

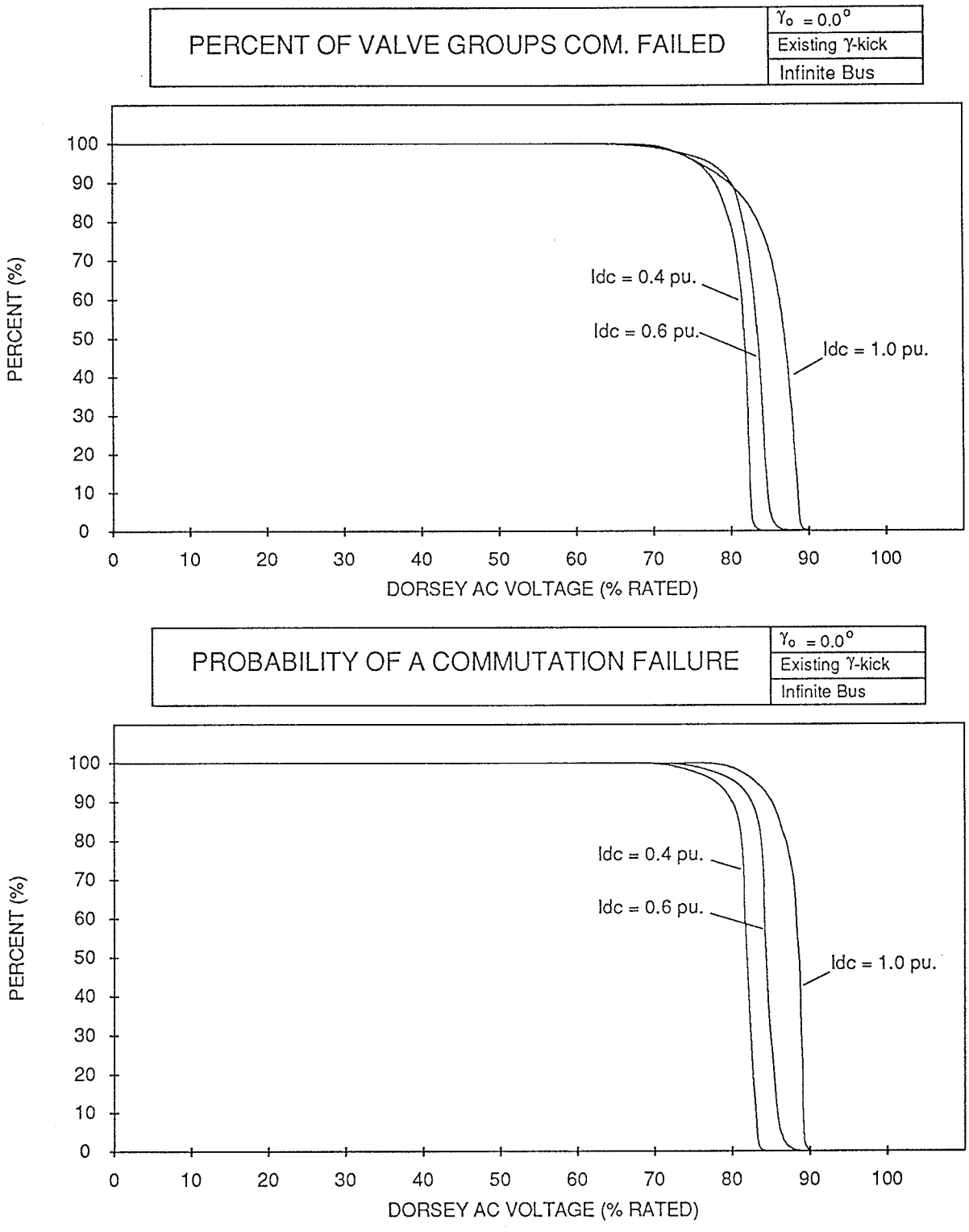

Figure 4.13 - Effect of direct current.

Since the inverter is operated at a steady state extinction angle of 18° at Dorsey, it may not initially be evident why the incidence of commutation failures increases with a different dc loading level (current magnitude). This can best be described by the commutation area required, and the amount of area lost with a voltage depression *(Figure 4.14)*. The higher direct current will lose more commutation area than an equivalent system operated at a lower direct current. Since the loss in commutation area has to be made up, the valve does this by taking margin left in the extinction angle. Since the higher current has to make up more commutation area, it will use more of the margin provided in the extinction angle. The incidence of commutation failures will therefore be higher for higher dc loading since the minimum extinction angle required for successful commutation would more often be insufficient.

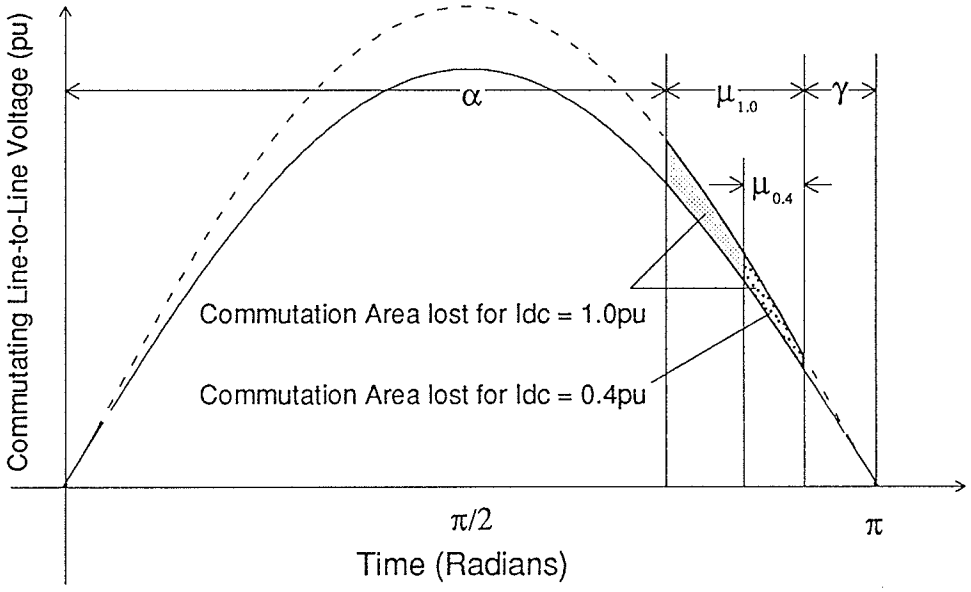

Figure 4.14 - Commutation area for changes in direct current.

As well, for constant rectifier voltage, as the direct current is changed, the inverter transformer tap will also move to maintain the desired current. The change in tap will vary the line to line voltage on the converter side of the transformer. This change will not change the relative commutation area but will affect the area available through the extinction angle. For a direct current of 1.0 pu, the inverter line to line voltage on the dc side of the transformer will be

lower than at a direct current of 0.4 pu. This means that any loss in commutation area may not be made up at the higher current - since the area associated with the extinction angle will be less.

Effect of Deionization Time

The previous simulations were modelled with a minimum required extinction angle of 0°. This meant that a commutation failure would not occur unless the commutation of current from one valve to another was not complete before the line to line voltage reversed across the valve. This approach is optimistic, since a 5° to 8° minimum deionization time is actually required. Therefore, a model was developed to simulate a minimum extinction angle required for successful commutation. If the extinction angle decreased below the minimum angle required, the valve that just gave up commutation would be refired to simulate a commutation failure.

From *Figures 4.15* and *4.16,* the effect on the incidence of commutation failures due to this minimum extinction angle is evident for direct currents of 0.4 pu. and 1.0 pu respectively. By increasing the minimum required extinction angle to 8°, the probability of a commutation failure also increased. The shift in the curves to the left represents fewer commutation failures for the same fault severity.

Effect of Extinction Angle

The steady state extinction angle at Dorsey is 18° and the effect of operating at a higher value was investigated at rated current (1 pu). A relatively strong ac system (SCR = 6.0) was modelled at the inverter in this case.

Increasing the ordered extinction angle will increase the area available for commutation due to remote ac S-L-G faults. As well, as the extinction angle is increased, the converter tap is lowered to obtain the desired full load current. Lowering the tap will increase the ac line-to-line voltage on the dc side of the converter transformer, which would also increase the available area for commutation upon a voltage depression.

Operating at a higher extinction angle also requires redesigning the converter, with increased ratings. This study neglected the redesign of the converter with a higher steady state extinction angle. Any increase in γ should not only consider commutation failure performance, but also extra converter capital and operating costs for a higher γ operation.

Figure 4.17 shows the probability of the incidence of a commutation failure as a function of fault severity. A steady state extinction angle of 18°, 25° and 30° was used in this analysis. With the higher extinction angle, the probability of a commutation failure was greatly reduced.

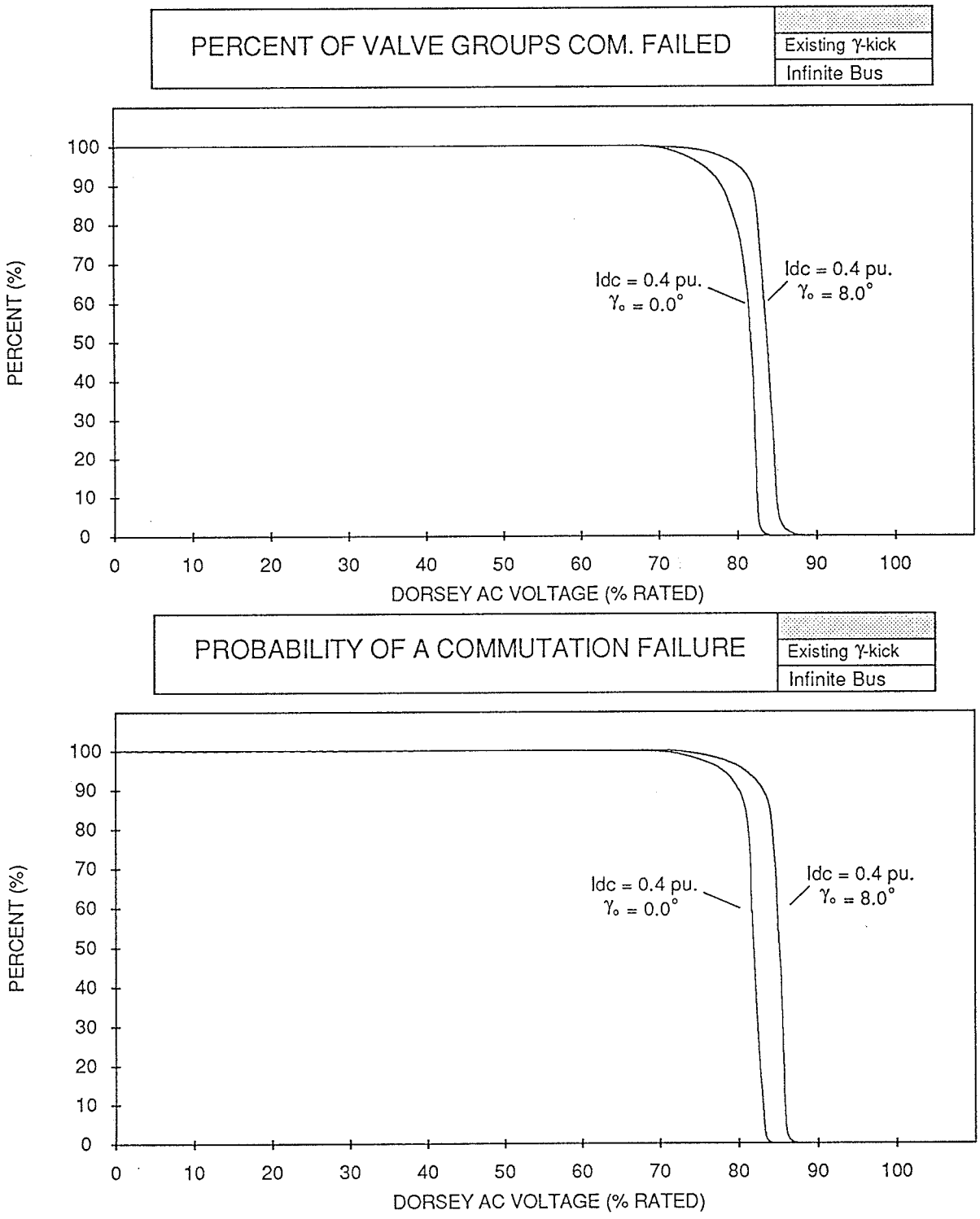

Figure 4.15 - Effect of deionization time for direct current of 0.4 pu.

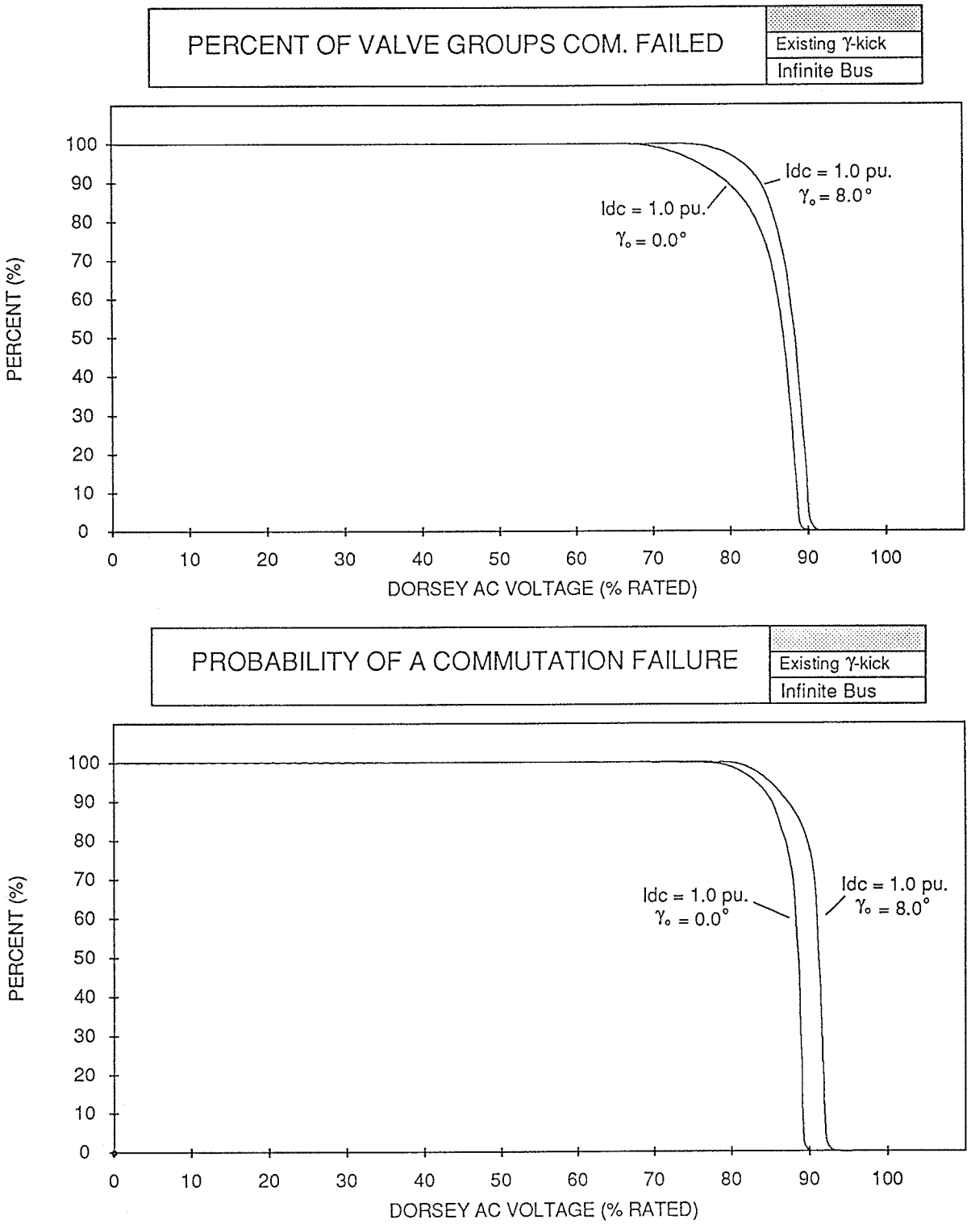

Figure 4.16 - Effect of deionization time for direct current of 1.0 pu.

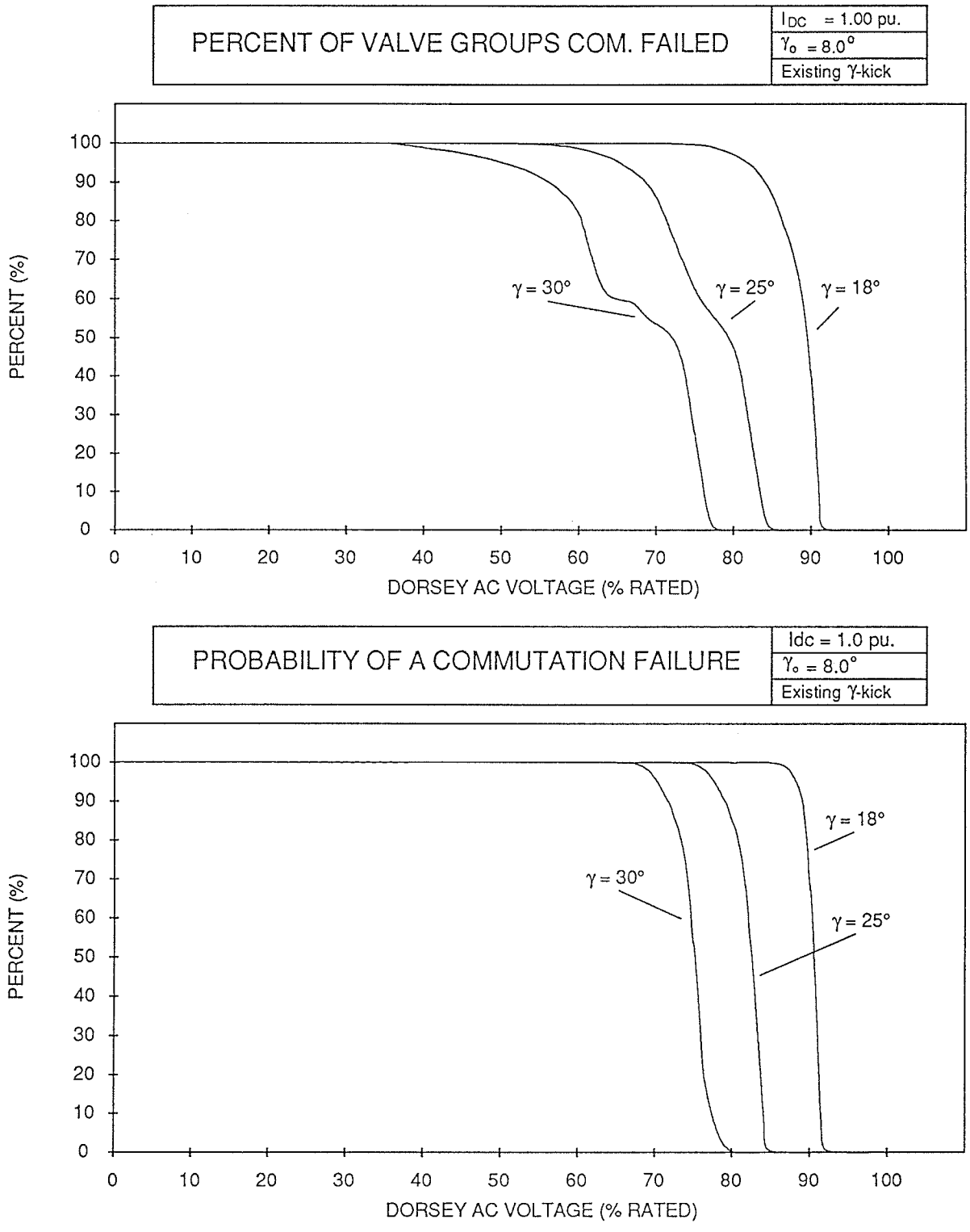

Figure 4.17 - Effect of extinction angle for direct current of 1.0 pu.

Effect of Inverter AC System Strength

To represent the effects of voltage distortions as well as phase shifts, the ac system model is very important. To simulate these effects, a Thevenin ac equivalent with all of the filters at the Dorsey converter bus was modelled. A relatively weak ac system with a short circuit ratio of 3.0 , as well as a stronger system with a short circuit ratio of 6.0 were modelled. Again, 100 simulations were done varying the start of the disturbance over the first cycle of the simulation.

One phase voltage at the Thevenin source was decreased for one cycle to represent the effects of a remote single line to ground fault. For the weak ac system, the distortions at the commutating bus was very significant, making it almost impossible to determine the lowest phase voltage. The probability of a commutation failure as well as the percentage of valve groups that failed commutation was therefore plotted as a function of the lowest phase voltage at the *Thevenin source* rather than at the Dorsey converter bus. The actual voltage at Dorsey will be slightly higher than the indicated voltage, shifting the curve slightly to the right. The shape of the curves will not change, only the displacement along the x-axis. The results for three cases were studied: SCR=3.0, SCR=6.0, Infinite Bus (*Figure 4.18*). The voltage plotted for the infinite bus case is the Dorsey voltage; whereas the voltage of the other two cases is the voltage at the Thevenin source. This explains why it appears that the infinite bus case has a higher probability of commutation failure than the case with a short circuit ratio of 6.0.

The plot of percentage of valve groups that failed commutation is skewed rather badly for the weak ac system (SCR=3.0), which indicates that the voltage distortions as well as the phase shift due to the change in power affected the number of valve groups that failed commutation for a given disturbance. In some cases, this aided in preventing some valves from failing, while at other times it increased the number of failures. The probability that a commutation failure will occur was not affected in the same way.

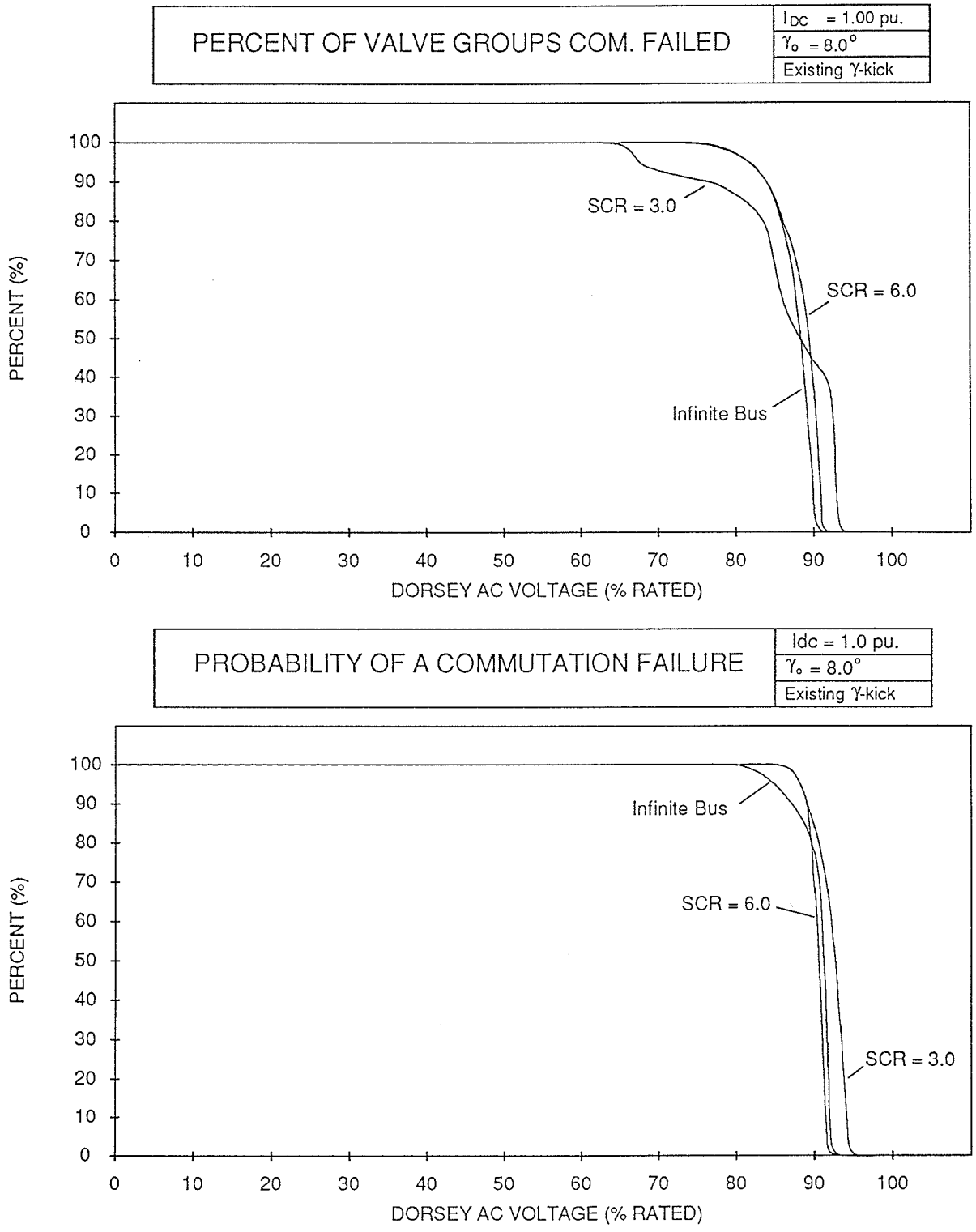

Figure 4.18 - Effect of SCR on the incidence of commutation failures.

Effect of Zero Sequence Detection

As previously mentioned, the control strategy for Dorsey Bipole 1 includes a large valve group-kick to the gamma controls of the valve group that failed commutation, and a small pole-kick to all of the other valve groups in the pole. This strategy is implemented upon the detection of a commutation failure. However, it is possible to predict a failure before it occurs by the zero-sequence voltage at the commutating bus, as discussed earlier. The pole-kick strategy for Bipole 1 was redesigned to include a zero sequence detection scheme. This strategy is illustrated in *Figure 4.19*

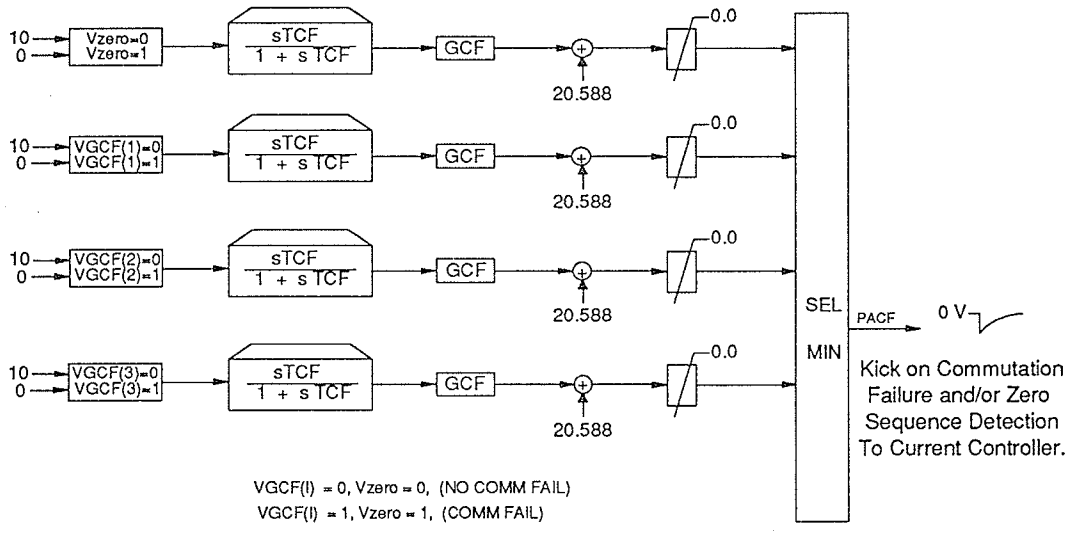

Figure 4.19 - Block diagram for a zero sequence pole-kick strategy.

With this scheme, upon the detection of a fault (other than a 3 phase fault), the pole kick will advance the firing angle at the inverter for each pole. The pole-kick was previously shown to increase the extinction angle from 18° to about 26° in roughly 40 - 50 milliseconds. In terms of preventing a commutation failure from occurring, the zero sequence detection had very little effect, probably due to the slow response upon its detection. A larger kick could be possible also; however more reactive power would be consumed at the inverter thereby decreasing the voltage further. In terms of subsequent failures, it would seem

that a zero sequence detection could reduce these occurrences; however in this study, in a period of 50 milliseconds the total number of commutation failures for each valve was recorded with and without the zero sequence detection. The results indicate less than 1% decrease in the total number of commutation failures - which indicates little motivation to include this control strategy at the pole level in preventing the incidence of commutation failures or to decrease the percentage of valve groups that failed. A longer simulation time and more detailed ac system models would have to be used to investigate the effect on subsequent failures.

The zero sequence detection scheme was also implemented at the valve group level with little change in results.

Conclusions

This chapter provided a detailed description of the ac and dc system models used in an EMTDC simulation of commutation failures, including model validation results. The computer results showed that there were a number of system conditions that affect the probability of commutation failures. The commutating voltage depression, the steady state direct current, the modelled thyristor deionization time, the steady-state extinction angle, and the ac system strength all affect the probability of a commutation failure occurring. However, a zero sequence detection scheme did not affect the probability of a commutation failure occurring.

Field Results

Introduction

This chapter describes the Manitoba HVdc transmission system, and presents commutation failure field results for the Manitoba Hydro system. A direct comparison between computer and field results is also made.

Nelson River HVdc Transmission System

The Nelson River HVdc System currently consists of 2 bipoles: Bipole 1 with mercury arc valves, and Bipole 2 with thyristors. The sending end rectifier (Radisson) capacity for Bipole 1 is 1667 MW (±463 kV, 1800 Amps.), with an overload capability of 1836 MW (1980 Amps.). For Bipole 2, the sending end rectifier (Henday) capacity is 2000 MW (±500 kV, 2000 Amps.), with an overload rating of 2200 MW (2200 Amps.)[11]. Both poles of Bipole 1 consist of 3 - 6 pulse valve groups at the rectifier and the inverter. The positive pole consists of 2 Y-Y valve groups and 1 Y-Δ, while the negative pole consists of 2 Y-Δ valve groups and 1 Y-Y. Both poles of Bipole 2, on the other hand consists of 2 - 12 pulse valve groups at the rectifier and the inverter. Both bipoles 1 and 2 are terminated in the south at Dorsey Converter Station, approximately 32 km. northwest of the center of Winnipeg. *Figure 5.1* shows a single line diagram of the Nelson River HVdc System as it is planned for the year 1993[12].

Three +300/-150 Mvar synchronous compensators at the Dorsey converter bus will be commissioned in 1991, while two of the 6 pulse mercury arc valves of the negative pole of Bipole one will be replaced with thyristor valves by 1993. As well, Limestone Generating Station will be at full power in 1992.

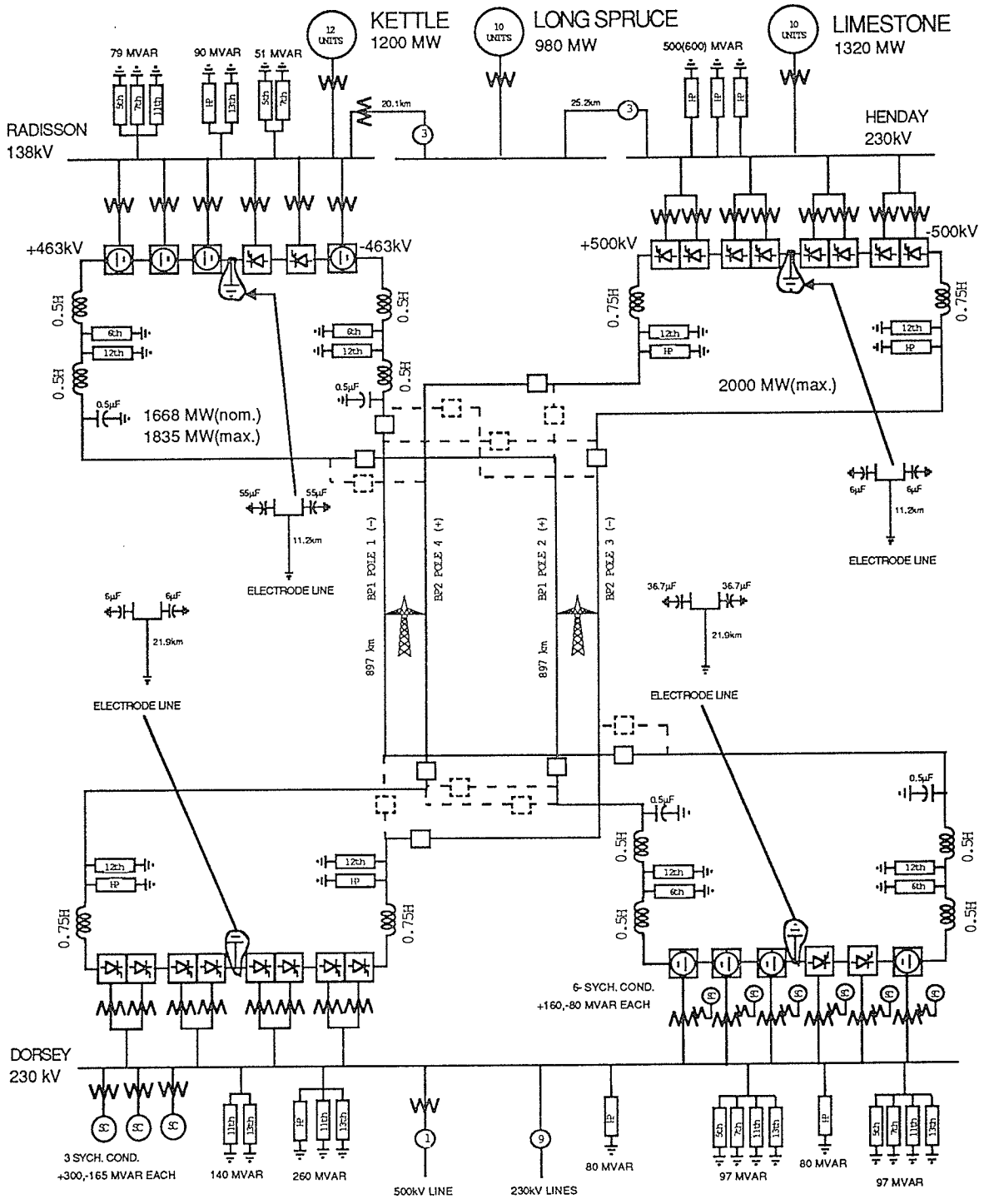

Figure 5.1 - Nelson river HVdc system (1993) (Courtesy of Manitoba Hydro).

Commutation Failure Results

A list of the commutation failures that occurred at Dorsey from 1984 to 1990 is included in Appendix A. The lowest phase voltage at Dorsey for each failure was recorded, as well as the number of synchronous compensators, the filters in service, the power level on the 500 kV line to the United States, the direct current, the number of valve groups in service, and the number of valve groups that failed commutation, as well as the cause of the disturbance.

Using this data, a comparison was attempted to the simulation results. The commutation failures were grouped by the lowest phase voltage during the disturbance, and the percent of valve groups that failed was calculated. The results of this calculation are shown in *Figure 5.2* for Bipole 1 and Bipole 2.

Because commutation failures are so dependent on the point-on-wave that the disturbance occurred, the field data did not provide enough of a sample for each single line to ground fault of similar severity and similar system conditions. This resulted in a scattering of points for the field data, which would have been matched by simulation results if 100 simulations were not executed at random start times. As well, the percent of valve groups that fail commutation will depend on the strength of the ac system, the direct current, as well as any effect from Bipole 2. Because of all of these factors, it was very difficult to extract any comparable data from the field results. As well, because results were only kept for faults causing a commutation failure, the probability of the incidence of a commutation failure could not be calculated due to the lack of information on the total number of disturbances, and the minimum phase voltage which did not cause a commutation failure.

The incidence of commutation failures for Bipole 1 and Bipole 2 were extracted from the field results and tabulated below, where the total is the total number of commutation failure events that occurred at Dorsey. Of the 103 events, there were 96 commutation failures that occurred on Bipole 1, and 66 commutation failures that occurred on Bipole 2.

Total Number Of Commutation Failures		
Bipole 1	Bipole 2	Total
96	66	103

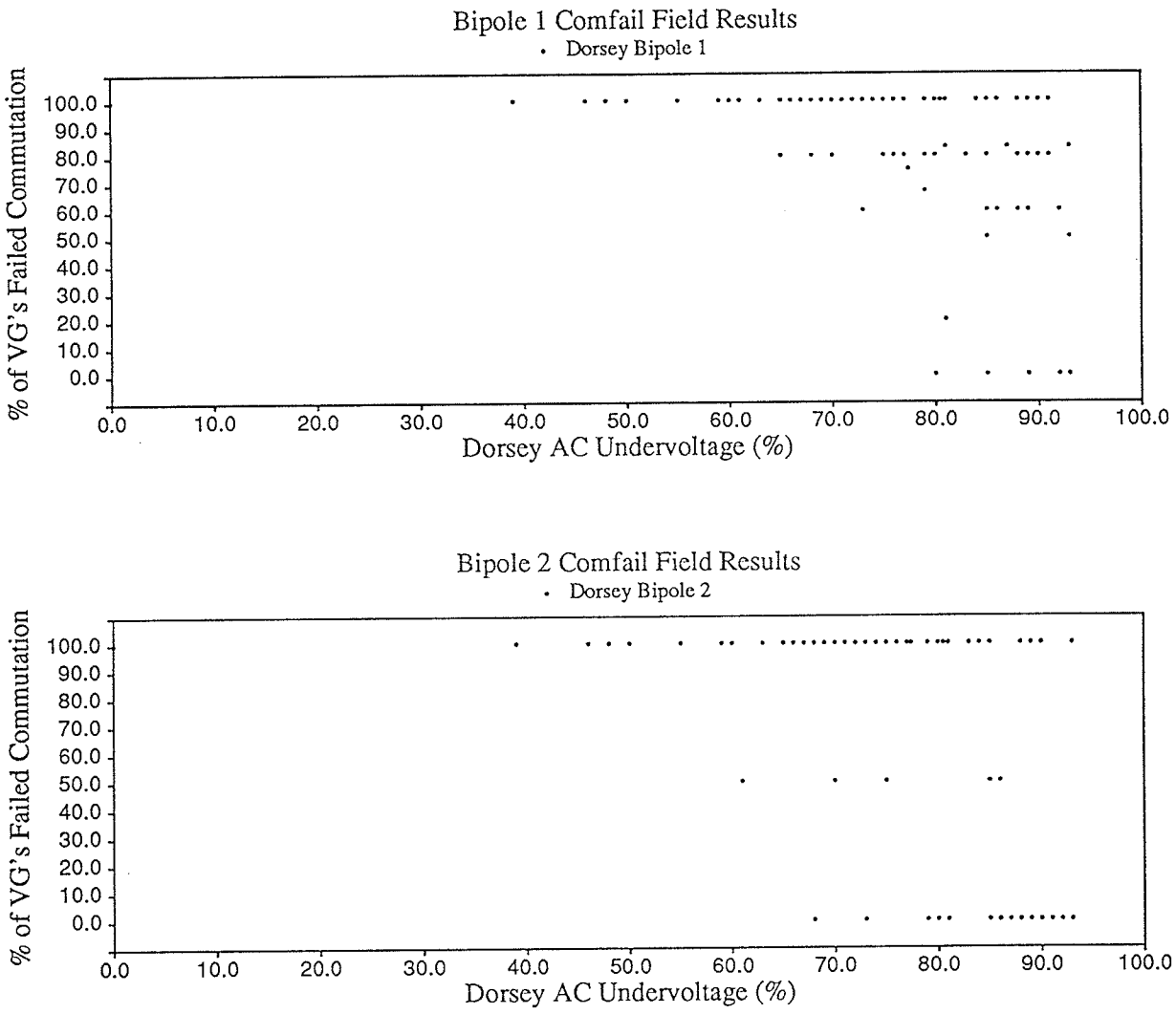

Figure 5.2 - Dorsey Bipole 1 and Bipole 2 commutation failure field results.

From this table, several results come into view:

- A commutation failure is almost twice as likely to occur on Bipole 1 than Bipole 2.

- There is less than a 1% chance of a commutation failure only occurring on Bipole 2.

- Contributing to these results may be that the final stage of Bipole 2 was not completed until 1985. As well, the deionization time of a thyristor valve is less than the deionization time of a comparable mercury arc valve.

In addition, for Bipole 1, the smallest voltage depression that caused a commutation failure was 93%, which occurred at 0.6 pu direct current. The lowest voltage depression that did not cause all of the valve groups to fail commutation was 65% at 0.3 pu direct current.

Field Traces

The commutation failures recorded at Dorsey Converter Station are documented in Appendix A. The failure which occurred on September 9th, 1984 was simulated with EMTDC. The system configuration at the time of the disturbance had all 6 Bipole 1 valve groups in service, with 5 synchronous compensators and the 500 kV line in service. This indicates a strong ac system at the time of the disturbance. Therefore, the ac equivalent with a short circuit ratio of 6.0 was used to simulate the disturbance. Although the commutation failure was caused by a remote line to ground fault, the equivalent voltage depression was applied at the Thevenin source to reproduce the commutation failure. Again, since commutation failures are very dependent on the point-on-wave when the disturbance occurs, 100 simulations were executed each with a random disturbance time. The table shown in Appendix B illustrates the format of the results. The valve groups that failed commutation differed from run to run, depending on the time of the disturbance. In each computer simulation, the disturbance was applied for 16.6 milliseconds (1 cycle), while the commutation failure that actually occurred at Dorsey lasted for approximately 20 milliseconds. The number of commutation failures caused by the actual disturbance are given below.

	VG11	VG12	VG13	VG21	VG22	VG23
Number of Commutation Failures	2	1	3	1	1	2

None of the simulation runs directly matched the number of valve groups that failed commutation at Dorsey. This may be due to voltage or phase distortions that were unable to be represented with the simple ac equivalent representation, or because the voltage depression was simulated at the Thevenin source rather than at the Dorsey commutating bus. The actual voltage at Dorsey is slightly higher in the simulation compared to the field results. The simulation that best described the commutation failure at Dorsey is highlighted in Appendix B. This case was re-executed monitoring the dc voltage and direct current of both poles. The field results were digitized and plotted on the same scale as the simulated results. DC voltage is shown in *Figure 5.3*, and line current is shown in *Figure 5.4*. Although the results do not match as well as the controlled model validation tests shown earlier, the results show good correlation, considering that a simple ac system equivalent was used in the model. Characteristic of a severe commutation failure is the drop in dc voltage to zero, as well as an increase in direct current because of this voltage drop. In both the simulation as well as the field results, a 60 Hz damped oscillation was observed in the recovery, which is characteristic of the Bipole 1 HVdc system.

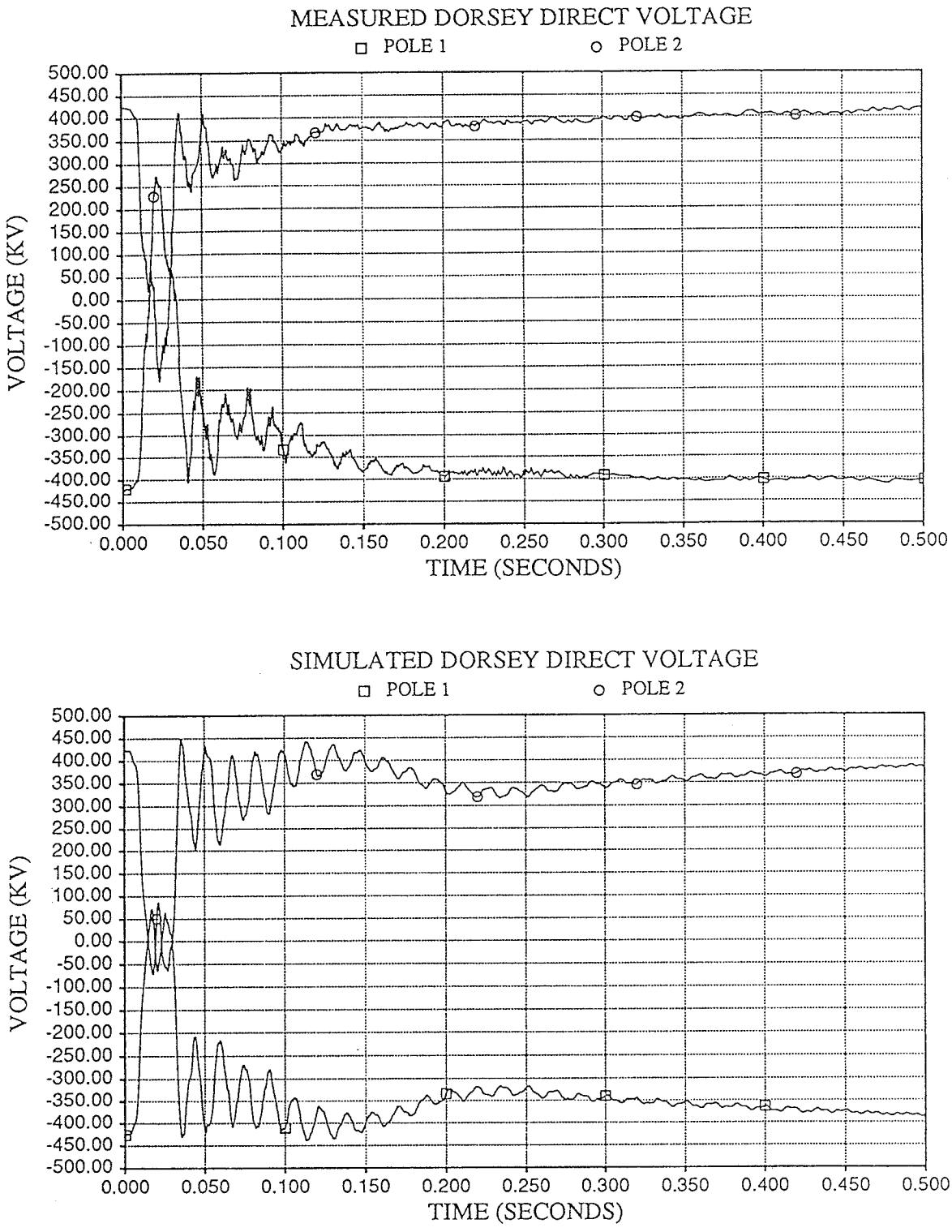

Figure 5.3 - DC voltage comparison between system recordings and computer simulations.

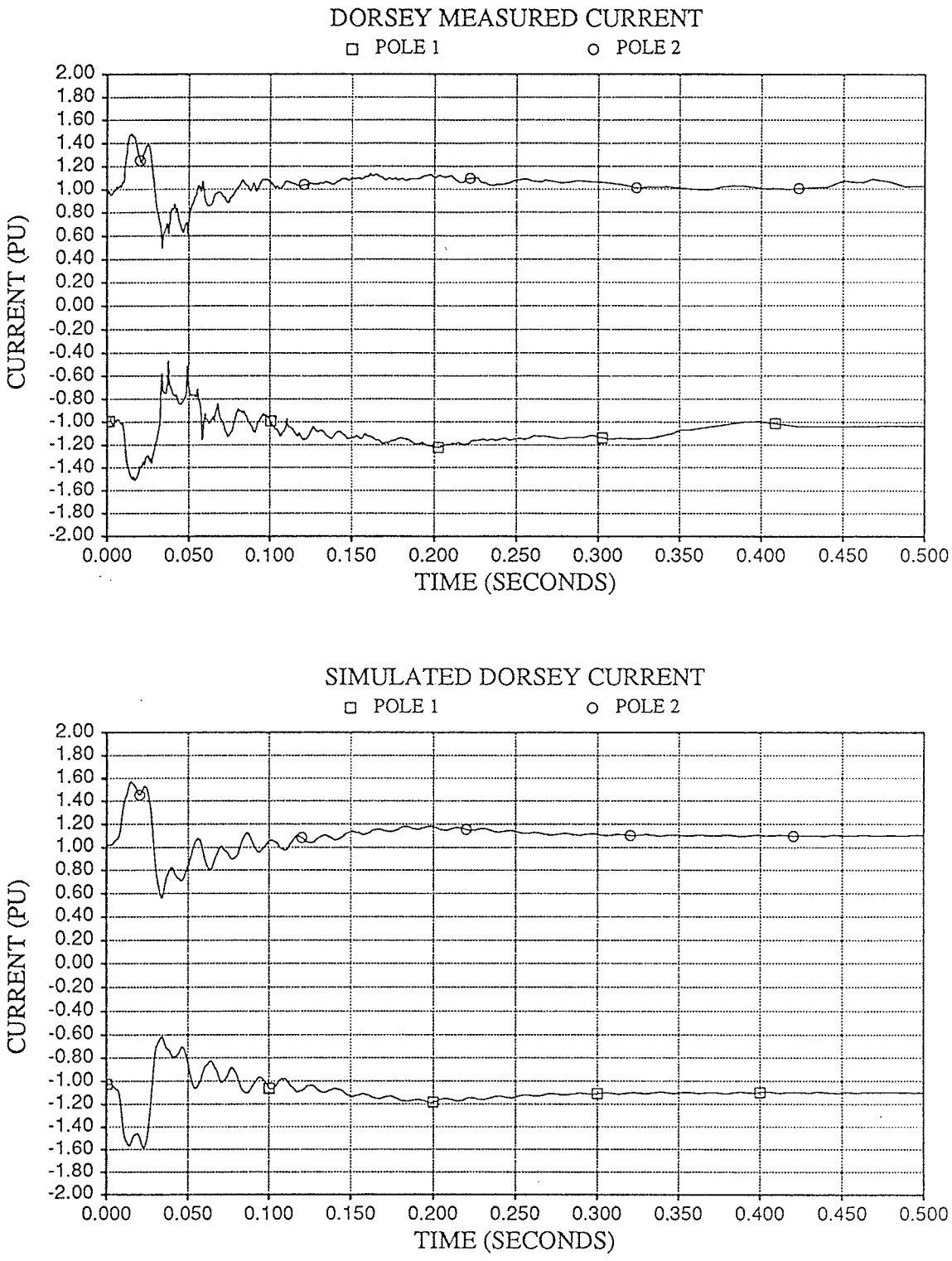

Figure 5.4 - Line current comparison between system measurements and computer simulation.

Conclusions

This chapter presented commutation failure field results for the Manitoba Hydro HVdc system. Good correlation between computer simulation results and field results was demonstrated, including a direct comparison to field traces.

Chapter 6

Summary & Future Work

Summary

Since a commutation failure is very dependent on the time of the disturbance, the incidence of a commutation failure is a stochastic process. This means that a proper sample of failures under similar conditions must be used to determine the probability that a commutation failure will occur under the chosen system conditions. Computer simulations were therefore performed at 100 randomly selected disturbance times for several predetermined operating conditions. In this way, commutation failures could be recorded, and the probability that a commutation failure would occur as well as the percentage of valve groups that failed commutation could be determined for each operating condition.

Comparison between operating conditions was made possible by graphing the percentage of commutation failures as a function of the severity of the disturbance. The severity of the disturbance was classified according to the lowest phase voltage at the commutating bus due to the single-line-to-ground fault. In this way, the chance of a commutation failure occurring was determined as a function of the dc loading (current magnitude), the deionization time of the valve, the ac system strength, and the steady state extinction angle.

A summary of the computer simulation results follows:

- The more severe the disturbance, the more likely a commutation failure would occur. It was shown that at rated current for Bipole 1, a remote single-line-to-ground fault would definitely cause at least one commutation failure if the lowest phase voltage decreased below 80%, based on an ac SCR of 3.0.

- At rated current for Bipole 1, a remote single-line-to-ground fault would not cause a commutation failure if the lowest phase voltage remained above 92%, based on an ac SCR of 3.0.

- As the dc loading (current magnitude) increased, the probability of a commutation failure increased as well, for the same ac disturbance.

- As the thyristor deionization time of the valve increased, so did the probability of a commutation failure. As well, the percentage of valve groups that failed commutation also increased.

- A low ac system strength resulted in severe voltage distortions and phase shifts from a single line to ground disturbance. This tended to decrease the percentage of valve groups that failed commutation, yet increased the probability that a commutation failure would occur.

- The most effective way to reduce the incidence of a commutation failure is to operate at a higher steady-state extinction angle. This was shown by the relative decrease in the incidence of commutation failures with an increase in the steady state extinction angle at the inverter. This will allow the voltage to decrease further without a commutation failure occurring; however, an increase in the steady-state extinction angle should not only consider commutation failure performance, but also extra converter capital and operating costs for a higher γ operation.

- Zero-sequence detection schemes can be used to advance the firing angle of all the valves at the inverter upon the incidence of an ac disturbance. However, this control may be more effective in decreasing the number of subsequent commutation failures rather than reducing the incidence of failures. It was found that faster controls do not offer substantial improvements in the incidence of commutation failures, for the fault severities pursued in this report.

The prevention of a commutation failure is not possible since current turn-off cannot be controlled for a conventional thyristor. Controls can be used to advance the firing angle of subsequent valves once a commutation failure has occurred, but controls will not prevent the original failure from occurring.

Future Work

The probability of the occurrence of a commutation failure was the main focus of this report. It would be a natural progression to research the number of

subsequent commutation failures associated with different fault severities. This would require an ac system equivalent which includes synchronous compensator models, frequency damping and angle damping models. As well, longer run times will have to be used to observe the complete recovery of the dc system to the power reduction from the commutation failure. A simulator may increase the speed of this process, but the results will not differ from EMTDC results. The simulator must also have a minimum extinction angle model to properly determine when the commutation failure occurs.

Other areas of research include a verified model for the turn-off process of a thyristor. The actual turn-off time may vary according to circuit parameters or temperature. The 8° deionization time adopted in this study was considered pessimistic.

Conclusions

The probability of a commutation failure from a remote ac system fault was found to depend on a number of system conditions, summarized below:

- The voltage depression at the commutating bus associated with the fault.
- The voltage distortions at the commutating bus associated with the fault.
- The phase shift at the commutating bus associated with the fault.
- The strength of the ac system at the time of the disturbance.
- The direct current at the time of the disturbance.
- The rise of direct current during the ac system fault.
- The controlled steady-state extinction angle.
- The deionization time of the valve.
- The point-on-wave that the disturbance occurred.

Along with the system conditions at the time of the fault, several different dc control strategies were analyzed to decrease the probability of a commutation failure. Among the control strategies implemented was a zero sequence detection scheme used to predict the likelihood of a commutation failure. From the results, however, the control action of the zero sequence detection scheme did not have a large impact on decreasing the probability of a commutation failure. In fact, the most effective way discovered to reduce the incidence of a commutation failure is to operate the inverter at a higher steady state extinction angle.

Operating at a higher extinction angle may require redesign of the converter, with increased ratings. Therefore, the increase in steady state extinction angle should not only consider commutation performance, but also extra converter capital and operating costs.

Appendix A

No.	Date	Time	AC Bus Voltage (%)	No. Of Syncs.	Filters	500kV Line (MW)	DC Current BIP1	DC Current BIP2	No. Of VG's BIP1	No. Of VG's BIP2	No. Of VG's CF BIP1	No. Of VG's CF BIP2	Cause & Remarks
1	84.04.12	17:08	88	5	F3 off	590	1850	1960	5	1	4	1	WH 66kV line (W4) tripped
2	84.04.26	05:55	90	5	7,8,9 off	300	1600	1010	5	2	4	0	24 & 66kV line faults
3	84.04.26	05:55	92	5	7,8,9 off	300	1600	1010	5	2	3	0	24 & 66kV line faults
4	84.04.26	05:55	91	5	7,8,9 off	300	1600	1010	5	2	4	0	24 & 66kV line faults
5	84.04.26	05:55	85	5	7,8,9 off	300	1600	1010	5	2	3	0	24 & 66kV line faults
6	84.05.26	05:55	88	5	7,8,9 off	300	1600	1010	5	2	4	0	24 & 66kV line faults
7	84.04.26	05:55	90	5	7,8,9 off	300	1600	1010	5	2	4	0	24 & 66kV line faults
8	84.04.26	05:55	92	5	7,8,9 off	300	1600	1010	5	2	3	0	24 & 66kV line faults
9	84.04.26	05:55	91	5	7,8,9 off	300	1600	1010	5	2	4	0	24 & 66kV line faults
10	84.04.26	05:55	85	5	7,8,9 off	300	1600	1010	5	2	3	0	24 & 66kV line faults
11	84.04.26	05:55	88	5	7,8,9 off	300	1600	1010	5	2	4	0	24 & 66kV line faults
12	84.04.27	06:18	88	5	F7,8 off	350	1660	1300	5	1	5	0	230kV line (D14G) fault
13	84.04.27	06:44	88	5	all on	350	1660	1300	5	2	3	0	230kV line (D14G) fault
14	84.04.27	11:08	86	5	all on	630	1800	1470	5	2	3	1	230kV line (D14G) fault
15	84.04.27	11:09	86	5	all on	630	1800	1470	5	2	3	1	230kV line (D14G) fault
16	84.04.27	11:10	88	5	all on	630	1800	1470	5	2	5	2	230kV line (D14G) fault
17	84.04.27	12:51	80	5	all on	630	1800	1470	5	2	4	0	230kV line (D14G) fault
18	84.04.27	12:54	73	5	all on	630	1800	1470	5	2	5	2	230kV line (D14G) fault
19	84.04.27	22:52	91	5	all on	590	1630	1050	5	2	4	0	230kV line (D14G) fault
20	84.04.27	23:12	86	5	F7,8 off	590	1630	1050	5	2	5	0	230kV line (D14G) fault
21	84.04.27	23:40	89	5	F7,8 off	460	1500	950	5	2	3	0	230kV line (D14G) fault
22	84.04.28	02:24	89	5	F7,8 off	370	1430	940	5	2	5	0	230kV line (D14G) fault
23	84.04.28	03:20	88	5	F7,8 off	350	1460	820	5	2	4	0	230kV line (D14G) fault
24	84.04.28	03:22	89	5	F7,8 off	350	1460	820	5	2	5	0	230kV line (D14G) fault
25	84.04.28	03:23	88	5	F7,8 off	350	1460	820	5	2	4	0	230kV line (D14G) fault
26	84.04.28	03:49	89	5	F7,8 off	350	1240	770	5	2	3	0	230kV line (D14G) fault
27	84.04.28	04:08	89	5	F7,8 off	350	1240	770	5	2	4	0	230kV line (D14G) fault
28	84.04.28	04:29	89	5	F7,8 off	350	1240	770	5	2	4	0	230kV line (D14G) fault
29	84.04.28	04:45	89	5	F7,8 off	350	1240	710	5	2	4	0	230kV line (D14G) fault
30	84.05.22	11:33	79	5	all on	970	1720	1070	5	2	4	2	D602F-Chisago 1075MW red
31	84.06.16	21:42	46	5	all on	800	1500	1025	5	2	5	2	Lightning
32	84.06.16	21:43	75	5	all on	800	1500	1025	5	2	4	1	Lightning
33	84.06.16	22:08	74	4	all on	800	1450	975	5	2	5	3	Lightning
34	84.06.21	11:32	89	5	all on	730	1800	1350	5	2	4	2	Lightning
35	84.06.21	12:02	81	5	all on	730	1800	1300	5	2	7	2	Lightning
36	84.06.21	20:50	73	5	all on	670	1750	675	5	2	5	2	Lightning
37	84.07.08	17:05	69	5	1,2,3,4,5,6	880	1370	1150	5	2	5	2	Lightning
38	84.07.12	11:20	85	5	all on	925	1780	1580	5	2	4		Lightning
39	84.07.12	14:24	86	5	all on	880	1780	1610	5	2	3		Lightning
40	84.07.16	16:48	65	5	all on	900	1715	1130	6	2	6	2	Lightning
41	84.08.07	04:04	73.5	4	1,2,3,4,5				6	2	6	0	RL2 ground fault
42	84.08.02	11:54	58	5	all on	870			5	2			Flashover to trees
43	84.08.02	13:21	54	5	all on	870			6	2			Flashover to trees
44	84.08.02	15:35	58	5	all on	850			6	2			Flashover to trees
45	84.08.02	16:34	65	S11 off	all on	830			6	2			Flashover to trees
46	84.09.21	08:49	79	5	all on	600	1800	1820	6	1	6	0	Lightning on 66kV line.
47	84.11.07	09:01	76	5	all on	610	1610	1030	6	2	6	2	115kV line (WT34) fault
48	84.11.07	09:03	85	5	all on	610	1610	1030	6	2	6	2	115kV line (WT34) fault
49	84.11.07	09:06	80	5	all on	610	1610	1030	6	2	6	2	115kV line (WT34) fault
50	84.11.14	21:35	91	4	7,8 off	210	1250	1270	6	2	2	0	Line (D14G) trip
51	85.12.27	18:30	60	6	7,8 off	400	1085	1170	6	4	6	4	LaVerendrye cap failure
52	86.01.09	06:59	68	6	all on	150	810	820	6	4	6	4	WH line fault
53	86.01.21	01:36	72	5	7,8 off	0	750	710		4		4	115kV line fault
54	86.02.06	13:29	93	5	all on	650	1040	1100	6	3	3	0	T31 energization

55	86.03.01	09:20	83	6	all on	780	1200	1080	5	4		4	High D1W/PCW problem
56	86.03.01	12:33	78	6	all on	760	1100	1060	5	4			High D1W/PCW problem
57	86.03.24	22:03	82	5	all on	350	940	1090	5	4			VG 23 CAB
58	86.03.24	22:28	88.5	4	all on	350	940	1090	5	4			T23 energization
59	86.04.09	07:07	81	5	all on	540	1200	1490	5	2	1	0	T31 energization
60	86.04.13	10:46	50	5	all on	out	960	1000	5	4	5		T21 energization
61	86.06.06	14:18	81	5	all on	850	1510	1000	5	4	5	4	Loss of line (A6V)
62	86.06.18	01:43	93	4	all on	850	1360	990	5	4	0	0	High current deblock VG12
63	86.06.18	13:58	92	4	all on	900	1375	1000	5	4	0	0	Synchronizing 13 to 230
64	86.06.25	21:47	72	5	all on	900	1480	1030	5	4	5	4	T23 energization
65	86.06.26	05:00	55	5		800	1160	1000	2	4	2	4	Lightning on line (D14G)
66	86.06.26	05:18	78	5					3	2	3		Lightning
67	86.06.26	05:27	78	5					4	2	2		Lightning
68	86.06.26	19:47	92	5	all on	920	1800	1050	4	4	0	0	SUVP - High deblock VG13
69	86.06.26	21:03	61	5	all on	950	1450	1050	5	4	5	2	Station fault at McPhilip
70	86.07.03	15:45	89	5	7,8 off	910	1530	1030	5	4	0	0	VAR starvation
71	86.07.03	16:36	85	5	7,8 off	900	1530	1030	5	4	4	0	Line D14G down
72	86.07.03	18:16	68	5	7,8 off	870	1530	1030	5	4	5	4	Lightning
73	86.07.03	18:18	70	5	7,8 off	870	1530	1030	5	4	5	4	Lightning
74	86.07.07	16:30	85	5	all on	950	1470	1125	5	4	0	0	VAR Starvation
75	86.07.26	14:45	75	6	all on	950	1270	1030	6	4	6		D13R Trip
76	86.07.26	15:18	74	6	all on	960	1310	1010	6	4	3		Lightning
77	86.07.26	15:22	74	6	all on	960	1310	1010	6	4	4		Lightning
78	86.08.15	22:08	39	6	all on	950	1270	1030	6	2	6	2	Line (D12C) trip
79	86.08.16	22:24	48	6	all on	960	1380	1570	6	2	6	2	Line (D12C) trip
80	86.08.17	20:58	87	6	all on	950	1470	1280	6	2	5	0	T42 energization - SUVP
81	86.08.19	09:43		6		800	1070	1010	6	4			Lightning - SUVP
82	86.09.22	15:08	63	6	all on	930	1150	1300	6	3	6	3	66kV line fault - SUVP
83	86.10.17	07:55	87	6	all on	560	1120	900	6	4	3		Lost S13 - VG13 CAB
84	86.12.20	20:08	75	6	F6 off	400	1100	1050	6	4	6	4	115kV fault
85	86.12.20	20:58	75	6	F6 off	400	1100	1050	6	4	6	4	115kV fault
86	86.12.20	19:32	67	6	F6 off	580	1100	1050	6	4	6	4	115kV fault
87	86.12.21	07:56	85	6	F6 off	240	1170	1145	6	4	3	2	VG11 AB
88	86.12.21	14:18	68	6	F6 off	470	1060	1245	6	4	6	4	115kV fault
89	87.02.24	15:49											115kV line (SV24) fault
90	87.03.21	13:07	59			260	900	930	5	4	5	4	R50M Trip
91	87.04.07	07:31	93	5		440	750	830	6	4	5	4	SUVP VG11 AB
92	87.04.19	20:23	83	5		760	1150	1000	5	4	4	4	SUVP VG23 deblock fail AB
93	87.05.13	15:45	76	5					5	4	4	4	30 ground fault - Brandon
94	87.06.06	06:50	73	5	F7,8 off	60	535	545	4	2	4	2	Lightning
95	87.07.06	19:23	80	5	all on	650	1230	1015	6	4	6		Lightning
96	87.07.07	13:02	84	5	all on	485	1165	1020	4	4	4	4	SUVP VG23 deblock fail
97	87.07.09	21:29	C=0	5	F7,8 off	210	650	900	5	3	5	3	Lightning
98	87.10.20	17:30	77.4	4	1,2,3,4,5,6,7,8	330	1650	1350	4	2	3	2	VG13 CAB
99	87.10.23	20:47	73	5	F7,8,9 off	230	1120	1110	5	2	3	2	VG23 CAB connecting to dc
100	87.11.06	15:40	80.5	4		10	1300	1205	5	2	5	2	T32 energization
101	87.12.16	16:09	90	5	all on	180	1420	1210	5	3	5	3	T32 energization
102	87.12.29	05:51	69	5	F7,8 off	490	640	760	5	4	5	4	D12C sky wire down
103	87.12.29	09:19	77	5	all on		860	1030	5	4	5	4	Icing on 4X47
104	87.12.29	10:57	70	4	all on		840	910	5	4	5	4	Icing on 4X47
105	87.12.29	10:57	73	4	all on		840	910	5	4	5	4	Icing on 4X47
106	87.12.29	13:41	71	4	all on		940	875	5	4	5	4	Icing on 4X47
107	87.12.29	14:04	72	4	all on		850	890	5	4	5	4	Icing on 4X47
108	87.12.29	14:16	74	4	all on		850	890	5	4	5	4	Icing on 4X47
109	87.12.29	14:26	69	4	all on		850	890	5	4	5	4	Icing on 4X47
110	87.12.29	14:37	73	4	all on		850	890	5	4	5	4	Icing on 4X47
111	87.12.29	14:47	66	4	all on		850	890	5	4	5	4	Icing on 4X47
112	87.12.29	16:15	77	3	all on		800	880	5	4	5	4	Icing on 4X47
113	88.01.06	11:20	76	5	all on	60	1065	1230	5	4	5	4	VG23 CAB
114	88.02.19	19:07	79	5	all on	-80	975	1045	6	4	4	4	VG21 CAB

115	88.05.07	00:14	55	5	F7,8,9 off	-100	520	400	5	2	5		LaVerendrye bus fault
116	88.05.17	14:00	80	5	all on	500	1420	1830	5	2	0	2	Ridgeway 66kV fault
117	88.05.18	18:39	67	5	all on	450	1420	1400	6	2	6	2	Lightning on R49R
118	88.06.04	14:06		3	all on	0	1000	910	6	3			Line fault (D14G)
119	88.07.05	04:13	80	4		-335	400		6	0	4		Lightning
120	88.07.05	15:18	80	4	all on	320	1410	1525	5	2	5	2	Lightning
121	88.07.05	15:53	81	4	all on	320	1410	1525	6	2	5	2	Lightning
122	88.07.05	15:56	77	4	all on	320	1410	1525	5	2	4	2	Lightning
123	88.10.17	19:51	70	4	all on	180	930	1230	5	2	4	1	AC fault WH
124	88.11.22	10:48	70	5	all on	20	1100	880	6	2	6	2	RS51 fault
125	88.11.04	17:30	73	4		-90	705	805	5	2			AC line fault
126	89.08.18	13:03	65	6	all on	20	560	810	5	4	4	4	Lightning at Ridgeway
127	89.10.20	17:11	65	4	all on	460	880	1210	5	4	5	4	VG21 deblock fail CAB
128	89.10.20	17:52	68	4	all on	340	770	1090	5	4	4	0	Enerrgization of T21

Disturbance Time (Seconds)	Commutation Failure Indicator							Percent	Commutation Failure Counter					
	VG 11	VG 12	VG 13	VG 21	VG 22	VG 23	TOT		VG 11	VG 12	VG 13	VG 21	VG 22	VG 23
0.00487375	1	1	1	1	1	1	6	100.0	1	2	1	2	2	1
0.00892115	1	1	1	1	1	1	6	100.0	2	1	2	2	2	2
0.00102806	***1***	***1***	***1***	***1***	***1***	***1***	***6***	***100.0***	***2***	***1***	***2***	***1***	***1***	***2***
0.00382447	1	1	1	1	1	1	6	100.0	1	2	2	2	2	2
0.00293899	1	1	1	1	1	1	6	100.0	2	1	2	1	1	2
0.01349878	1	1	1	1	1	1	6	100.0	1	2	1	3	3	2
0.01338339	1	1	1	1	1	1	6	100.0	1	2	1	3	3	2
0.00172186	1	1	1	1	1	1	6	100.0	2	1	2	1	1	2
0.00723028	1	1	1	1	1	1	6	100.0	2	1	2	1	1	2
0.01359797	1	1	1	1	1	1	6	100.0	2	2	2	1	1	2
0.00673437	1	1	1	1	1	1	6	100.0	1	2	1	2	2	1
0.01350951	1	1	1	1	1	1	6	100.0	1	2	1	3	3	2
0.01446223	1	1	1	1	1	1	6	100.0	2	2	2	2	2	2
0.01068354	1	1	1	1	1	1	6	100.0	2	1	2	1	1	2
0.01236820	0	1	0	1	1	1	4	66.7	0	2	0	2	2	1
0.01584816	1	1	1	1	1	1	6	100.0	2	1	2	1	1	2
0.00067449	1	1	1	1	1	1	6	100.0	2	1	2	2	1	2
0.00145364	1	1	1	1	1	1	6	100.0	2	1	2	1	1	2
0.01349020	1	1	1	1	1	1	6	100.0	1	2	1	3	3	2
0.01251006	0	1	0	1	1	1	4	66.67	0	2	0	2	2	1
0.01351452	1	1	1	1	1	1	6	100.0	1	2	1	3	3	2
0.01497602	1	1	1	1	1	1	6	100.0	1	2	1	2	2	1
0.01257014	0	1	0	1	1	1	4	66.7	0	2	0	2	2	1
0.00290990	1	1	1	1	1	1	6	100.0	2	1	2	1	1	2
0.01057053	1	1	1	1	1	1	6	100.0	2	1	2	1	1	2
0.00096345	1	1	1	1	1	1	6	100.0	2	1	2	1	1	2
0.01396680	1	1	1	1	1	1	6	100.0	2	2	2	2	2	2
0.01064634	1	1	1	1	1	1	6	100.0	2	1	2	1	1	2
0.00861788	1	1	1	1	1	1	6	100.0	2	1	2	2	2	2
0.00374317	1	1	1	1	1	1	6	100.0	1	2	1	2	2	2
0.01138592	1	1	1	1	1	1	6	100.0	2	1	2	1	1	2
0.01664734	1	1	1	1	1	1	6	100.0	2	1	2	2	2	2
0.01471448	0	1	0	1	1	1	4	66.7	0	2	0	2	2	2
0.00283098	1	1	1	1	1	1	6	100.0	2	1	2	1	1	2
0.00260782	1	1	1	1	1	1	6	100.0	2	1	2	1	1	2
0.01338840	1	1	1	1	1	1	6	100.0	1	2	1	3	3	2
0.00223541	1	1	1	1	1	1	6	100.0	2	1	2	1	1	2
0.00911689	1	1	1	1	1	1	6	100.0	2	1	2	2	2	2
0.00413990	0	1	0	1	1	1	4	66.7	0	2	0	2	2	1
0.00145674	1	1	1	1	1	1	6	100.0	2	1	2	1	1	2
0.01379848	1	1	1	1	1	1	6	100.0	2	2	2	2	2	2
0.01030874	1	1	1	1	1	1	6	100.0	2	1	2	1	1	2
0.00783968	1	1	1	1	1	1	6	100.0	2	1	2	2	2	2
0.00847602	1	1	1	1	1	1	6	100.0	2	1	2	2	2	2
0.00607681	1	1	1	1	1	1	6	100.0	2	2	2	2	2	2

0.01375103	1	1	1	1	1	1	6	100.0	2	2	2	2	2	2
0.00553107	1	1	1	1	1	1	6	100.0	2	2	2	2	2	2
0.00862813	1	1	1	1	1	1	6	100.0	2	1	2	2	2	2
0.00477052	1	1	1	1	1	1	6	100.0	1	2	1	2	2	2
0.01515913	0	1	0	1	1	1	4	66.7	0	2	0	2	2	1
0.01439762	1	1	1	1	1	1	6	100.0	2	2	2	2	2	2
0.00415921	0	1	0	1	1	1	4	66.7	0	2	0	2	2	1
0.00340891	1	1	1	1	1	1	6	100.0	2	2	2	2	2	1
0.01096725	1	1	1	1	1	1	6	100.0	2	1	2	1	1	2
0.00770092	1	1	1	1	1	1	6	100.0	2	1	2	2	1	2
0.01111794	1	1	1	1	1	1	6	100.0	2	1	2	1	1	2
0.00624061	1	1	1	1	1	1	6	100.0	2	2	2	2	2	2
0.01362658	1	1	1	1	1	1	6	100.0	2	2	2	2	1	2
0.00961137	1	1	1	1	1	1	6	100.0	2	1	2	2	2	2
0.00407434	0	1	0	1	1	1	4	66.7	0	2	0	2	2	1
0.01149631	1	1	1	1	1	1	6	100.0	2	1	2	1	1	2
0.01112866	1	1	1	1	1	1	6	100.0	2	1	2	1	1	2
0.00731945	1	1	1	1	1	1	6	100.0	2	1	2	1	1	2
0.00592160	1	1	1	1	1	1	6	100.0	2	2	2	2	2	2
0.01474905	0	1	0	1	1	1	4	66.7	0	2	0	2	2	2
0.00632453	1	1	1	1	1	0	5	83.3	2	2	2	2	2	0
0.00543642	1	1	1	1	1	1	6	100.0	2	2	2	2	2	2
0.01573944	1	1	1	1	1	1	6	100.0	2	1	2	1	1	2
0.00634742	1	1	1	1	1	0	5	83.3	2	2	2	2	2	0
0.00774813	1	1	1	1	1	1	6	100.0	2	1	2	2	2	2
0.01589561	1	1	1	1	1	1	6	100.0	2	1	2	1	1	2
0.0054216	1	1	1	1	1	1	6	100.0	2	2	2	2	2	2
0.00066519	1	1	1	1	1	1	6	100.0	2	1	2	2	1	2
0.00052905	1	1	1	1	1	1	6	100.0	2	1	2	2	1	2
0.00342774	1	1	1	1	1	1	6	100.0	2	2	2	2	2	1
0.01286817	1	1	1	1	1	1	6	100.0	1	2	1	2	2	2
0.01634765	1	1	1	1	1	1	6	100.0	2	1	2	2	1	2
0.00112247	1	1	1	1	1	1	6	100.0	2	1	2	1	1	2
0.01337981	1	1	1	1	1	1	6	100.0	1	2	1	3	3	2
0.00136209	1	1	1	1	1	1	6	100.0	2	1	2	1	1	2
0.00424314	0	1	1	1	1	1	5	83.3	0	2	1	2	2	1
0.01188540	1	1	1	1	1	1	6	100.0	1	2	1	2	2	1
0.00042868	1	1	1	1	1	1	6	100.0	2	1	2	2	1	2
0.00997400	1	1	1	1	1	1	6	100.0	2	1	2	1	1	2
0.00736976	1	1	1	1	1	1	6	100.0	2	1	2	1	1	2
0.01100755	1	1	1	1	1	1	6	100.0	2	1	2	1	1	2
0.01175928	0	1	0	1	1	1	4	66.7	0	2	0	2	2	1
0.00435495	1	1	1	1	1	1	6	100.0	1	2	1	2	2	1
0.00652075	0	1	0	1	1	1	4	66.7	0	2	0	2	2	1
0.00859952	1	1	1	1	1	1	6	100.0	2	1	2	2	2	2
0.00189376	1	1	1	1	1	1	6	100.0	2	2	2	1	1	2
0.00792766	1	1	1	1	1	1	6	100.0	2	1	2	2	2	2
0.00069690	1	1	1	1	1	1	6	100.0	2	1	2	2	1	2
0.00371408	1	1	1	1	1	1	6	100.0	1	2	1	2	2	2
0.00845766	1	1	1	1	1	1	6	100.0	2	1	2	2	2	2

0.00422740
0.01029277
0.00624704
0.01429439
0.01039720

0	1	0	1	1	1	4	66.7
1	1	1	1	1	1	6	100.0
1	1	1	1	1	1	6	100.0
1	1	1	1	1	1	6	100.0
1	1	1	1	1	1	6	100.0

0	2	0	2	2	1
2	1	2	1	1	2
2	2	2	2	2	2
2	2	2	2	2	2
2	1	2	1	1	2

Assalit, H.B., "Thyristor Turn-Off Time Trade-Offs," IEEE Proc. Industry Applic. Soc., 1981

Billon, V.C. , Taisne, J.P., Arcidiacono, V., Mazzoldi, F., "The Corsican Tapping: From Design To Commissioning Tests of the Third Terminal of the Sardinia-Corsica-Italy HVdc Link," IEEE Transactions on Power Delivery, Vol. 4, No.1, January 1989

Bowles, J.P. ,"AC System and Transformer Representation for HVdc Transmission Studies, "IEEE Transactions on Power Apparatus and Systems, Vol. PAS-89, No.7,," September/October 1970

Bowles, J.P. , Martin, C.J.B. , Rumpf, E., "Control in HVdc Systems - The State of the Art Part 1: Two-Terminal-Systems," CIGRE Study Committee No.14 (DC Links)

Gibson, H., Ballad, J.P., Chester, J.K., "Characterization, Evaluation and Modelling of Thyristors For HVdc Converter Valves," International Conference on AC and DC Power Transmission (4th: London, England), September 23-26, 1985

Hayashi, T., "Analysis of Commutation Failure in Case of Switching on Shunt Capacitor into AC System," IEEE PES Summer Meeting, New York, N.Y., January 30-February 4, 1977

Hingorani, N.G. , Burberry, M.F. , Simulation of AC System Impedance in HVdc System Studies, "IEEE Transactions on Power Apparatus and Systems, Vol. PAS-89, No. 5/6, May/June 1970

Kimbark, E.W., Direct Current Transmission - Volume 1 (John Wiley & Sons) 1971

Rashwan, M.M. , Thio, C.T. ,"Control, Protection, and Operating Performance of the Nelson River HVdc System," PES Summer Meeting, July 1983

Taylor, P.D., Thyristor Design and Realization, (John Wiley & Sons), Chichester N.Y., 1987

Woodhouse, M.L. ,"Voltage and Current Stresses on HVdc Valves," IEEE Transactions on Power Delivery, Vol. PWRD-2, No.1, January 1987

References

[1]Woodhouse, M.L., "Voltage and Current Stresses on HVdc Valves," IEEE Transactions on Power Delivery, Vol. PWRD-2, No.1, January 1987

[2]Kimbark, E.W., Direct Current Transmission - Volume 1 (John Wiley & Sons, 1971), p.295

[3]Kimbark, E.W., Direct Current Transmission - Volume 1 (John Wiley & Sons, 1971), p. 237.

[4]Kimbark, E.W., Direct Current Transmission - Volume 1 (John Wiley & Sons, 1971), p. 158.

[5]Kimbark, E.W., Direct Current Transmission - Volume 1 (John Wiley & Sons, 1971), p. 87.

[6]Bowles, J.P., "AC System and Transformer Representation For HVdc Transmission Studies," IEEE Transactions on Power Apparatus and Systems, Vol. PAS-89, No.7, September/October 1970

[7]Manitoba Hydro, Specification No. 1950 - Dorsey and Radisson Stations - Supply of Thyristor Valves to Replace Mercury Arc Valves, February 3 1989.

[8]Bowles, J.P., "AC System and Transformer Representation For HVdc Transmission Studies," IEEE Transactions on Power Apparatus and Systems, Vol. PAS-89, No.7, September/October 1970

[9]P. Kuffel, BP1 and BP2 System Data (An Internal Manitoba Hydro Memo Written to File) 91 05 01

[10]The validation tests were performed May 24, 1990. The EMTDC system configuration representing the system at the time of the tests was provided by P. Kuffel (Manitoba Hydro), and the chart recorder and transient fault recorder traces were documented by G.B. Mazur (Manitoba Hydro).

[11]Rashwan, M.M., Thio, C.V., "Control, Protection, and Operating Performance of the Nelson River HVdc System," PES Summer Power Meeting, July 1983

[12]Internal Document, Manitoba Hydro